

ABSTRACT

Title: THE MECHANISM OF RHENIUM
FIXATION IN REDUCING SEDIMENTS

Marvourneen Kimranee Dolor,
Master of Science, 2005

Directed By: Professor George R. Helz,
Department of Chemistry and Biochemistry

There is a wide range of uses of information related to rhenium's geochemical behavior. Field studies indicate that rhenium is highly enriched in reducing sediments. However the mechanisms by which this high degree of enrichment is achieved are unclear. Perrhenate's (ReO_4^-) sorption onto a clay mineral, kaolinite, was investigated and found to be weak. This behavior is consistent with rhenium's conservative behavior in the oceans. Sorption was enhanced by the presence of a reducing agent, lithium borohydride. The presence of sulfide, a reducing agent found in nature, enhanced sorption slightly. Sulfide apparently does not reduce ReO_4^- rapidly as shown by the failure of polysulfide species to appear in solution. Instead, sulfide causes the formation of thioperrhenates.

The mechanism of thiolation is the successive replacement of oxygen atoms in ReO_4^- by sulfur atoms, but ReO_3S^- and ReS_4^- are the only thioperrhenates observed by UV-Vis spectroscopy. The di- and tri- thioperrhenates, ReO_2S_2^- and ReOS_3^- are absent due to their relative instability. Thiolation of ReO_4^- appears to be general-acid catalyzed. Quantitative yield of ReS_4^- from ReO_4^- was never achieved.

Thioperrhenates undergo polymerization in solution to yield a colloidal Re-S species, probably related to Re_2S_7 , which contains polysulfide ions in its structure. This Re-S polymer is stable under different experimental conditions and thermodynamic calculations confirm that it is a very stable, insoluble species. Sulfide may play an important role in Re enrichment in sediments by leading to the formation of this solid Re-S species.

THE MECHANISM OF RHENIUM FIXATION IN REDUCING SEDIMENTS.

By

Marvourneen Kimranee Dolor.

Thesis submitted to the Faculty of the Graduate School of the
University of Maryland, College Park, in partial fulfillment
of the requirements for the degree of
Master of Science
2005

Advisory Committee:
Professor George R. Helz, Chair/ Advisor
Professor Neil V. Blough
Professor John A. Tossell

© Copyright by
Marvourneen Kimranee Dolor
2005

Dedication

To you Mummy, for all your loving e-mails, for all your prayers and for always believing in me: Thank You.

Love,
Your first-born

Acknowledgements

First off, I would like to thank Dr. Helz for sharing his knowledge as an experimentalist, scientific writer and environmental professional. I have learnt so much from Dr. Helz and most of all I've learnt just how much I have left to learn.

I thank my family for being supportive and always expressing their pride in all my achievements, no matter how small I thought they were. I thank my mother for being so enthusiastic about all my academic efforts over the years. I thank my sister, Tamilia for being so supportive. I thank my brother, Francois, for inspiring me by earning his black-belt, days before I completed this thesis. I thank my grandmother for all her prayers. I also thank and all my aunts, uncles and cousins for their support.

I would like to thank Dr. Belinda Wallace for being an inspiration and always lending an ear to all my complaints and rants. I thank J, Natasha, Beverly, Tanay and Aravindan for the nights on the town, the pot-luck dinners and the spontaneous gatherings.

I thank Dr. Carla Neuberger for “teaching me the ropes”, answering all my questions and always being willing to help me solve a problem. I thank Dr. William McDonough and Dr. Richard Ash for sharing their ICP-MS expertise, and allowing me to use the E2. I thank Dr. Phil Piccoli for his help with EPMA analysis. I thank Dr. John Tossell for making unpublished calculations available for this work.

Financial support for this work was provided by the National Science Foundation. Grant No.EAR0229387.

Table of Contents

Dedication.....	ii
Acknowledgements.....	iii
Table of Contents.....	iv
List of Tables.....	vi
List of Figures.....	vii
Chapter 1: Introduction.....	1
<u>1.1 Impetus for Study</u>	1
<u>1.2 The Problem</u>	3
1.2.1 Coastal Anoxia.....	3
1.2.2 Model Anoxic Basin – Chesapeake Bay.....	4
1.2.3 Model Anoxic Basin – The Black Sea.....	5
<u>1.3 Rhenium</u>	5
1.3.1 The Basics.....	5
1.3.2 Geochemical Cycle.....	9
<u>1.4 Comparable Metals</u>	12
1.4.1 Technetium – Rhenium’s Chemical Analogue.....	12
1.4.2 Molybdenum – Rhenium’s possible Geochemical Analogue.....	14
<u>1.5 This Work</u>	16
Chapter 2: Experimental Methods.....	17
<u>2.1 Materials</u>	17
<u>2.2 Instrumentation</u>	17
2.2.1 pH meter.....	17
2.2.2 Ultraviolet-Visible Spectrophotometry.....	18
2.2.3 Inductively Coupled Plasma-Mass Spectrometry.....	20
2.2.4 Electron Probe Microanalyzer (EPMA).....	23
<u>2.3 Methods</u>	23
2.3.1 Preparation of H ₂ S/HS ⁻ and Determination of Total Sulfide.....	23
2.3.2 Preparation of Ampoules.....	24
Chapter 3: Results.....	26
<u>3.1 Investigation of Perrhenate (0.3mM) Sorption on simple oxides and kaolinite</u>	26
<u>3.2 Investigation of Perrhenate (1 μM - .01 μM) Sorption to kaolinite</u>	35
3.2.1. Sorption to kaolinite in the presence of 10 mM Borohydride.....	38
3.2.2. Sorption to kaolinite in the presence of 10 mM Hydrogen Sulfide.....	42
<u>3.3 Investigation of Thioperrhenate Formation</u>	44
3.3.1 Reaction between perrhenate and sulfide over 10.5 hours.....	44
3.3.2 Ampoules containing 1mM perrhenate equilibrated at 25 °C.....	52
3.3.3 Ampoules containing 1mM perrhenate equilibrated at 75 °C.....	55
3.3.4 Ampoules containing 10 μM perrhenate equilibrated at 75 °C.....	58
3.3.5 Solubility of Dirhenium Heptasulfide (Re ₂ S ₇).....	60
<u>3.4 Investigation of thioperrhenate formation and sorption on kaolinite</u>	62
3.4.1 Experiment with kaolinite over 30 hours.....	62

3.4.2 Experiment with Kaolinite in the presence of polysulfides and lower Perrhenate concentration.....	69
Chapter 4: Discussion	74
Appendix I. Tables of experimental observations	84
Appendix II. Tables of UV-Vis data for ampoules containing ~1mM [ReO ₄ ⁻]. Temperature 25°C. Pathlength: 1cm and 0.1 cm.	88
References.....	104

List of Tables

1.	Physical properties of some simple perrhenates.	7
2.	Action of reducing agents on perrhenate.	7
3.	ICP-MS operating conditions.	20
4.	Aridus Operating Conditions. The exact values for sweep gas and nitrogen gas were determined daily during tuning.	20
5.	Thioperrhenate concentrations of mixtures presented in Fig. 15.	53
6.	Solubility of Re_2S_7 experiments: pH, final $[\text{HS}]$ and $[\text{Re}_{(\text{aq})}]$.	61
A1.	Description of contents of centrifuge tubes used in Kaolinite sorption experiments. Reducing agent: sulfide.	84
A2.	Description of contents of centrifuge tubes used in Kaolinite sorption experiments. Reducing agent: borohydride.	85
A3.	Visual observations of ampoules containing $\sim 1 \text{ mM } [\text{ReO}_4^-]$. Temperature: $25 \text{ }^\circ\text{C}$ and $75 \text{ }^\circ\text{C}$.	86
A4.	Visual observations of ampoules containing $\sim 10 \text{ } \mu\text{M } [\text{ReO}_4^-]$. Temperature: $75 \text{ }^\circ\text{C}$.	87

List of Figures

1.	Calibration curve of perrhenate ion obtained from UV-Vis spectroscopy.	19
2.	Graph illustrating that the pH range of perrhenate solutions was maintained after an equilibration time of 20 hours in the absence of kaolinite.	27
3.	Perrhenate sorption on 10 g/L δ -Al ₂ O ₃ (BET: 102.9 m ² /g) at ionic strengths 0.01M and 0.1M NaCl.	30
4.	Perrhenate sorption on 10 g/L SiO ₂ (BET: 182 m ² /g) at ionic strengths 0.01M and 0.1M NaCl.	31
5.	Perrhenate sorption of 200g/L KGa1b (BET: 12.5 m ² /g) at ionic strengths 0.01M and 0.1M NaCl.	32
6.	Molybdate sorption on KGa1 (BET: 9.14 m ² /g) and Perrhenate sorption on KGa1b (BET: 12.5 m ² /g) at ionic strength 0.1M NaCl.	33
7.	Molybdate sorption on δ -Al ₂ O ₃ (BET: 102.9 m ² /g) and Perrhenate sorption on δ -Al ₂ O ₃ (BET: 102.9 m ² /g) at ionic strength 0.1M NaCl.	34
8.	UV-Vis spectra of ~0.2mM NaReO ₄ and 0.1M LiBH ₄ equilibrated in an N ₂ -filled glovebox.	39
9.	Bar graphs showing Re sorption on kaolinite in the presence of borohydride.	41
10.	Bar graphs showing Re sorption on kaolinite in the presence of sulfide.	43
11.	UV-Vis spectrum of 0.002M NaReO ₄ and 0.05M NH ₃ -H ₂ O.	46
12.	UV-Vis spectrum of 0.002M NaReO ₄ and 0.05M NH ₃ -H ₂ O bubbled with H ₂ S(g) for 2 hours.	48
13.	UV-Vis spectrum of 0.002M NaReO ₄ and 0.05M NH ₃ -H ₂ O bubbled with H ₂ S(g) for 5.5 hours.	49
14.	UV-Vis spectrum of 0.002M NaReO ₄ and 0.05M NH ₃ -H ₂ O bubbled with H ₂ S(g) for 10.5 hours.	50
15.	Change in concentration of perrhenate and thioperrhenate species vs. time in contact with H ₂ S(g) at P _(H₂S) = 1atm.	51

16.	UV-Vis spectra of sulfide and 1mM perrhenate mixtures equilibrated for 8 weeks at 25°C.	54
17.	UV-Vis spectra of sulfide and 1mM perrhenate mixture equilibrated for 3 weeks at 25°C then 75°C for 5 weeks.	56
18.	Representative spectrum, from XDS, illustrating the elements present in the precipitates, predominantly rhenium and sulfur.	57
19.	UV-Vis spectra of sulfide and 10 μ M perrhenate mixtures equilibrated for 33 days at 75°C.	59
20.	UV-Vis spectrum of 0.002M NaReO ₄ and 0.05M NH ₃ -H ₂ O bubbled with H ₂ S(g) for 10.5 hours; 200 g/L kaolinite was added at 4.5 hours.	64
21.	Change in concentration of perrhenate and thioperrhenate species and change in pH vs. time in contact with H ₂ S(g) at P _(H₂S) = 1atm; 200 g/L kaolinite was added at 4.5 hours.	65
22.	Change in total rhenium, perrhenate and thioperrhenate concentrations over the course of the experiment.	67
23.	UV-Vis spectrum of 0.002M NaReO ₄ and 0.05M NH ₃ -H ₂ O bubbled with H ₂ S(g) for 10.5 hours then placed in glovebox. Sample taken at 30.5 hours; 200 g/L kaolinite was added at 4.5 hours	68
24.	UV-Vis spectrum of 2 μ M NaReO ₄ , 0.15 mM Na ₂ S ₄ and 50mM NH ₃ -H ₂ O before H ₂ S bubbling and after being bubbled with H ₂ S(g) for 10.5 hours; 200 g/L kaolinite was added at 4.5 hours.	71
25.	Change in rhenium concentration and pH over the course of the experiment.	73
26.	UV-Vis spectra of 0.3mM ReO ₄ ⁻ sorption on 200g/L kaolinite, ionic strength 0.01M NaCl.	75

Chapter 1: Introduction

1.1 Impetus for Study

The goal of my research is to determine and thereby understand the fixation mechanisms of rhenium in reducing sediments. The term ‘reducing’ is used to refer to both suboxic (no O₂ or H₂S present) and anoxic (H₂S present but no O₂) conditions (Colodner et al., 1995). This condition usually occurs when the rate of oxygen consumption via respiration is faster than the rate of oxygen replenishment via ventilation (Adelson et al., 2001).

Rhenium has proved useful in establishing the environmental conditions present when organic-rich sediments were deposited (Colodner et al., 1993). This is because rhenium is enriched only in reducing sediments and this enrichment is considerable (Colodner et al., 1993). Other metals besides Re are enriched in reducing sediments and the research done towards elucidating the fixation of other metals is very insightful in terms of suggesting the direction in which work on rhenium should proceed. Rhenium, however, is unmatched in its degree of enrichment (Colodner et al., 1993). Molybdenum and uranium are enriched in anoxic sediments over oxic sediments by factors of 10 to 50, while Colodner et al. (1993), have found that enrichment of rhenium is a factor of 300.

Calvert and Pedersen (1993) have performed numerous studies on a suite of trace elements and have drawn interesting conclusions. They state that sediments lacking in enrichment of molybdenum and rhenium as well as cadmium, copper,

nickel, zinc, chromium and vanadium can only be reliably used to suggest that sedimentation occurred under oxic conditions. These metals are enriched in anoxic sediments *and* in subsurface anoxic deposits that underlie surface oxic horizons (Calvert and Pedersen, 1993). This leads to ambiguity when attempting to determine whether the water body itself was anoxic at the time of deposition (Calvert and Pedersen, 1993).

Crusius et al. (1996) have drawn slightly different conclusions from others who have studied rhenium's enrichment in sediments. They studied the suboxic sediments of the Sea of Japan, sediments in the oxygen minimum of the Pakistan margin and the sediments underlying the anoxic waters of the Black Sea. They concluded that, Re is enriched in suboxic sediments, slightly after the reduction of $\text{Fe}^{(\text{III})}$ and $\text{U}^{(\text{VI})}$ while Mo is enriched in more reducing sediments, in the presence of free H_2S (Crusius et al., 1996). A much larger portion on the ocean floor is suboxic and not anoxic and so removal of Re to suboxic sediments may be the largest sink of Re in seawater (Crusius et al., 1996). Crusius et al. (1996) assert that downcore records now hold the potential to be used to hindcast ancient redox environments. Together, Mo and Re concentrations as well as depth of enrichment can be used to determine whether the water column or the sediments were oxic, suboxic or anoxic (Crusius et al., 1996).

Morford and Emerson (1999) also analyzed a suite of redox sensitive elements, molybdenum, rhenium, vanadium, uranium, and cadmium to evaluate enrichment (or lack thereof) in sediments from the Northwest African margin, the U.S. Northwest margin and the Arabian Sea. They confirmed the findings of

Colodner et al. (1993,1995) and Calvert and Pedersen (1993) and concluded that, while all of the metals tested are reduced under anoxic conditions, Re is the superior tracer of reducing conditions. Re shows the highest degree of enrichment due to its low particulate concentrations (Morford and Emerson, 1999).

There is a wide range of uses of information related to rhenium's behavior and this is further incentive for my research. Environmental scientists, chemists and engineers, nuclear chemists, geochemists, geologists and petroleum engineers can all use the same information about rhenium's geochemical behavior to solve different problems.

1.2 The Problem

1.2.1 Coastal Anoxia

Coastal anoxia leads to numerous problems in the coasts and estuaries where it occurs. In these areas, this problem affects the wildlife, commercial and recreational fisheries, and the tourism industry (Rabalais et al., 2002). The alleged cause of coastal anoxia is cultural eutrophication. This is the inadvertent fertilization of natural water bodies by nitrate- and phosphorous-rich agricultural run off (Laws, 2000).

Not all environmentalists agree that cultural eutrophication is the sole cause of anoxic conditions in aquatic systems. For example Adelson et al. (2001) point out that many factors, such as advective/diffusive processes, external changes in water and land use, as well as weather and climate, all affect deep-water ventilation. Deep-water ventilation in turn controls whether or not a water body will be anoxic. Cronin

at al. (2000) also discuss the fact that over the time-scale of centuries, changes in coastal and estuarine hydrology will be significant and have profound effects on ventilation rates.

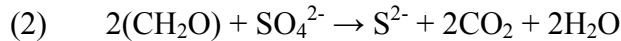
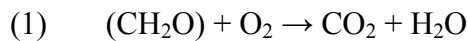
1.2.2 Model Anoxic Basin – Chesapeake Bay

Chesapeake Bay is the largest estuary in the United States. It was formed by a rise in sea level following the last glaciation and is basically the drowned lower course of the Susquehanna River. The bay has an area of about 11,400 km², but its average depth is only 6-7 m. In general estuaries are highly productive systems due to the physical circulation pattern that provides a natural mechanism for recycling food and inorganic nutrients. (Laws, 2000).

In 1936 Newcombe and Horne studied the Chesapeake Bay and found that there was oxygen depletion in the bottom waters during the summer months (Newcombe and Horne, 1938). This has continued to be a common occurrence in the decades since then (Laws, 2000). However, there has been disagreement about whether this problem has become more severe in the past 20-30 years (Laws, 2000). This is due to the inadequacy of archived data on the volume of anoxic water, a value that varies from year to year (Adelson et al., 2001). Long-term, self-consistent data are needed in order to establish accurate trends for use by environmental management agencies. Thus far the only viable potential source of such information is geochemistry, such as the study of Mo and Re (Adelson et al., 2001)

As mentioned above, anoxia occurs where there is no O₂ but H₂S is present. Biological processes generate this H₂S. Phytoplankton biomass fuels oxygen consumption, a significant portion of which is due to (1) aerobic, heterotrophic

bacterial metabolism and microbial sulfur cycling (Tuttle, 1987). Microbial sulfur cycling involves two key processes: (2) sulfate reduction catalyzed by anaerobic bacteria in Bay sediments and (3) sulfide oxidation occurring in the top layer of the sediments or in the deep waters below the pycnocline (3) (Tuttle, 1987).



1.2.3 Model Anoxic Basin – The Black Sea

In the compilation, Black Sea Oceanography, editors Izdar and Murray describe the modern Black Sea as the model anoxic basin. It is the world's largest permanently anoxic basin (area = 423,000 km²; volume = 534, 000 km³). It is unique in terms of its isolation from the rest of the world's oceans. Only the narrow and shallow Bosphorus Strait provides water exchange with the Mediterranean. Concentrations of hydrogen sulfide reach values of 350 μM in the deep water and the oxygen-hydrogen sulfide interface exists between 80 and 200 m water depth. (Izdar and Murray, 1991).

1.3 Rhenium

1.3.1 The Basics

Rhenium was not discovered until 1925 and as Colton (1965) suggests, this is probably due to the fact that rhenium is one of the rarest of the non-radioactive elements. Peacock (1966) asserts that natural rhenium has two isotopes, 185 and 187, which are present in the ratio 1: 1.62. Rhenium is in the same group as manganese in

the periodic table, but its behavior more closely resembles molybdenum (Colodner, 1991).

Rhenium is recovered commercially as a by-product of the treatment of molybdenum ores and also copper ores. In each case the ores are roasted in air; rhenium heptaoxide is formed and volatilizes out of the furnace. It may be recovered either from the stack or flue dusts or removed from the waste gases using a dry cyclone or wet scrubber. The recovered heptaoxide is usually dissolved in water and the rhenium finally recovered by crystallization of potassium perrhenate (Colton, 1965). It is possible to precipitate potassium perrhenate because it is sparingly soluble (Peacock, 1966).

There are three well-established oxides for rhenium. As is typical for second and third transition elements in this part of the periodic table, the maximum oxidation state of the elements is very stable in the oxygen compounds. Rhenium heptaoxide, Re_2O_7 , is the product formed by heating the element, or lower oxides, in oxygen. It dissolves in water to give perrhenic acid, HReO_4 , which is a strong acid that gives rise to a series of salts.

In contrast to the permanganates, the perrhenates are colorless and have virtually no oxidizing power. They are usually white crystalline compounds and Raman spectra indicate that the perrhenate ion exists in solution as the tetrahedral ReO_4^- ion, and not the octahedral ReO_6^{5-} ion as was previously suggested (Colton, 1965). The physical properties of a few perrhenates are included in Table 1. Perrhenates' behavior towards reducing agents has also been studied, and a summary

of some of the results is given in Table 2. These results show that in the majority of cases reduction stops at $\text{Re}^{(\text{IV})}$ (Peacock, 1966).

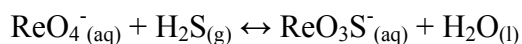
Table 1. Physical properties of some simple perrhenates (Colton, 1965).

Compound	M.p.(°C)	Density	Solubility (moles/100 g H ₂ O x10 ²)			Heat of solution (kcal/mole)
			0°	30°	50.3°	
LiReO ₄ .2H ₂ O	87.5	3.69	100	140	140	1.6
LiReO ₄	426	4.61	—	—	—	—
NaReO ₄	414	5.24	37.8	53.2	63.6	1.83
KReO ₄	555	4.38	0.124	0.508	1.11	7.68
NH ₄ ReO ₄	decomp.	7.53	1.03	3.25	5.99	6.21
RbReO ₄	598	4.73	0.116	0.468	1.05	7.70
CsReO ₄	616	4.76	0.0861	0.287	0.640	7.69

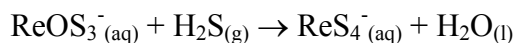
Table 2. Action of reducing agents on perrhenate (Peacock, 1966).

<i>Medium (N)</i>	<i>Reducing agent</i>	<i>Reduced State</i>
HCl (1-4)	Sn ²⁺ , Ti ³⁺ , V ²⁺ , Cr ²⁺	4
H ₂ SO ₄ (1)	Sn ²⁺ , Ti ³⁺ , V ²⁺ , Cr ²⁺	4
H ₂ SO ₄ (18)	Cr ²⁺	(6) 5 + 4
	Sn ²⁺	5? 4+7
		(disproportionates)
HCl (8-10)	Cr ²⁺	3
	2I ⁻	5
	3I ⁻	4
H ₂ SO ₄ (<3.6)	Zn/Hg	0 + 1
H ₂ SO ₄ (10 – 18)	Zn/Hg	4
HCl (0.6 – 3.2)	Zn/Hg	2+3
HCl (4.8 – 6.4)	Zn/Hg	3+4
H ₂ SO ₄ (9)	Cd/Hg	4
H ₂ SO ₄ (10 – 18)	Bi/Hg	5
HCl	N ₂ H ₄	4
HCl	H ₃ PO ₂	4
HCl (~11)	H ₃ PO ₂	3

According to Peacock (1966), thio-perrhenates are formed when a bivalent sulfur atom replaces an oxygen atom in the perrhenate ion. When hydrogen sulfide is passed into a neutral solution of a perrhenate, the colorless solution becomes yellow-green and thio-perrhenates are formed according to the equation:



The solution also contains dark poly-thio compounds. The thio-perrhenates are all more soluble than the oxygen analogues; they decompose slowly even in neutral solution. Peacock (1966) asserts that the prolonged action of hydrogen sulfide on perrhenate solutions does not appear to lead to the complete replacement of the oxygen atoms by sulfur. On the other hand, Muller et al. (1967) and Ranade et al. (1970), assert that tetrathio-perrhenate can be formed when a perrhenate solution, in concentrated ammonia solution is bubbled with H₂S gas:



On the addition of acid to thio-perrhenate solution, rhenium heptasulfide is precipitated. Rhenium heptasulfide, Re₂S₇, is a black powder, which is readily converted to the perrhenate ion by the action of alkaline hydrogen peroxide solution on nitric acid. Rhenium disulfide may be prepared either by the thermal decomposition of the heptasulfide in vacuum or by direct combination of the elements at red heat. Rhenium disulfide, ReS₂, is a dense black, chemically inert solid (Colton, 1965). Its structure is similar to that of molybdenum disulfide (Peacock, 1966).

1.3.2 Geochemical Cycle

According to Koide et al. (1987), the concentration of Re, (as the perrhenate ion, ReO_4^-) in seawater ranges from 30.5 pM to 81.5 pM. Anbar et al. (1992) determined seawater concentrations of rhenium, and state that it ranges from 38.9 pM to 39.5 pM. Anbar et al. (1992) assert that the larger range reported by Koide et al. (1987) may be a reflection of the less sophisticated analytical methods used. Koide et al. (1987) used a Graphite Furnace Atomic Absorption Spectrometer, while Anbar et al. (1992) used isotope dilution and negative thermal ionization mass spectrometry. Colodner et al. (1993 and 1995) used inductively couple plasma-mass spectrometry preceded by anion exchange to determine seawater concentrations of rhenium. Their results were consistent with the values obtained by Anbar et al. (1992), 38.9 pM.

These values are remarkably higher than those of neighboring elements like iridium, platinum and gold whose seawater concentrations do not exceed 1 pM. On the other hand, the crustal rock and deep sediment concentrations of rhenium are usually at least an order of magnitude less than its periodic table neighbors. The unusual seawater concentration is attributed to the non-reactivity of the perrhenate ion. (Koide et al., 1987).

Rhenium is not a required trace element in plants and/or animals and is thus not significantly cycled with biogenic matter in the water column. This leads to low particulate concentrations in seawater (Colodner et al., 1993, Ravizza et al., 1996 and Morford and Emerson, 1999). Yang (1991) has observed that Re is enriched by a factor of 1000 in brown algae. This implies that brown algae are a biological sink of Re in the world's oceans. A supporting finding is that technetium (rhenium's

chemical analogue), exhibits similar behavior (Birks, 1975). However, red and green algae do not exhibit Re enrichment and the reason for this finding has not been reported (Yang, 1991).

Colodner et al. (1993) have determined some important facts about the geochemical cycle of Re by studying water and sediments from the Black Sea and Chesapeake Bay. Rhenium in the continental crust is easily mobilized during weathering by oxic aqueous solutions, and is delivered to the oceans primarily by rivers. The residence time of Re in the oceans with respect to river inflow is estimated to be 750,000 yr. This is similar to the oceanic residence times of Mo and U of 780,000 and 250,000-500,000 yr, respectively. (Colodner et. al, 1993)

Colodner et al. (1992) compared the post-depositional mobility of rhenium to two other platinum-group elements, platinum and iridium. They assert that, for elements with several possible valence states, oxidized and reduced forms may show different susceptibilities to adsorption and precipitation reactions. There are phases that are specific to oxic or anoxic sediments, such as Fe-Mn oxyhydroxides or sulfides, that may be precipitated with these metals or adsorb them. Therefore, there are numerous undetermined factors that will dictate the distribution and mobility of rhenium between pore waters and sediments. (Colodner et al., 1992).

Colodner et al. (1992) found that in Atlantic abyssal sediments, platinum group element ratios in the geological record could change during diagenesis (the physical and chemical changes occurring in sediments between the times of deposition and solidification). Some of these chemical changes involve redox processes within the sediments. (Colodner et al., 1992).

Their work confirmed previous findings that Re is removed into anoxic sediments at or below the sediment water interface (Colodner et al., 1992). However, it is still unclear whether mineral surfaces, specifically ferromanganese oxides, have any ability to scavenge rhenium. Colodner et al. (1992) observed this behavior in the particle-rich layer in the Black Sea. Both Colodner et al. (1992) and Xiong and Wood (1999, 2001) postulate that metalliferous hydrothermal sediments are also a potential accumulation site for Re from seawater. However, Morford and Emerson disagree and conclude that hydrothermal processes play a negligible role in Re geochemistry (Morford and Emerson, 1999).

Xiong and Wood (1999, 2001) have studied the speciation and solubility of Re in model hydrothermal solutions. So far all of their results are tentative and have not been verified by real-world values. They concluded that in anoxic environments, at a temperature range of 100 °C to 200 °C, ReS_2 is the species that determines rhenium's low solubility (Xiong and Wood, 1999, Xiong and Wood, 2001). In a more recent paper Xiong (2003) goes on to postulate that at ambient temperatures ReS_2 controls solubility. Thermodynamic models are presented that indicate that $\text{Re}(\text{OH})_4^0$ is the dominant species in anoxic environment and not ReO_4^- (Xiong, 2003). This is a unique view of rhenium's speciation in natural waters. The extrapolation from high temperature hydrothermal environments to ambient temperature was not articulated very clearly and this makes these results difficult to evaluate.

1.4 Comparable Metals

1.4.1 Technetium – Rhenium’s Chemical Analogue

The understanding of rhenium’s marine geochemistry will provide entry to the understanding of technetium, an element that is just above rhenium, in group VIIA of the periodic table. Technetium has only unstable isotopes whose origins are primarily nuclear weapon detonations and nuclear reactor wastes. These two elements have remarkably similar chemistries. (Koide et al., 1987).

According to Wakoff and Nagy (2004), the U.S. Department of Energy’s Hanford Site in southeastern Washington State produced special nuclear materials for the nuclear weapons program between 1944 and 1988. The byproducts of these efforts are large volumes of liquid waste streams that are now stored in tanks.

Uranium fission products in the high level waste contained in these tanks include ^{99}Tc , $t_{1/2} = 2.1 \times 10^5$ years (Wakoff and Nagy, 2004). ^{99}Tc is the major concern in long-term risk assessments because of its relatively long half-life and the chemical stability of the pertechnetate ion (TcO_4^-) under aerobic conditions (Wakoff and Nagy, 2004).

Tc exhibits a wide range of redox and solubility characteristics in the radiation fields and chemical mixtures that existed in some tanks (Wakoff and Nagy, 2004). Therefore there is considerable uncertainty about the current chemical speciation and distribution of ^{99}Tc in the tanks. In order to establish strategies for tank waste retrieval and closure, a better understanding of the interactions between ^{99}Tc and tank waste solids is critical (Wakoff and Nagy, 2004). The first finding is that sorption of

Tc or its chemical analogue Re on oxides is minimal under oxic conditions above pH 7 (Wakoff and Nagy, 2004).

More recent studies by Maes et al. (2004) investigated technetium's interaction with humic substances. Evidence for the types of interactions was obtained from Extended X-ray Absorption Fine Structure (EXAFS) spectroscopy. They found that when high concentrations (mM to μM) of TcO_4^- are introduced to chemically reducing environments, small $\text{Tc}^{(\text{IV})}$ oxidic polymers are formed (Maes et al., 2004). These polymers may either form colloids and precipitate or may interact with (dissolved and immobile) humic substances. Observation of $\text{Tc}^{(\text{IV})}$ colloid sorption onto humic substances is very different from the generally accepted metal-humate complexation. These observations point to new possibilities for the reaction pathways of metals and radionuclides in humic-rich environments (Maes et al., 2004). $\text{Re}^{(\text{IV})}$ may also exhibit such behavior with humic substances in natural waters.

Bacterial Reduction

Bacterial reduction of soluble TcO_4^- to insoluble Tc species has been viewed as a potential solution to the problem of ^{99}Tc leaching into groundwater systems around nuclear sites. Lloyd et al. (1999, 2000) have done numerous experiments and have determined that *Geobacter sulfurreducens*, *Desulfovibrio desulfuricans* and *Escherichia coli* are three species of bacteria that mediate the reduction of $\text{Tc}^{(\text{VII})}$ to $\text{Tc}^{(\text{IV})}$. Because these are biological systems there are many other variables that affect this reduction other than the presence of $\text{Tc}^{(\text{VII})}$ and the respective bacteria. Some of these factors include the presence of sulfide, $\text{Fe}^{(\text{II})}$, $\text{Fe}^{(\text{III})}$ and low O_2 concentrations (Lloyd et al., 1999 and Lloyd et al., 2000). Studies of these factors are still underway,

however, there is the possibility that ReO_4^- can also be reduced and immobilized in this way.

1.4.2 Molybdenum – Rhenium’s possible Geochemical Analogue

Over the past decade, work has been done in the Helz lab to elucidate the behavior of molybdenum in anoxic waters. Since, Mo is reduced in anoxic waters, where H_2S is present this has involved investigating the behavior of thiomolybdates as well as molybdate’s behavior with iron monosulfide, FeS . Erickson and Helz (2000) determined that in the presence of the sulfide, molybdate undergoes sulfidation in four steps that conserve Mo(IV) and lead to tetrathiomolybdate:



Anoxic sediment pore waters are enriched relative to overlying waters in Brønsted acids. This promotes conversion of geochemically passive MoO_4^{2-} to particle-reactive thiomolybdates ($\text{MoO}_x\text{S}_{4-x}^{2-}$) (Vorlicek and Helz, 2002). A possible source of fixed, but acid-labile sulfide in oxic waters is the slow hydrolysis and oxidation of MoS_4^{2-} (Erickson and Helz, 1999).

Adelson et al.(2001) continued this work and investigated whether molybdenum could be used as a paleoenvironmental indicator of anoxia. They determined that it could, despite the fact that Mo is not scavenged from the water column. This is because sulfide rich water-sediment interfaces can only exist when the deep parts of the water body are anoxic (Adelson et al., 2001). Molybdate to thiomolybdate conversions occur at this water-sediment interface when H_2S concentrations are high (Erickson and Helz, 1999, Adelson et al., 2001). Thus when the water-column is anoxic, Mo fixation occurs (Adelson et al., 2001).

Experiments up to that point had suggested that Mo fixation occurred more readily in pore waters than in overlying waters. Vorlicek and Helz (2002) proceeded to test this hypothesis using kaolinite ($\text{Al}_2\text{Si}_2\text{O}_5[\text{OH}]_4$) as a representative mineral catalyst. They found that kaolinite did affect the thiomolybdate interconversions (Vorlicek and Helz, 2002). The effects were pH-dependent leading them to suggest that weak-acid surface sites promote hydrolysis (Vorlicek and Helz, 2002).

Interesting observations from this work led to another hypothesis, that polysulfide ions facilitate Mo scavenging (Vorlicek et al., 2004). Two main sets of experiments were performed: homogenous reactions of MoOS_3^{2-} and MoS_4^{2-} in polysulfide solutions and scavenging of thiomolybdates by pyrite surfaces. Results showed that although H_2S is indeed important in Mo speciation, zero-valent sulfur is important as well. From this finding they were able to present a model of marine MoO_4^{2-} fixation in Mo-Fe-S cuboidal structures. These structures are associated with pyrite in anoxic sediments and black shales. This model involves the formation of appropriate polysulfide species that are subsequently scavenged by pyrite (Vorlicek et al., 2004).

There is evidence that suggests that Re and Mo are chemically similar. However, the work by Crusius et al. (1996), mentioned above, as well as work by Crusius and Thomson (1999) presents the possibility that perrhenate and molybdate behavior in reducing environments are significantly different. Crusius and Thomson (1999) found that Re was not incorporated into one core where diagenetic pyrite was present, while Mo was. In this work we compare our findings for Re sorption to work done by Goldberg et al. (1996) on Mo sorption.

1.5 This Work

The aim of this work is to investigate the conditions that lead to rhenium enrichment in reducing sediments. My initial approach to the problem was to determine whether Re exhibits similar behavior to Mo. I used oxides and a common clay mineral in sorption experiments. I modeled these experiments after similar ones performed on Mo by Goldberg et al. (1996) and Vorlicek et al. (2004).

I was then interested in the reduction of Re by a stronger reducing agent than sulfide and selected borohydride, BH_4^- . I also investigated the formation of thioperrhenates from a strongly alkaline perrhenate solution. After determining that a mixture of thioperrhenates did indeed form, I investigated Re sorption on kaolinite in the presence of sulfide. I hypothesized that thioperrhenates would sorb more strongly to kaolinite than perrhenate.

I wanted to establish whether rhenium sulfide would form under environmental conditions, and what the molecular formula of this sulfide was likely to be. I also wanted to determine whether precipitation of this solid could account for the high enrichment of rhenium in anoxic sediments. The first step in this investigation was determining whether thioperrhenates are the precursors of rhenium sulfide. I equilibrated thioperrhenate mixtures in fused ampoules at room temperature as well as at 75 °C. My plan was to develop a possible timeline for the formation of thioperrhenates from perrhenate and their subsequent transformation to rhenium sulfide.

Chapter 2: Experimental Methods

2.1 Materials

Aluminium Oxide C (δ - Al_2O_3) and Aerosil 200 (SiO_2) were obtained from the Degussa Corporation. Aluminium Oxide C has a reported Brunauer-Emmett-Teller (BET) surface area of $102.9 \text{ m}^2/\text{g}$ (Goldberg et al. 1998). Silica has a reported BET surface area of $182 \text{ m}^2/\text{g}$ (Young, 1981). Kaolinite ($\text{Al}_2\text{Si}_2\text{O}_5[\text{OH}]_4$) as KGa1b, was purchased from Purdue University Source Clay Repository and used without pretreatment. The BET surface area of KGa1b is $12.5 \text{ m}^2/\text{g}$ (Bereznitski et al., 1998).

The following reagents were purchased and used as received: NaCl (J. T. Baker), NaOH (J. T. Baker), HCl (J. T. Baker), NaH_2PO_4 (J. T. Baker), Na_2HPO_4 (J. T. Baker), NH_4Cl (J. T. Baker), $\text{NH}_3\text{-H}_2\text{O}$ (J. T. Baker) Re_2S_7 (Sigma-Aldrich) and NaReO_4 (Sigma-Aldrich, 99.99 % purity). All solutions were prepared from $>18 \text{ M}\Omega \text{ cm}$ resistivity water (B-Pure, Barnstead). Glassware was soaked in 5% HNO_3 and rinsed thoroughly with deionized water before use.

2.2 Instrumentation

2.2.1 pH meter

All pH measurements were made with an Orion model 420A meter equipped with an Orion model 8103 combination microelectrode. At the beginning of each day, the meter was calibrated between pH 7 and 10 with VWR commercial buffers. The error associated with all pH measurements was ± 0.05 .

2.2.2 Ultraviolet-Visible Spectrophotometry

UV-Vis was used to measure rhenium concentrations since the perrhenate anion absorbs at the wavelengths 206nm and 228nm. A 1.00 cm quartz cuvette was used for analysis. The spectra were recorded on a Hewlett Packard Model 8452 Diode Array Spectrophotometer, using deionized water as the blank solution. The wavelength range of this instrument is 190nm to 820nm.

Figure 1 shows the calibration curve obtained. Since the ϵ value at 228nm corresponds best with the literature value, 228nm was the absorption maximum used to determine perrhenate concentration in subsequent sorption experiments.

Calibration Curve Perrhenate, 090104

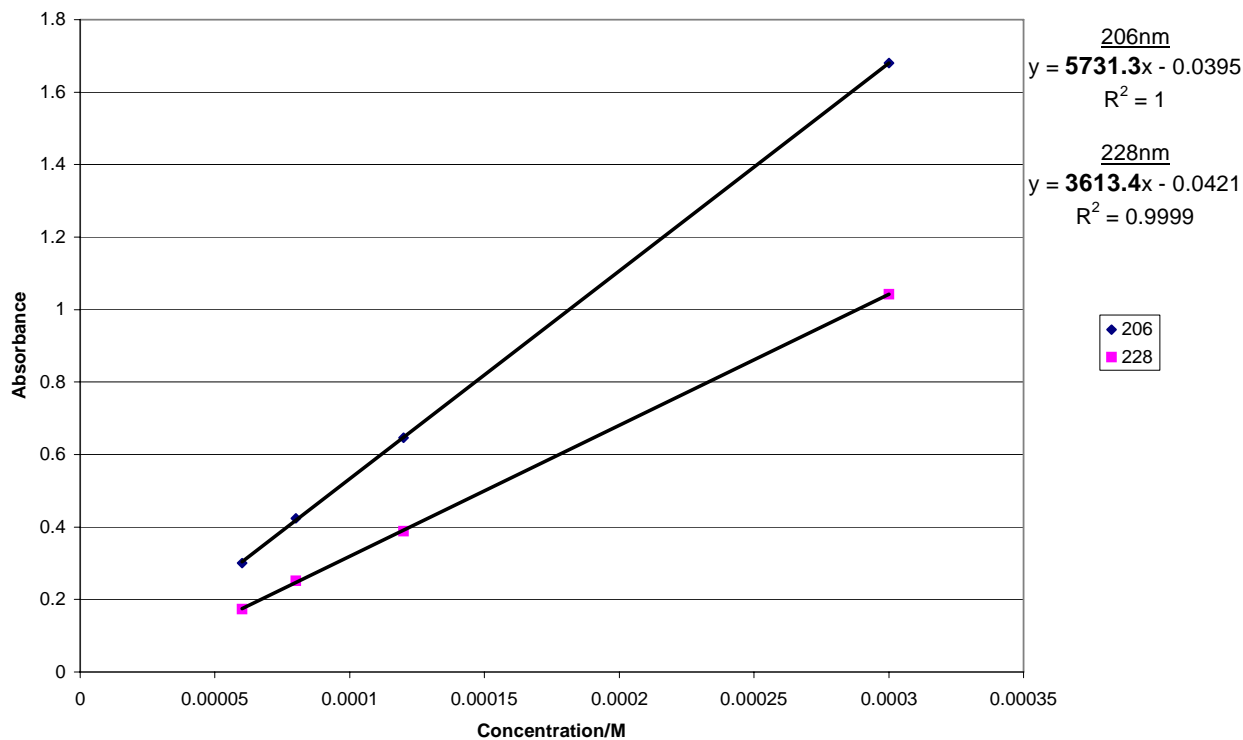


Fig. 1. Calibration curve of perrhenate ion obtained from UV-Vis spectroscopy. The experimental extinction coefficients (ϵ) values are the slopes of the calibration curves: $\epsilon_{206\text{nm}}=5731 \text{ Lmol}^{-1}\text{cm}^{-1}$ and $\epsilon_{228\text{nm}}= 3613 \text{ Lmol}^{-1}\text{cm}^{-1}$. These compare well to the literature values: $\epsilon_{206\text{nm}}=6060 \text{ Lmol}^{-1}\text{cm}^{-1}$ and $\epsilon_{228\text{nm}}=3610 \text{ Lmol}^{-1}\text{cm}^{-1}$ (Colton, 1965).

2.2.3 Inductively Coupled Plasma-Mass Spectrometry

I used the low detection limit of ICP-MS to investigate perchlorate sorption on the common clay minerals listed above. I used a Finnigan Element 2 Instrument, interfaced with a CETAC Aridus Sample Introduction System for all analyses. Tables 3 and 4 describe the operating conditions for the ICP-MS and Aridus respectively.

Table 3. ICP-MS Operating Conditions

ICP rf power, W	1350
detector	conversion dynode at ~8kV discrete dynode Secondary Electron Multiplier
run mode	reverse geometry: Magnetic Sector Field followed by Electric Sector Analyzer (ESA)
mass window	10
scanning per peak	10
run time per sample, s	75

Table 4. Aridus Operating Conditions. The exact values for sweep gas and nitrogen gas were determined daily during tuning.

Fluoropolymer Desolvating Membrane	
sweep gas L/min	2.5-3.0
nitrogen gas mL/min	6.0-9.0
membrane temperature	160
Spray Chamber	fluoropolymer with pumped drain
temperature	100
Autosampler	ASX-100

In ICP-MS, mass spectrometry is used to quantify the ions generated by the inductively coupled plasma (Bea, 1999). This plasma is an electrodeless discharge in argon at atmospheric pressure (Jarvis et al., 1992). Energy from a radio frequency

generator is coupled to the plasma and maintains it (Jarvis et al., 1992). An assembly of quartz tubes, known as the torch, houses the plasma. The torch provides physical separation between the region where electricity is added and the region containing the sample (Jarvis et al., 1992). Thus, the chemical composition of the sample solution can vary substantially without affecting the electrical processes that sustain the plasma (Jarvis et al., 1992). This is the main reason for the minimal physical and chemical interferences in ICP compared to those seen in other spectrochemical sources (Jarvis et al., 1992)

Ions from the central part of the torch are directed into the mass spectrometer by small orifices in the sampler and skimmer cones (Jarvis et al., 1992). These cones have to be replaced at least every month since the aerosol that does not go through the orifices is deposited on the back of these cones. This deposited material can revolatize and enter the mass-spectrometer during subsequent runs. This is a particular concern when previous users used laser ablation for sample introduction, since this method tends to deposit more material on the cones.

After passing through the cones and into the mass spectrometer the ion beam is collimated and focused by several ion lenses (Bea, 1992). This directs it into the quadrupole ion filter, which stops at every mass of interest, (Bea, 1992) 185 and 187 in our analyses. A detector records the number of ions passing through the filter in counts per second for each mass (Bea, 1992). The computer interfaced with the instrument then provides reports in units determined by the user such as ppb or molarity. These values are calculated by software using the calibration curve generated earlier in the run.

A five-point external calibration curve was used for my analyses. The concentrations used were: 1 nM, 10 nM, 50 nM, 100 nM and 200 nM. This curve served two purposes. It provided a means to convert counts per second supplied by the instrument into concentrations. It also served as an indicator that the instrument had been correctly tuned. Tuning was performed prior to each day's run to establish the optimum Sample Gas and nitrogen flow rates.

The standards were dilutions of a Rhenium standard (Specpure) and HNO₃ (Ultra-pure). All standards and unknowns were made to be 2% v/v HNO₃. Nitric acid provides the most ideal matrix for analysis. This was determined by analyzing standards and blanks in both deionized water and 2% v/v HNO₃. I found lower background counts when nitric acid was used.

I also found that there was considerable instrument drift over the course of one run. This was determined by analyzing a standard solution as an unknown sample at the end of a run. The first step I took to improve accuracy was to bracket each sample with two standards to obtain a calibration curve for each sample. This meant the generation of 15-20 calibration curves per analysis. I then used the counts per second for each unknown to calculate the molarity. This helped to improve accuracy but did not account for the different matrix environments of the samples and standards. I used a 0.5 ppb Tungsten internal standard in all the samples in order to determine the exact changes in counts per second during the course of a run. I used the ratio of the Tungsten-184 and Tungsten-186 counts in each sample versus the counts in a blank to determine the corrected Rhenium-185 and Rhenium-187 counts per second.

2.2.4 Electron Probe Microanalyzer (EPMA)

The electron probe microanalyzer (EPMA) is a high resolution Scanning Electron Microscope with EDS and WDS capabilities. EDS was used to determine the composition of the precipitates formed in the experiments where 1mM perrhenate and 10mM sulfide were equilibrated at 75 °C (Section 3.4). The instrument used was a JEOL 8900R Superprobe Electron Probe Microanalyzer.

The mixtures were filtered, using 0.02 μm pore-size filter paper. For each sample, I placed a piece of the filter paper containing residue on a piece of carbon tape mounted on a glass slide. The samples were then coated with a 200-300 Å thick layer of carbon. This makes the sample conductive so the electron beam will interact with it. The pressure inside the EPMA was 10^{-4} Torr. I used information gathered from the energy dispersive X-ray Spectrometer (XDS) to determine the elements present in the precipitates.

2.3 Methods

2.3.1 Preparation of $\text{H}_2\text{S}/\text{HS}^-$ and Determination of Total Sulfide

A one molar NaOH solution was prepared, placed in a three-neck round bottom flask, and deoxygenated with N_2 gas. High Purity H_2S gas (Matheson Tri-Gas) was then bubbled through the solution for a minimum of 45 minutes. Nitrogen gas was again passed through the solution for 15 minutes. A two-way valve was used to ensure that no oxygen could enter the flask when switching between the two gases. Stopcocks on both the inlet and outlet adapters were closed immediately after the N_2

gas was turned off to ensure no oxygen leaked into the flask while it was transferred to the N₂ filled glovebox.

Total sulfide measurements were made by potentiometric titration with HgCl₂. An aliquot of the solution was added to 60 mL of deoxygenated, deionized water made basic with 0.2g of NaOH. These mixtures were prepared inside a N₂ filled glovebox. The pH of the final solutions was approximately 13. The vials were sealed with Teflon coated, screw-on lids, and removed from the glovebox just before titration. The samples were titrated against 4.85 mM or 0.2883 mM HgCl₂, using a Brinkmann Metrohm716 DMS Titrino Automatic titrator equipped with a Ag/Ag₂S indicating electrode and a double junction reference Ag/AgCl electrode.

The end point of the titration is the steepest point on the plot of potential vs. mL of titrant delivered. Titrations were performed in triplicate and the average of the three volumes obtained was used to calculate total sulfide concentration.

2.3.2 Preparation of Ampoules

NaHS was prepared from NaOH and H₂S gas as described in Section 2.3.1. Two phosphate buffers at pH 6.21 and 7.20 and two ammonia buffers at pH 9.24 and 10.28 were prepared. Two hundred and fifty milliliters of each of these buffers was deoxygenated with N₂ gas and passed into an N₂ filled glove box.

Each ampoule was filled with approximately 20 mL of liquid inside an N₂ filled glovebox. After all ampoules were filled they were capped with a piece of rubber tubing closed off on one end with a balloon. The ampoules were then passed out of the glove box and prepared for sealing. This involved wrapping pieces of

aluminum foil around the rubber tubing to prevent burning of the rubber. The ampoules were then sealed with a propane/O₂ flame.

There were a large number of different experiments performed in this study. I will report the procedures for each of these experiments as I present the results in the next chapter.

Chapter 3: Results

3.1 Investigation of Perrhenate (0.3mM) Sorption on simple oxides and kaolinite.

The purpose of these experiments was to evaluate sorption of ReO_4^- as a function of pH on kaolinite, a common clay mineral. In this study, this mineral serves as a proxy for marine sediments. The kaolinite, KGa1b ($\text{Al}_2\text{Si}_2\text{O}_5[\text{OH}]_4$) is reasonably well characterized and this will simplify the task of deducing the conditions under which the perrhenate anion is sorbed in nature. In addition to kaolinite, two oxides, Aluminum Oxide C ($\delta\text{-Al}_2\text{O}_3$) and Aerosil 200 (SiO_2) were used.

Initially, the procedure for adsorption of molybdate established by Goldberg et al. (1996) was followed. This called for an equilibration time of 20 hours. However all samples experienced pH drift to approximately pH 3. It is likely that the large amounts of kaolinite adsorbed the hydroxyl ions from the solution, driving the pH down. Figure 2 shows that the pH range is maintained in control solutions containing perrhenate but no kaolinite. Using a shorter equilibration time of 30 minutes alleviated this problem. Figure 2 also shows that the perrhenate did not precipitate over time or sorb to the vessel walls in the absence of sorbing solid. Since UV-Vis spectrometry was being used to analyze samples, the NaCl concentrations used were 0.1M and 0.01M instead of 1.0M and 0.1M as Goldberg used. 1.0M NaCl solutions led to UV-Vis detection errors.

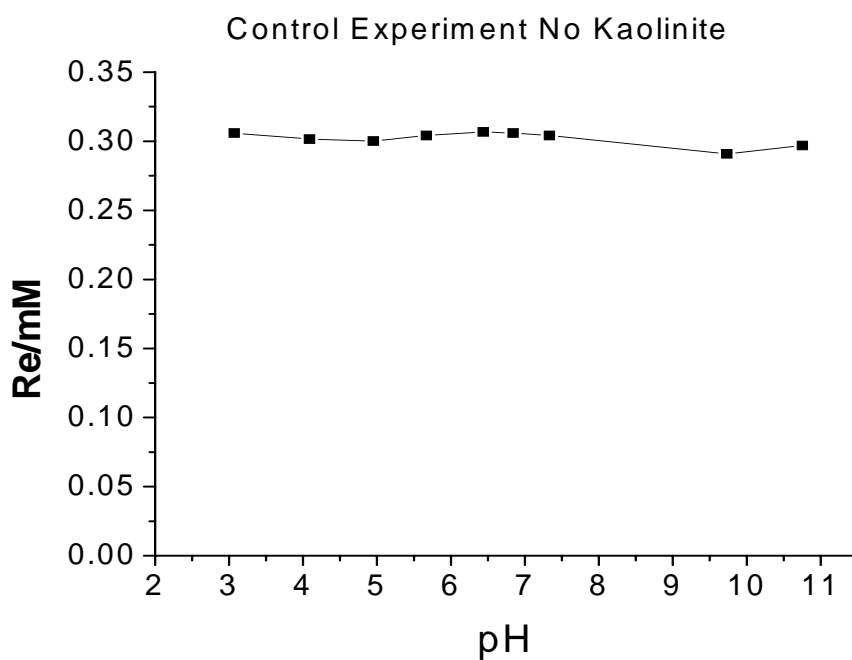


Fig. 2. Graph illustrating that the perrhenate concentration and pH range was maintained after an equilibration time of 20 hours in the absence of kaolinite. $[\text{ReO}_4^-]$ was determined using peak absorbances at 228nm in the UV-Vis spectra of the solutions.

The mass concentration of each solid, (silica, alumina and kaolinite) was different. The mass of solid to be used was determined by first calculating how much solid would be needed to sorb all rhenium atoms present in a certain volume of perrhenate solution. I assumed that one rhenium atom might require as much as 1nm^2 of surface area. The mass used in the experiment was 10 times this calculated mass to ensure that sorption sites were not a limiting factor. The procedure followed for all three solids was identical. Two hundred and fifty milliliters of 0.3mM NaReO_4 and either 0.1M NaCl or 0.01M NaCl , depending on the experiment, was added to an Erlenmeyer flask containing the required mass of solid: 50g of kaolinite, 2.5g of alumina or 2.5g of silica.

The pH was brought up to approximately 11 using NaOH and allowed to equilibrate for 30 minutes with magnetic stirring. The pH was then titrated down to pH 3 using HCl, taking samples at 0.5 pH-unit increments. In order to ensure that any changes in perrhenate concentration were a result of reversible sorption, the pH was then titrated back up to pH 11 using NaOH. At each new pH the mixture was allowed to equilibrate for 30 minutes and an aliquot was obtained. Each aliquot was then centrifuged, filtered with both $0.45\ \mu\text{m}$ (polysulfone membrane, Pall Gelman) and $0.02\ \mu\text{m}$ (aluminum oxide membrane, Whatman) syringe-filters and analyzed via UV-Vis spectroscopy.

Using the UV-Vis absorption maxima of $\lambda=228\text{nm}$, perrhenate concentrations were calculated. These were then graphed vs. pH for both ionic strengths used (0.1M and 0.01M NaCl), Figs. 3 to 5. I found that perrhenate was weakly sorbed to all minerals used, at pH less than 8.5. This means that sorption is a possible means for

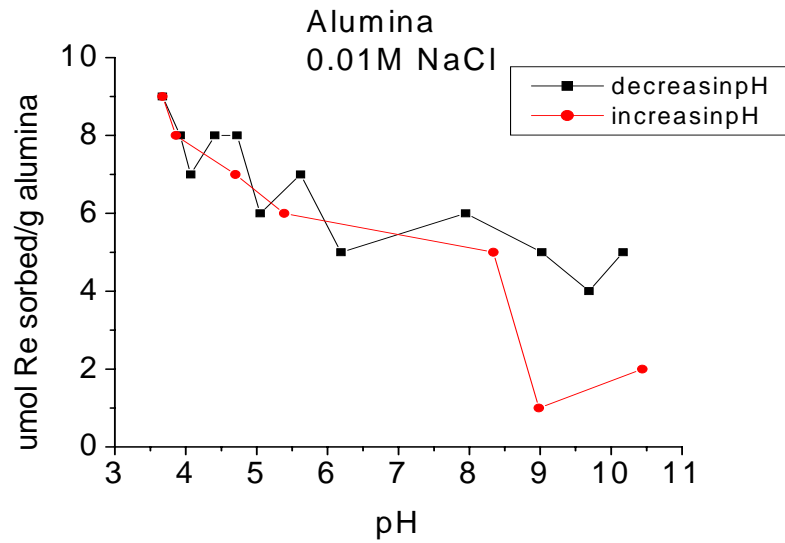
perrhenate fixation at the pH of marine environments, assuming that the pH of seawater is 8.2. The weakness of this sorption explains the low levels of Re in oxic sediments. This supports the hypothesis that sorption of the perrhenate anion is not the only Re removal mechanism responsible for the high degree of enrichment of Re in anoxic sediments.

Rhenium sorption on KGa1b, Fig. 5, is about an order of magnitude weaker than sorption on δ -Al₂O₃, Fig.3, and SiO₂, Fig. 4. The BET surface area of KGa1b (12.5 m²/g) is approximately an order of magnitude smaller than that of δ -Al₂O₃ and SiO₂ (102.9 m²/g and 182 m²/g respectively). Thus, the maximum amounts of Re per unit area (pH 3) are 0.29, 0.15 and 0.03 μ mole/m² for δ -Al₂O₃, SiO₂ and kaolinite respectively.

For all three solids the % of Re sorbed was calculated for pH 8.2 (Figs. 3 to 5). For δ -Al₂O₃ 20% of perrhenate was sorbed at ionic strength 0.01M NaCl and 17% perrhenate was sorbed at ionic strength 0.1M NaCl. For SiO₂ 20% of perrhenate was sorbed at ionic strength 0.01M NaCl and 16% perrhenate was sorbed at ionic strength 0.1M NaCl. For KGa1b 20% of perrhenate was sorbed at ionic strength 0.01M NaCl and 18% perrhenate was sorbed at ionic strength 0.1 M NaCl.

In Figs. 6 and 7, I compared my findings at [ReO₄⁻] = 0.3 mM to Goldberg et al.'s (1996) results for molybdate sorption at [MoO₄²⁻] \approx 0.3 mM. Figure 6 compared sorption on kaolinite while Fig. 7 compared sorption on Aluminum Oxid C. These comparisons illustrate the relative weakness of perrhenate sorption. This may be due to differences in the behavior of the two anions or it may reflect the much shorter equilibration time used in perrhenate sorption experiments.

a)



b)

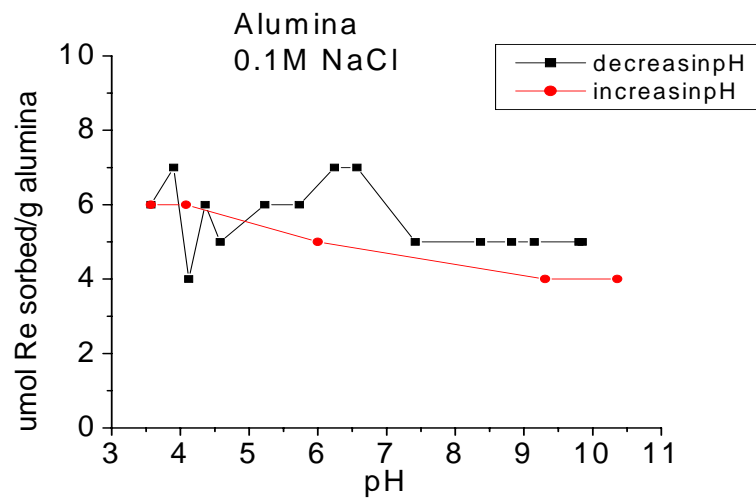


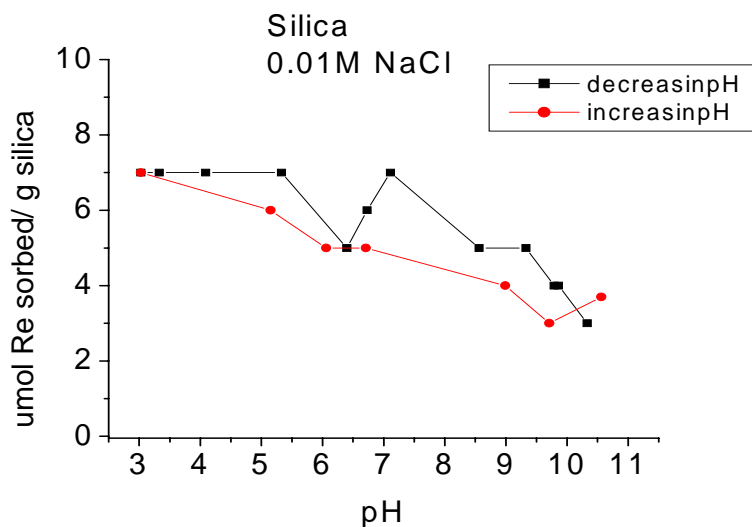
Fig. 3.

Initial $[\text{ReO}_4^-] = 0.3\text{mM}$

a) ReO_4^- sorption on 10 g/L $\delta\text{-Al}_2\text{O}_3$ (BET: 102.9 m^2/g) at ionic strength 0.01M NaCl. Approximately 20% of ReO_4^- was sorbed at pH 8.2.

b) ReO_4^- sorption on 10 g/L $\delta\text{-Al}_2\text{O}_3$ (BET: 102.9 m^2/g) at ionic strength 0.1M NaCl. Approximately 17% of ReO_4^- was sorbed at pH 8.2.

a)



b)

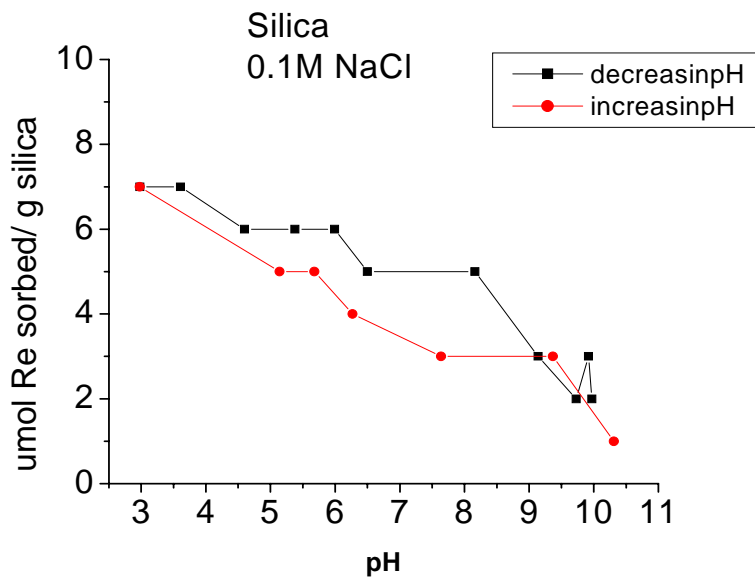


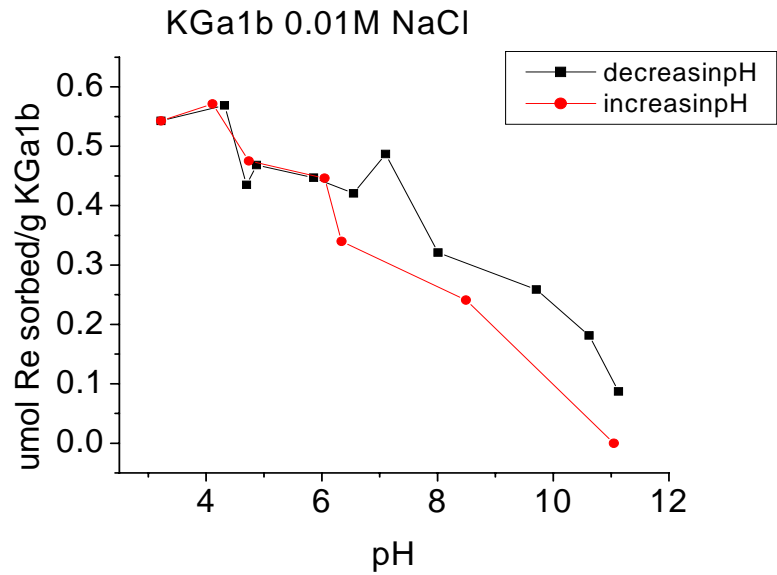
Fig. 4.

Initial $[\text{ReO}_4^-] = 0.3\text{mM}$

a) ReO_4^- sorption on 10 g/L SiO_2 (BET: $182\text{ m}^2/\text{g}$) at ionic strength 0.01M NaCl. Approximately 20% of ReO_4^- was sorbed at pH 8.2.

b) ReO_4^- sorption on 10 g/L SiO_2 (BET: $182\text{ m}^2/\text{g}$) at ionic strength 0.1M NaCl. Approximately 16% of ReO_4^- was sorbed at pH 8.2.

a)



b)

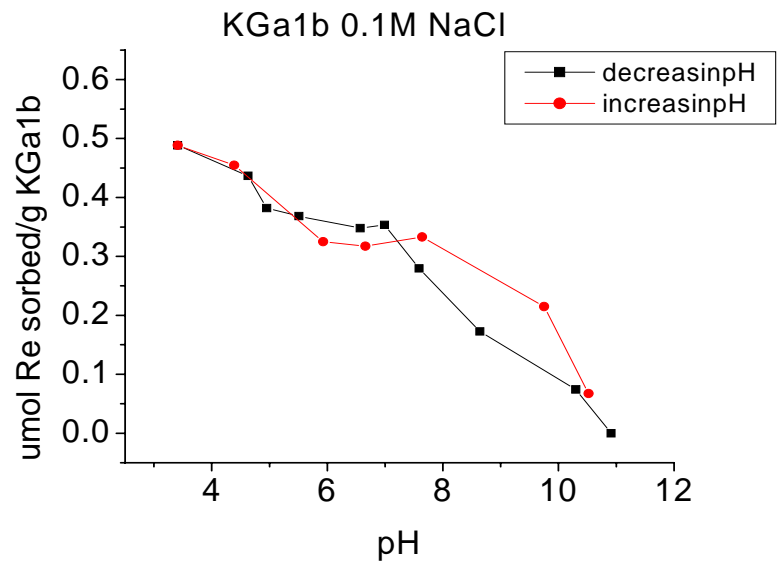


Fig. 5.

Initial $[\text{ReO}_4^-] = 0.3\text{mM}$

a) ReO_4^- sorption on 200 g/L KGa1b (BET:12.5 m^2/g) at ionic strength 0.01M NaCl. Approximately 20% of ReO_4^- was sorbed at pH 8.2.

b) ReO_4^- sorption on 200 g/L KGa1b (BET:12.5 m^2/g) at ionic strength 0.1M NaCl. Approximately 18 % of ReO_4^- was sorbed at pH 8.2.

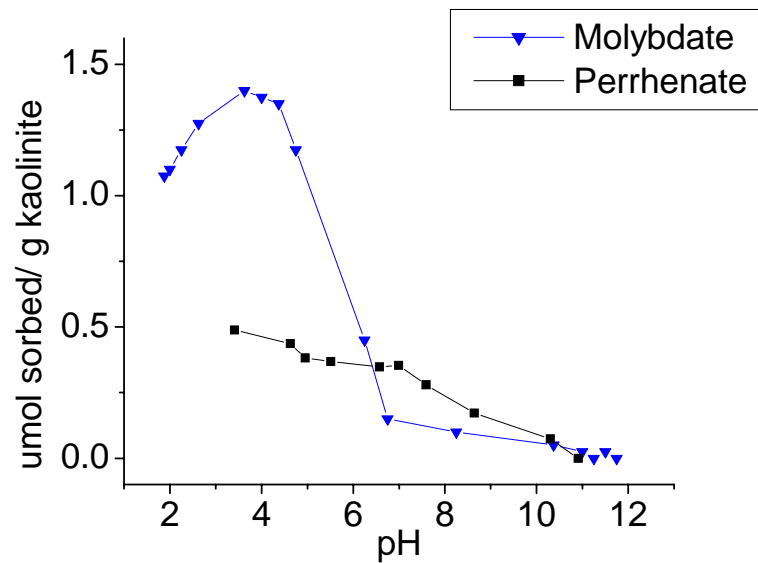


Fig. 6. MoO_4^{2-} sorption on 200 g/L KGa1 (BET:9.14m²/g) at ionic strength 0.1M NaCl (Goldberg et al., 1996). Initial $[\text{MoO}_4^{2-}] = 0.292$ mM. ReO_4^- sorption on 200 g/L KGa1b (BET:12.5m²/g) at ionic strength: 0.1M NaCl. Initial $[\text{ReO}_4^-] = 0.3$ mM.

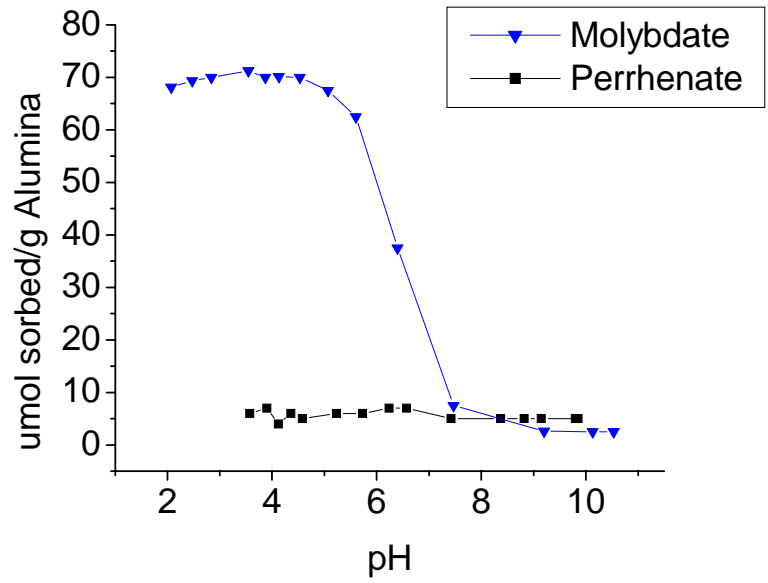


Fig.7. MoO_4^{2-} sorption on 4.0 g/L $\delta\text{-Al}_2\text{O}_3$ (BET:102.9 m^2/g) at ionic strength 0.1M NaCl (Goldberg et al., 1996). Initial $[\text{MoO}_4^{2-}] = 0.292$ mM.
 ReO_4^- sorption on 10 g/L $\delta\text{-Al}_2\text{O}_3$ (BET:102.9 m^2/g) at ionic strength: 0.1M NaCl. Initial $[\text{ReO}_4^-] = 0.3$ mM.

3.2 Investigation of Perrhenate ($1 \mu\text{M}$ - $.01 \mu\text{M}$) Sorption to kaolinite

The above experiments are useful insofar as they illustrate the potential of these minerals to sorb perrhenate ions. However, it has been observed that rhenium is enriched in reducing sediments (Colodner et al., 1993, Calvert and Pedersen, 1993, Crusius et al, 1996, Morford and Emerson, 1996). Thus, the next step was to use a reducing agent in the presence of a clay mineral to investigate rhenium enrichment under simulated anoxic conditions. Also, 0.3mM is approximately 7 orders of magnitude larger than seawater concentrations of perrhenate, which are on the order of 10^{-11} M (Koide et al., 1987, Anbar et al., 1992 and Colodner et al., 1993 and 1995). Thus I also wanted to use the low detection limit of ICP-MS analysis to investigate perrhenate sorption on these minerals at concentrations less enriched in Re relative to seawater concentrations. By using a range of perrhenate concentrations I expected to obtain sorption isotherms of perrhenate for each mineral surface.

For reduction experiments involving both sulfide and borohydride, the centrifuge tubes were treated identically. The exact contents of the tubes used in these experiments are described in Tables A1 and A2 in the Appendix. The centrifuge tubes were filled inside a N_2 filled glovebox. They were then allowed to equilibrate on a rocker, inside the N_2 filled glovebox for approximately 24 hours. The tubes were then passed out of the glovebox centrifuged for 15 minutes and filtered using $0.02 \mu\text{m}$ (Whatman) syringe filters. Samples were stored in a refrigerator for no more than one week prior to analysis. All samples were made to be 2% v/v HNO_3

prior to ICP-MS analysis and samples expected to contain higher concentrations of Re were diluted by a factor of 10.

A note on ICP-MS measurements:

In Experimental Methods section 2.2.3 I discuss two correction methods used to compensate for ICP-MS analytical drift over the course of one run. In the experiments outlined in this section (Results, 3.2), I bracketed each sample with a standard and generated numerous calibration curves. This method was not ideal however, because the matrices of the samples and standards were very different. The standards contained a Rhenium standard in 2% HNO₃, while the samples contained reducing agent, borate buffer and sodium perrhenate in 2% HNO₃.

In later experiments I used an internal standard of tungsten to monitor changes in sensitivity. This was a better correction method because it accounted for the matrix of the sample. I would advise future workers to use a combination of these two methods. The disadvantage is the long run time this would require, however, I think that this is the only way to account for possible changes in instrument sensitivity which can be as drastic as 50% over a 3 hour period.

There are two sources of analytical error in all ICP-MS measurements presented. The first is due to personal errors. Some sources of these errors were reading the level of liquid in a volumetric flask or pipet as well dispensing volumes from 100 μ L and 1000 μ L pipettes. I used my estimates of significant figures to quantify the degree of uncertainty present due to these errors. In all of my volume measurements the number of significant figures used was 3, where the first 2 figures

were certain and the last digit was uncertain. So for example a 1.00 mL sample delivered to a centrifuge tube was reported as 1.00 ± 0.05 mL.

The second type of error was instrumental error reported by the instrument as a relative standard deviation for each sample analyzed. This was on average $\pm 10\%$ (or $1/10$) of the reported value. For results presented in Figs. 9 a) and 10 a) the samples were diluted by adding 1.00 ± 0.05 mL sample to 9.00 ± 0.05 mL nitric acid. The total relative standard deviation in the undiluted concentration is given by:

$$\sigma_{[Re]}/[Re] = [(0.05/1)^2 + (0.05/9)^2]^{1/2} + 1/10 = 0.15$$

Thus, for a sample with undiluted concentration of $1.103 \mu\text{M}$ the uncertainty is 0.15 of $1.103 \mu\text{M}$. The final concentration including uncertainty is $1.1 \pm 0.2 \mu\text{M}$. Similar calculations were performed for data presented in Figs. 9. b) and c) and Figs. 10. b) and c). The samples were diluted by adding 3.00 ± 0.05 mL sample to 2.00 ± 0.05 mL nitric acid.

$$\sigma_{[Re]}/[Re] = [(5/3000)^2 + (5/2000)^2]^{1/2} + 1/10 = 0.13$$

3.2.1. Sorption to kaolinite in the presence of 10 mM Borohydride

The experiment was performed using borohydride (BH_4^-) as the reducing agent. Borohydride has been used by other workers to reduce the perrhenate anion (Broadbent and Johnson, 1962, and Pacer, 1973). Broadbent and Johnson (1973) added sodium borohydride to cold aqueous solution of ammonium perrhenate and acetic acid. The authors found that the addition of acid was necessary for the reduction perrhenate by borohydride to occur at a reasonable rate (Broadbent and Johnson, 1973).

I performed an experiment to evaluate the reaction between perrhenate and borohydride in the absence of acid. I equilibrated 10mL of 100 mM LiBH_4 and 0.2mM NaReO_4 inside an N_2 -filled glovebox. UV-Vis spectrometry was used to determine ReO_4^- concentration at 24 hour intervals. The spectra are presented in Fig. 8. Perrhenate concentration drops by approximately 0.01mM every 24 hours. This means that the reduction of the perrhenate ion is occurring very slowly under these experimental conditions. I have assumed that the reduced rhenium species do not absorb around 228nm, where perrhenate has an absorbance maximum.

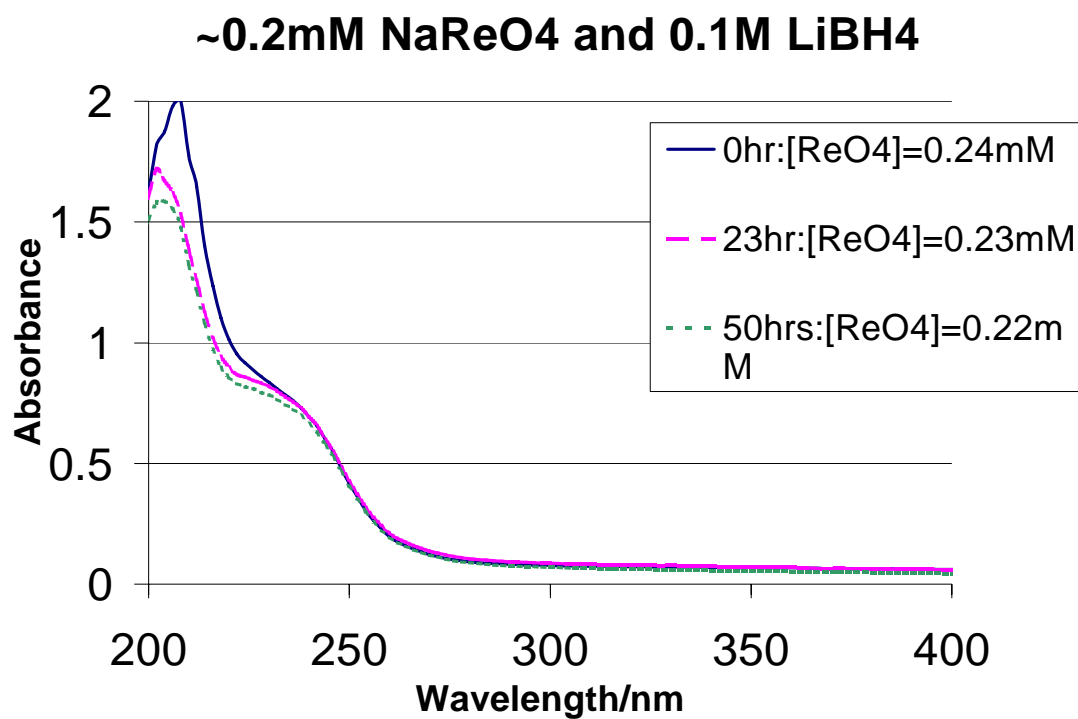
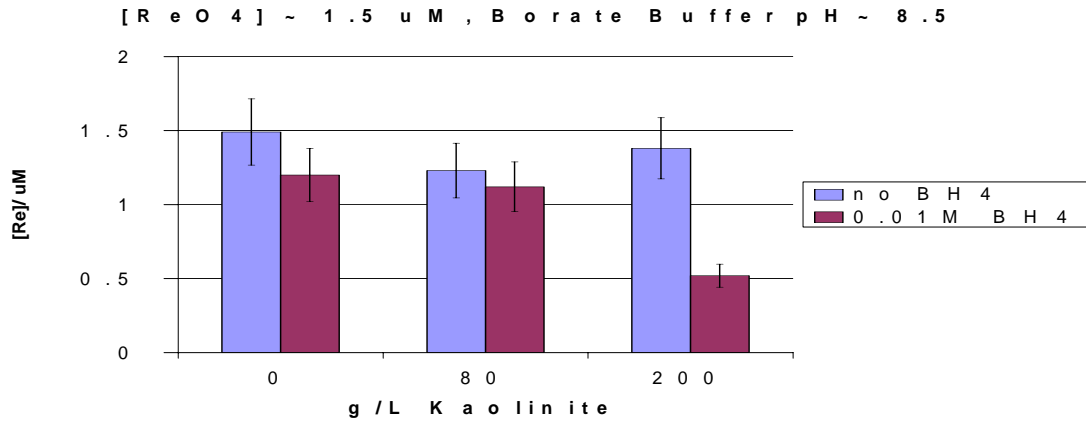


Fig. 8. UV-Vis spectra of ~0.2mM NaReO₄ and 0.1M LiBH₄ equilibrated in an N₂-filled glovebox. Cell pathlength 1cm.

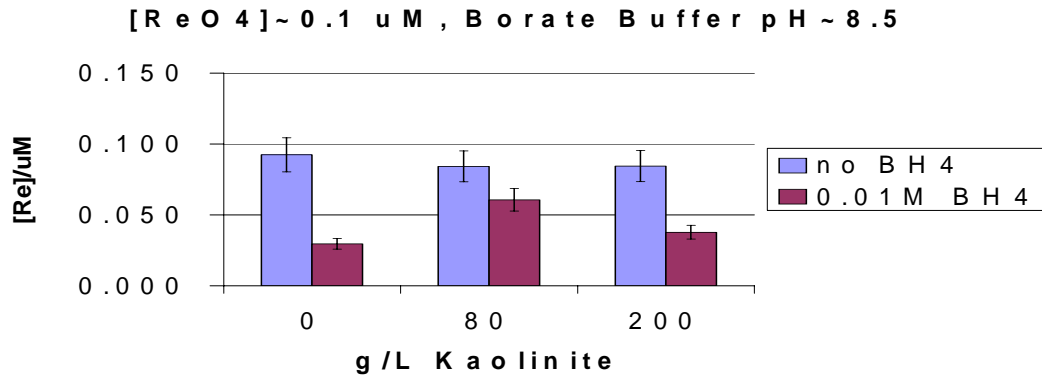
The results from this experiment are compiled in the bar graphs in Fig. 9. These experiments yielded results that supported my initial hypothesis: perrhenate sorption on mineral surfaces is promoted by reducing agents. In all cases the sample containing borohydride experienced more Re loss than the samples with no borohydride. All Re concentrations were dilution corrected before the graphs were compiled.

In Fig. 9 a) the control sample, which contains no borohydride and no kaolinite, contains the highest Re concentration. The sample with the most kaolinite in the presence of reducing agent contains the lowest Re concentration. This supports the proposed hypothesis. In Fig. 9 b) the control sample contains the highest Re concentration. In Fig. 9 c) the samples containing kaolinite in the presence of borohydride, show significant loss of rhenium.

a)



b)



c)

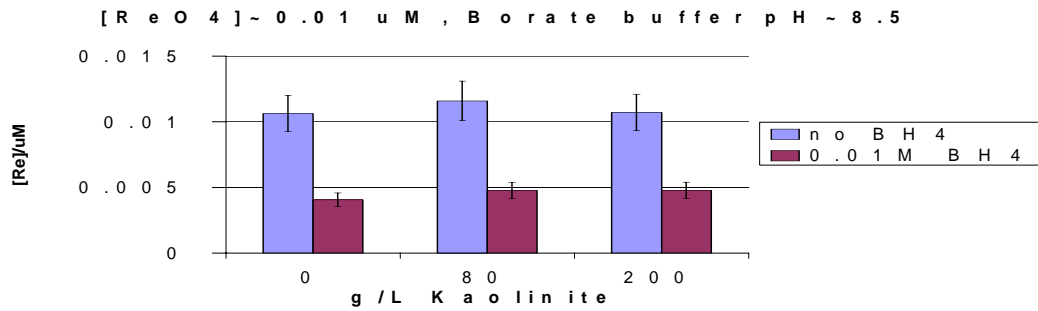


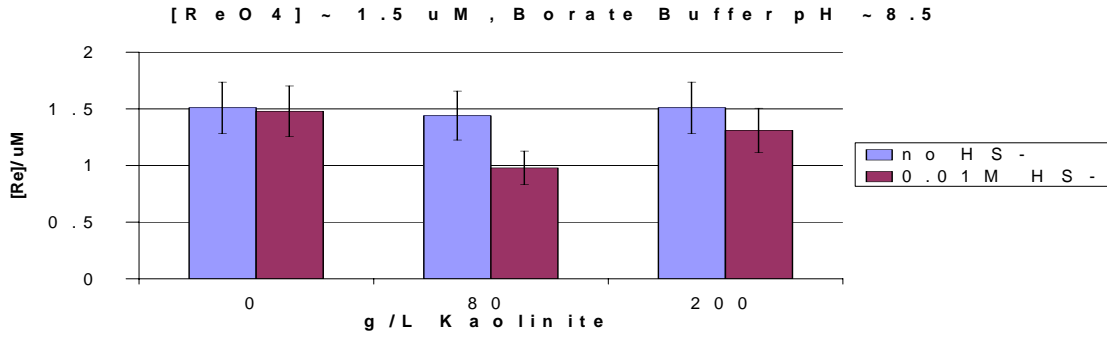
Fig. 9. Bar graphs showing Re sorption on kaolinite in the presence of borohydride. The title of each graph contains the approximate magnitude of the concentration used in each experiment. Centrifuge tube contents were equilibrated for 24 hours

3.2.2. Sorption to kaolinite in the presence of 10 mM Hydrogen Sulfide

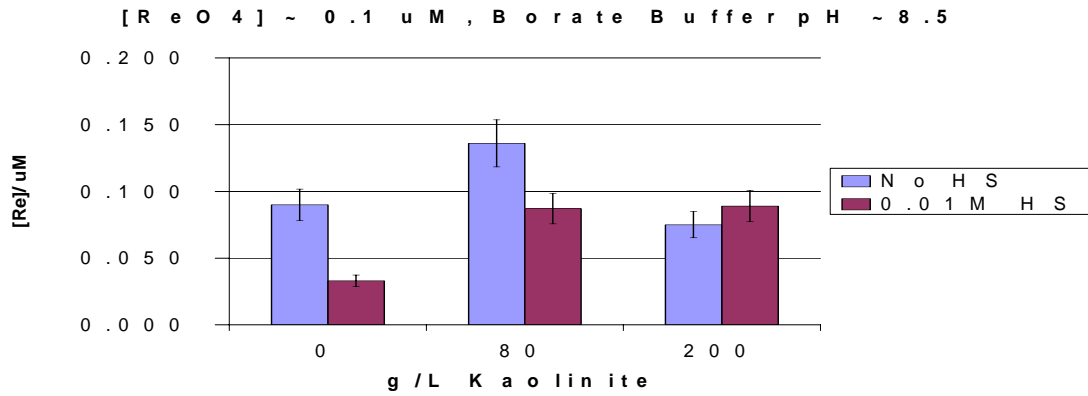
The above experiment was repeated using a reducing agent that would be found in nature, sulfide (HS^-). The results from this experiment are compiled in the bar graphs in Fig. 10. These results showed that in the majority of cases, the sample containing sulfide experienced more Re loss than the samples with no sulfide. I expected that the samples with the highest concentration of kaolinite in the presence of sulfide would show the most depletion in rhenium concentration. Figure 10 a) illustrates that the tube with less kaolinite in the presence of sulfide shows the most depletion. In Fig. 10 b) the sample with no kaolinite, shows the greatest depletion. One explanation of these results is analytical drift. Another possible explanation of these results is that kaolinite releases a small amount of rhenium into the system.

In later results, I show that the reaction between sulfide and perrhenate proceeds over months. The experiment outlined above had an equilibration time of 24 hours, and so does not show the complete effect of sulfide on perrhenate sorption.

a)



b)



c)

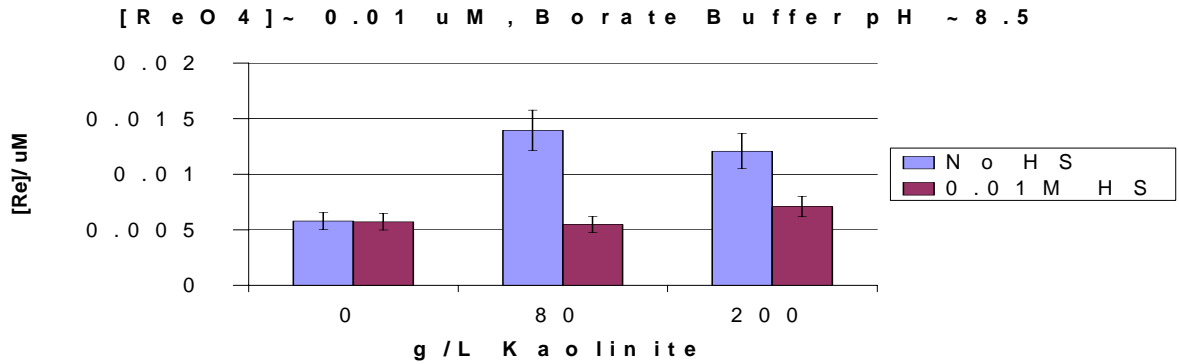


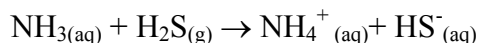
Fig. 10. Bar graphs showing Re sorption on kaolinite in the presence of sulfide. The title of each graph contains the approximate magnitude of the concentration used in each experiment. Centrifuge tube contents were equilibrated for 24 hours

3.3 Investigation of Thioperrhenate Formation

3.3.1 Reaction between perrhenate and sulfide over 10.5 hours

This experiment was performed in order to determine the products formed when perrhenate was bubbled with H₂S gas without kaolinite present. Fifty milliliters of 0.002M NaReO₄ and 0.05M NH₃-H₂O was prepared and placed in a three-neck round-bottom flask. An aliquot was taken and a 1:10 dilution made. The solution was deoxygenated by bubbling with N₂ gas for 15 min. Hydrogen sulfide was then bubbled through the solution for a total of 10.5 hours. Aliquots were taken at 90-minute intervals and 1:10 dilutions made. UV-Vis spectra of all samples and dilutions were taken.

I did not measure the pH of these samples, however the probable pH of the samples can be estimated as follows. The reaction between ammonia and sulfide in the reaction vessel is:



This reaction is expected to go to completion, and since initial [NH₃]=0.05M, final [HS⁻]=0.05 M. At saturation with P_{H₂S}=1 atm, [H₂S]_(aq)=0.1M. Using the K_a of hydrogen sulfide, the probable pH can be calculated from the following equation:

$$K_a = 10^{-7.01} = [\text{H}^+][\text{HS}^-]/[\text{H}_2\text{S}] = [\text{H}^+](0.05\text{M})/(0.1\text{M})$$

The pH calculated is 6.7. This value is comparable to measured pH values in experiments described in Section 3.4 where kaolinite was added to the reaction vessel.

Figures 11-14 are a few representative UV-Vis spectra. In Fig. 11, the spectrum of the 1:10 dilution can be used to measure the concentration of perrhenate in the solution. The perrhenate anion absorbs at 206nm, $\epsilon_{206\text{nm}} = 5731 \text{ Lmol}^{-1}\text{cm}^{-1}$, and 228nm, $\epsilon_{228\text{nm}} = 3613 \text{ Lmol}^{-1}\text{cm}^{-1}$, (Fig. 1.). The absorbance at 228nm is 0.8 and the undiluted concentration can be calculated using the equation $A = \epsilon bc$, where b is a pathlength of 1cm. This concentration is approximately 0.002 M perrhenate. The same calculation can be performed for the absorbance at 206nm.

.05M NH₃, 0.002M NaReO₄, No H₂S

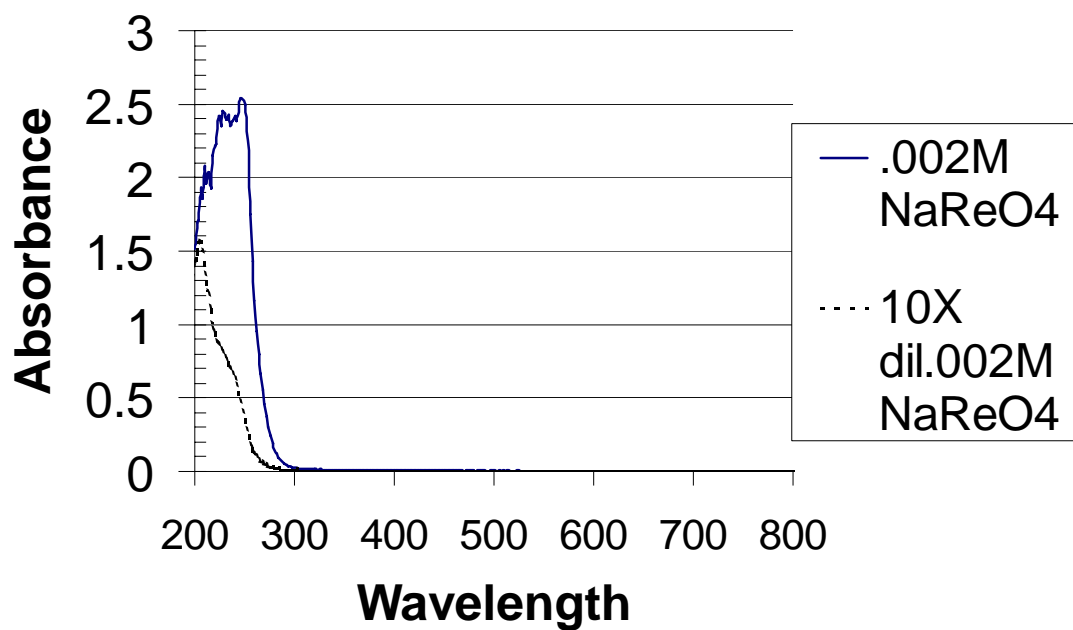


Fig. 11. UV-Vis spectrum of 0.002M NaReO₄ and 0.05M NH₃-H₂O. Cell pathlength: 1 cm. There are no peaks at any of the wavelengths that indicate the presence of thioperrhenates. In the next three figures, peaks at 300nm, 350nm and 505nm become apparent.

In Figs. 12-14, the large absorbances below 275nm are due to a mixture of ReO_4^- , HS^- and H_2S . Absorption at $\lambda = 300 \text{ nm}$ and $\lambda = 350 \text{ nm}$ indicates the presence of ReO_3S^- a yellow compound, and absorption at $\lambda = 505 \text{ nm}$ corresponds to ReS_4^- a red-violet compound (Muller et al., 1967, Wilkinson et. al, 1987). The final mixture was a pale reddish-brown. A qualitative assessment of the UV-Vis spectra obtained, Figs. 12-14, indicates that thiolation of the perrhenate anion did in fact occur. Since both ReO_2S_2^- and ReOS_3^- absorb at around $\lambda = 400 \text{ nm}$, it may be deduced that these two thioperrhenates are not present in large concentrations. However, successive replacement of oxygen atoms by sulfur atoms may still be the way in which thiolation proceeds since ReO_2S_2^- and ReOS_3^- may not be stable under experimental conditions.

Absorbances at wavelengths that indicate the presence of thioperrhenates were extracted from the UV-Vis spectra. These absorbances were then used to determine $[\text{ReS}_4^-]$: $\epsilon_{505\text{nm}} = 9521 \text{ Lmol}^{-1}\text{cm}^{-1}$ and $[\text{ReO}_3\text{S}^-]$: $\epsilon_{350\text{nm}} = 525 \text{ Lmol}^{-1}\text{cm}^{-1}$. These extinction coefficients were obtained from Muller et al. (1967, 1970 and 1981), who used $(\text{C}_6\text{H}_5)_4\text{AsReS}_4$, $(\text{C}_6\text{H}_5)_4\text{PReS}_4$, $(\text{CH}_3)_4\text{NReS}_4$, TlReO_3S and RbReO_3S . The vibrational and electronic spectra of these compounds were measured and used to establish the wavelengths where these species absorbed; the extinction coefficients at each wavelength was also determined (Muller et al., 1967). The calculated concentrations were plotted vs. time in contact with H_2S at $P_{(\text{H}_2\text{S})} = 1\text{atm}$, Fig.15. Perrhenate (ReO_4^-) concentrations were determined by difference:

$$[\text{ReO}_4^-] = \text{Initial } [\text{ReO}_4^-]_{(\text{from Fig. 11})} - [\text{ReS}_4^-] - [\text{ReO}_3\text{S}^-]$$

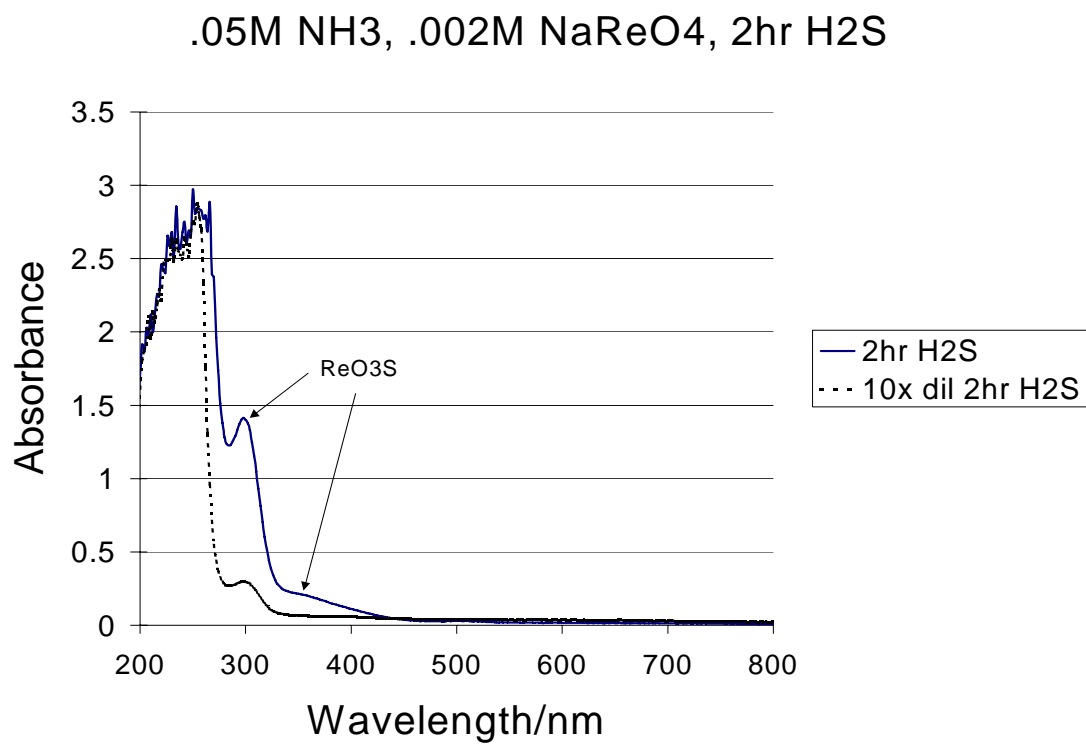


Fig. 12. UV-Vis spectrum of 0.002M NaReO₄ and 0.05M NH₃-H₂O bubbled with H₂S for 2 hours. Cell pathlength: 1cm.

.05M NH₃ .002M NaReO₄ 5 1/2 hr H₂S

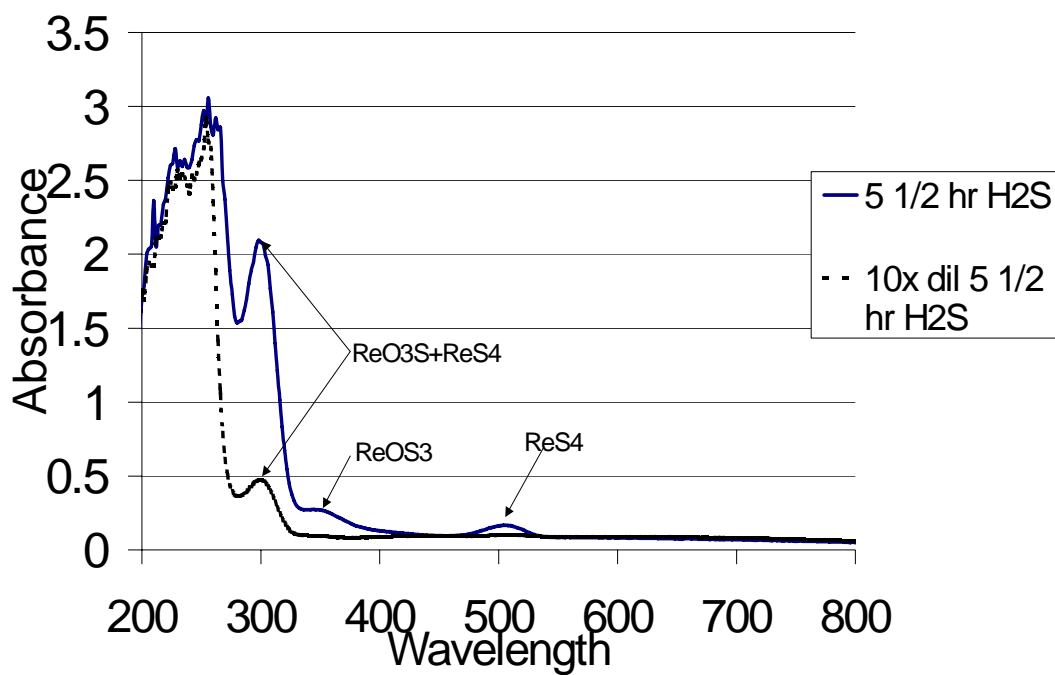


Fig. 13. UV-Vis spectrum of 0.002M NaReO₄ and 0.05M NH₃-H₂O bubbled with H₂S for 5.5 hours. Cell pathlength: 1cm.

.05M NH₃ .002M NaReO₄ 10 1/2 hr H₂S

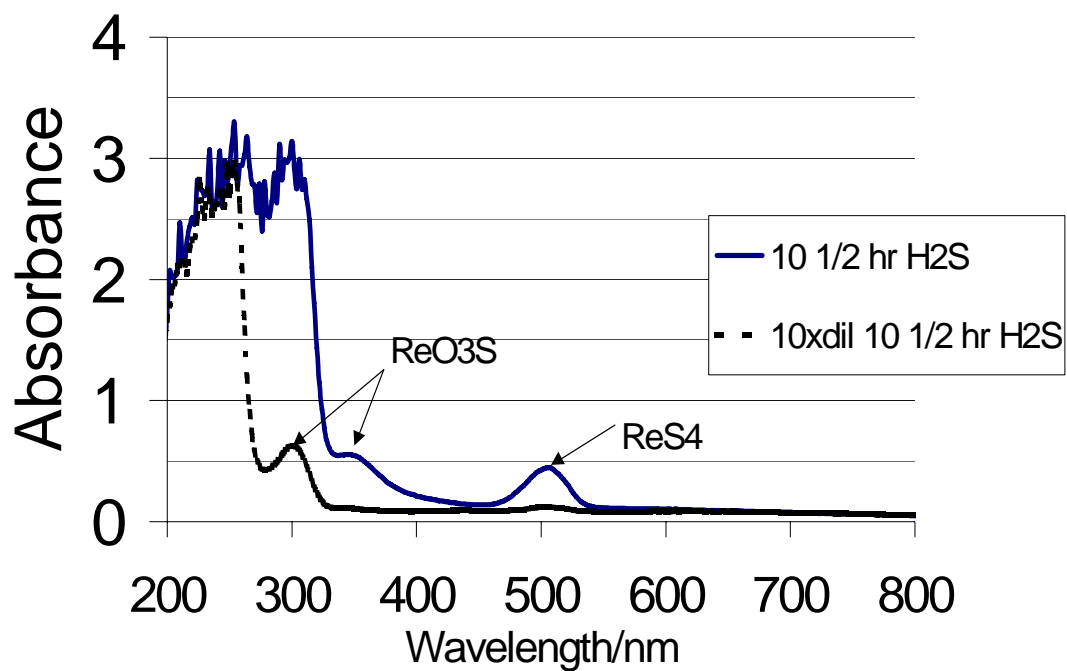


Fig. 14. UV-Vis spectrum of 0.002M NaReO₄ and 0.05M NH₃-H₂O bubbled with H₂S for 10.5 hours. Cell pathlength: 1cm

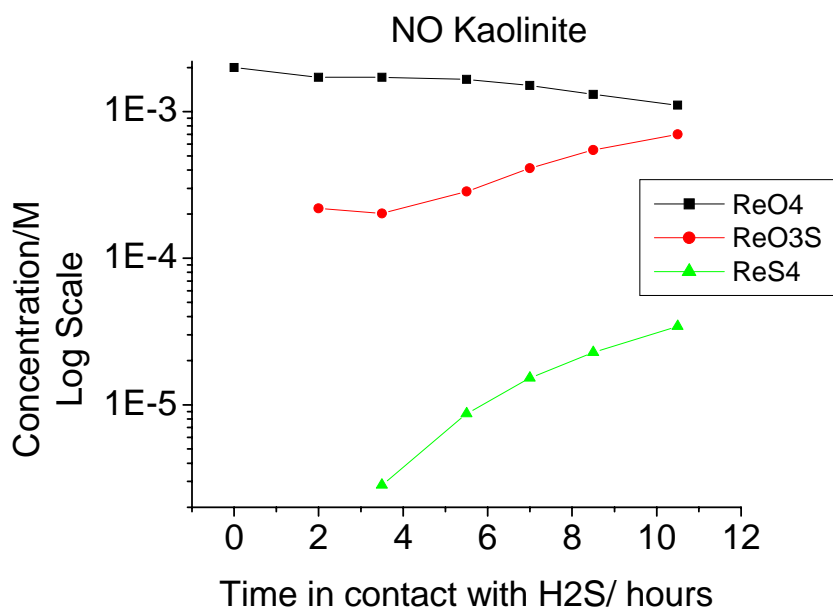


Fig. 15. Change in concentration of perrhenate and thioperrhenate species vs. time in contact with H₂S at P_(H₂S) = 1atm. Concentration is on a log-scale.

This experiment indicates that thiolation occurs but is not complete. All of the oxygen atoms in ReO_4^- have not been replaced by sulfur atoms. Thus the final product is a mixture of ReO_4^- , ReO_3S^- and ReS_4^- and not solely ReS_4^- as was expected. The next step was to investigate the reaction between perrhenate and sulfide over long time periods. This was achieved by sealing perrhenate and sulfide mixtures in ampoules.

Each ampoule contained 1 mM perrhenate and 95 mM buffer. The sulfide concentration ranged from 1 mM to 10 mM. The ampoules were then allowed to equilibrate for weeks. After, approximately 3 weeks, 4 ampoules were placed in a drying oven at 75 °C. These ampoules represented each of the four pHs used in these experiments and contained 10 mM NaHS.

The colors observed in these ampoules were very intense and I felt that this might make UV-Vis analysis difficult. To alleviate this potential problem, more ampoules were prepared that contained 10 μL NaReO_4 , 95 mM buffer, and either 1mM or 10mM NaHS. All of these ampoules were placed in a drying oven at 75 °C.

3.3.2 Ampoules containing 1mM perrhenate equilibrated at 25 °C

The first group of ampoules analyzed were the ones equilibrated at room temperature, 25 °C. Visual observations of color changes and Tyndall beam experiments are compiled in Table A3 in the Appendix. The total sulfide and pH were measured and UV-Vis spectra obtained. These results, using a cell of pathlength 0.1cm, are summarized in Fig. 16. I expected the most thiolation to occur in those ampoules containing the highest concentration of sulfide, and this did in fact

occur. I measured the extent of thiolation by comparing the absorbance at wavelengths attributed to thioperrhenates: ReO_3S^- : 350 nm and ReS_4^- : 505 nm (Wilkinson et al., 1987). Table 5 provides the concentrations calculated using extinction coefficients from Muller et al., (1967).

Table 5. Thioperrhenate concentrations of mixtures presented in Fig. 15. I did not measure [Total Re] so I cannot calculate $[\text{ReO}_4^-]$, as I did in previous experiments.

Buffer Type/95mM	pH	[HS]/mM	[ReO3S]/uM	[ReS4]/uM
H2PO4:HPO4/3:1	6.49	4.7		66.2
H2PO4:HPO4/3:1	6.43	0.92	457	38.8
H2PO4:HPO4/3:1	6.36	0.13	152	
H2PO4:HPO4/1:3	7.47	6.3		99.8
H2PO4:HPO4/1:3	7.33	1.8	166	10.4
H2PO4:HPO4/1:3	7.31	0.63	87.6	
NH4:NH3/ 1:3	10.19	9.6		0.473
NH4:NH3/ 1:3	10.20	2.7		
NH4:NH3/ 1:3	10.19	0.96		

The most thiolation occurred in the ampoules buffered at the lowest pH: 6.4. This suggests that thioperrhenate formation is general acid-catalyzed, as has been demonstrated for the analogous molybdenum system (Erickson and Helz, 2000). The UV-Vis spectrum of the ampoule at pH 6.4 containing the highest concentration of sulfide (4.7mM) has an elevated baseline (Fig. 16). This suggests the presence of colloidal particles in the mixture. After filtration with a 0.02 μm syringe filter (Whatman), the spectrum of the mixture was unaltered. The chemical make-up of this colloid is needed to determine the reaction pathway of thioperrhenate formation. A simple extraction experiment with 1-octanol indicated that this colloid is not hydrophobic, since it remained in aqueous solution.

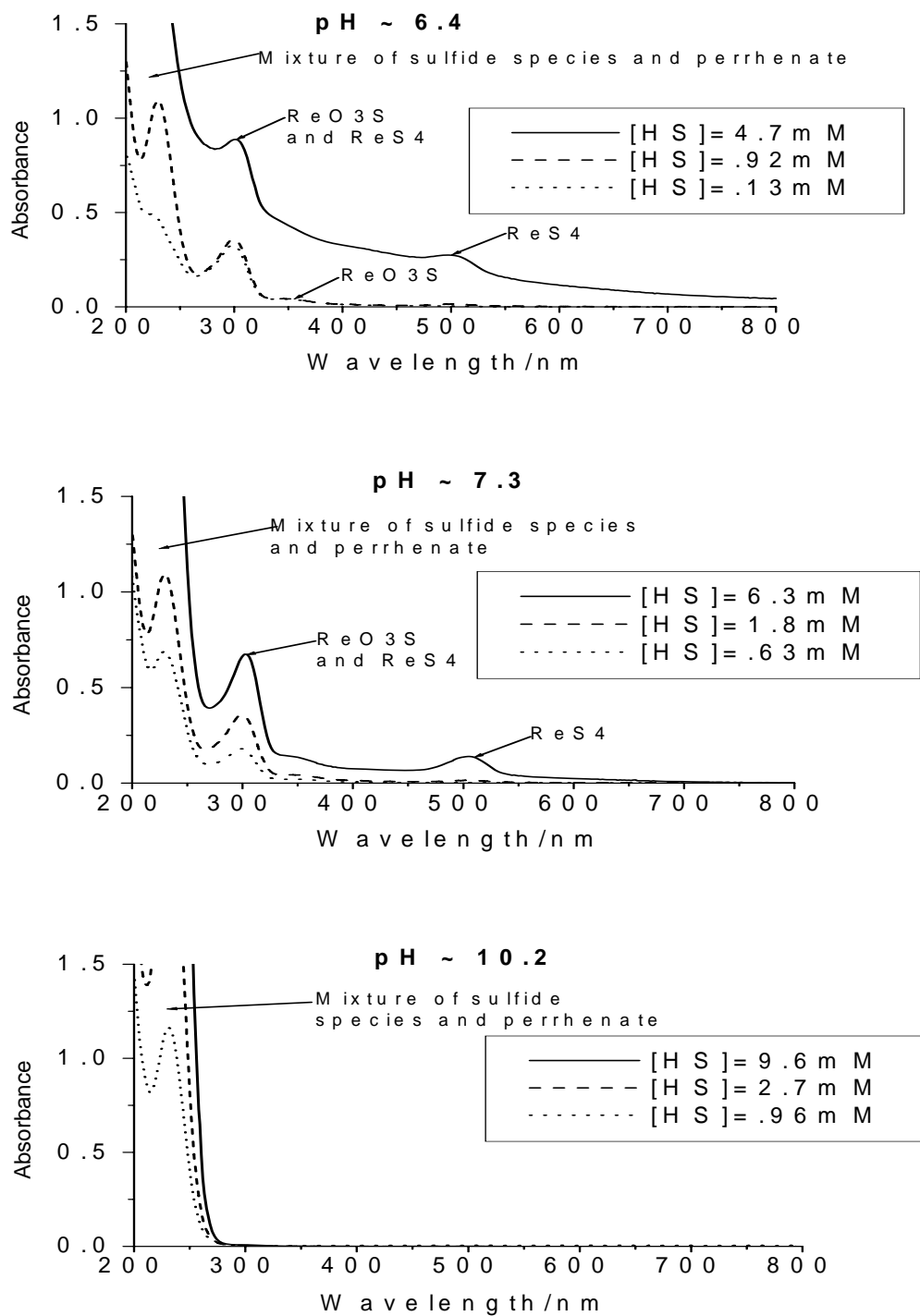


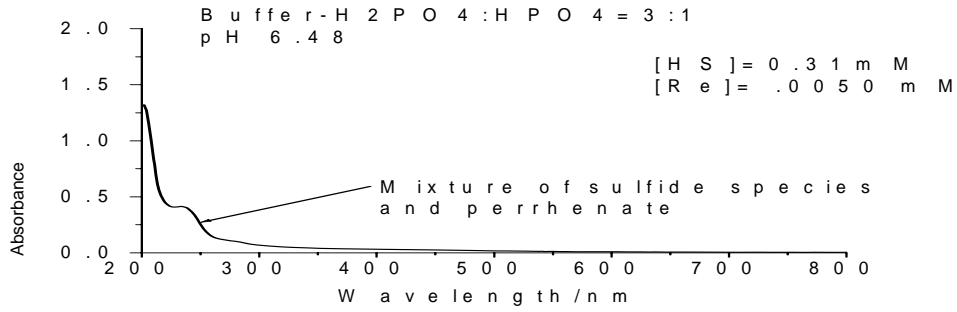
Fig. 16. UV-Vis Spectra of sulfide and 1mM perrhenate mixtures equilibrated for 8 weeks at 25 °C. Path length = 0.1 cm.
 pH 6.4 buffer contains 71.25mM H₂PO₄⁻/ 23.75mM HPO₄⁻²
 pH 7.3 buffer contains 23.75mM H₂PO₄⁻/ 71.25mM HPO₄⁻²
 pH 10.2 buffer contains 23.75mM NH₄⁺/ 71.25mM NH₃

3.3.3 Ampoules containing 1mM perrhenate equilibrated at 75 °C

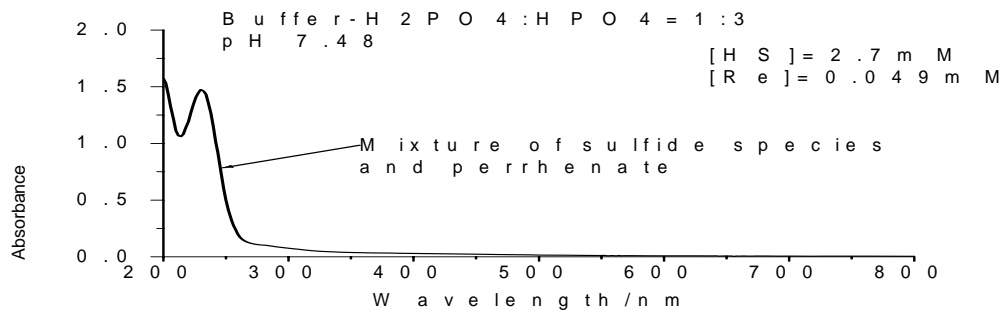
The second group of ampoules analyzed were the ones equilibrated at 75 °C in a drying oven. Observations of color changes and Tyndall beam experiments are compiled in Table A3 in the Appendix. The samples at pH 6.48, 7.48 and 9.21 were all a dark brown opaque color and contained a black precipitate. The sample at pH 10.19 was pink and contained a smaller amount of the black precipitate. All four samples were filtered using 0.45 μm (Pall) and 0.02 μm (Whatman) syringe filters. The dark brown mixtures yielded pale brown filtrates and black residues, while the pink mixture yielded a pink filtrate and black residue.

The total sulfide and pH were measured and UV-Vis spectra obtained for the filtrates. Additionally the total Re concentration was measured via ICP-MS. These results are summarized in Fig. 17. The rhenium concentration of the filtrates increases with increasing pH, Fig. 17 and this indicates that rhenium is present in the precipitates formed in the samples. The residues obtained after filtration were qualitatively analyzed using an Electron Probe Microanalyzer. All four residues contained rhenium and sulfur, indicating that the residues were rhenium sulfides. None of the residues contained enough oxygen to suggest that they were oxides. Figure 18 is a representative spectrum obtained. A semi-quantitative Re:S ratio was obtained from this method and indicates that there are approximately 3 rhenium atoms for every 7 sulfur atoms in the solid.

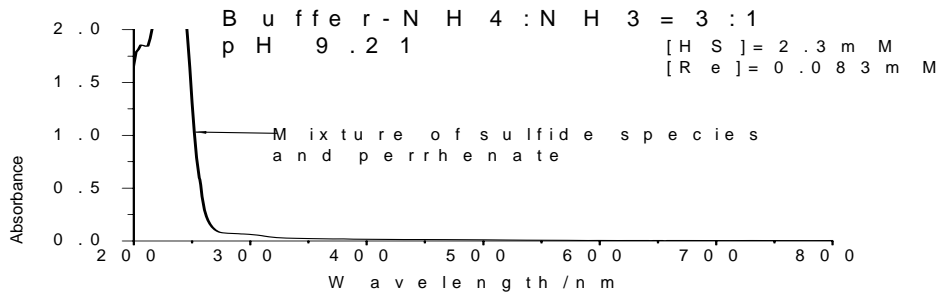
a)



b)



c)



d)

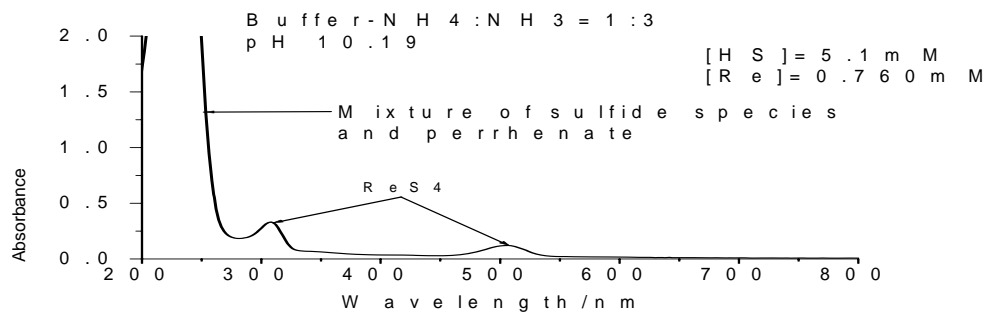


Fig. 17. UV-Vis Spectra of sulfide, 1mM perrhenate and 95mM buffer equilibrated at 25 °C for 3 weeks then 75 °C for 5 weeks. Filtered with 0.45 μm and 0.02 μm syringe filters. Cell path length 0.1cm.

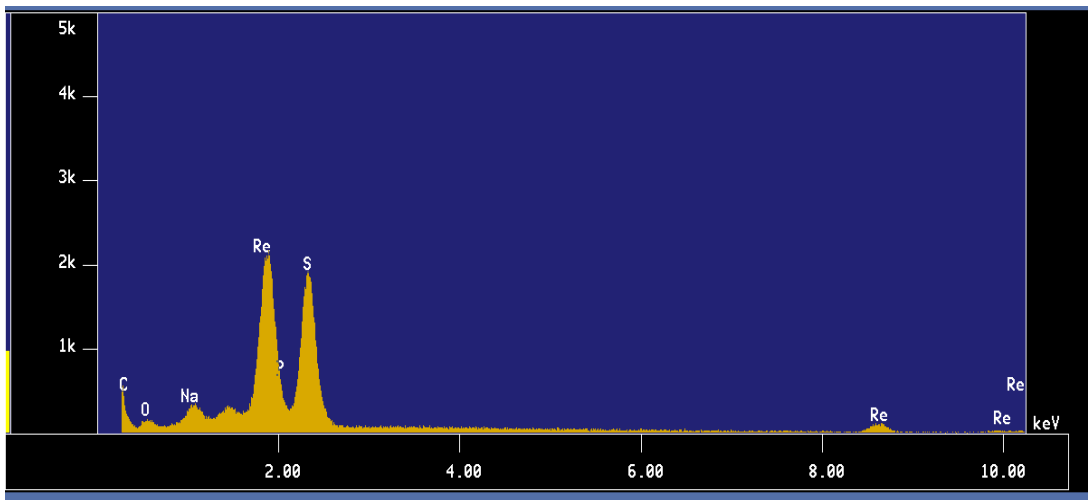


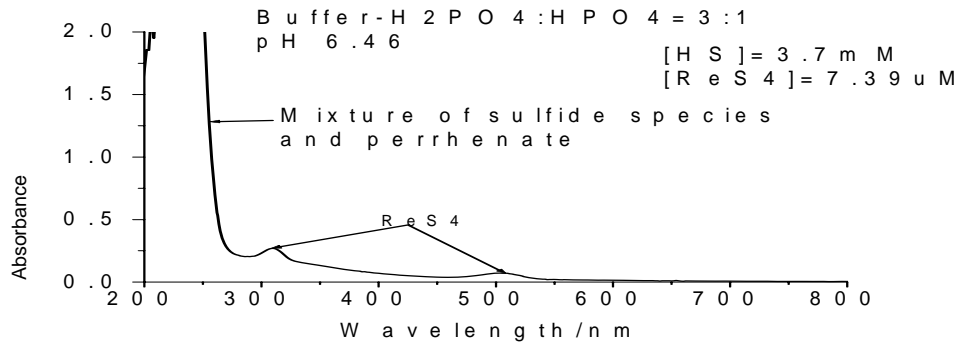
Fig. 18. Representative spectrum illustrating the elements present in the precipitates, predominantly rhenium and sulfur. The sodium, oxygen and carbon are components of the filter paper and residual filtrate. This information was gathered from the energy dispersive X-ray Spectrometer (XDS), a component of the Electron Probe Microanalyzer (EPMA).

3.3.4 Ampoules containing 10 μM perrhenate equilibrated at 75 $^{\circ}\text{C}$

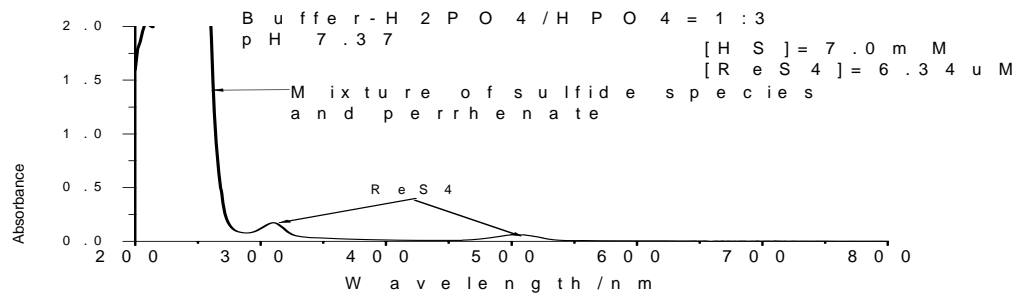
The final group of ampoules analyzed were the ones containing 10 μM perrhenate, equilibrated at 75 $^{\circ}\text{C}$ in a drying oven. These ampoules were prepared because the ampoules at 1mM perrhenate concentration had such an intense brown color after equilibration, I thought they would need to be diluted for UV-Vis analysis. Since I was trying to evaluate the equilibrium reaction occurring between perrhenate and sulfide I did not want to add water to the system before analysis and inadvertently disrupt any possible chemical equilibrium. I later found that this intense brown color was due to a black solid that I was able to remove from solution by filtration (Section 3.3.3).

After an equilibration time of 33 days the total sulfide and pH were measured and UV-Vis spectra obtained. Visual observations were recorded in Table A4, found in the Appendix. These results, using a cell of pathlength 1 cm, are summarized in Fig. 19. Based on my results in Section 3.3.2, I expected the most thiolation to occur in those ampoules at the lowest pH, and this did in fact occur. This supports the hypothesis that thioperrhenate formation is general acid-catalyzed. I measured the extent of thiolation by comparing the absorbance at wavelengths attributed to thioperrhenates.

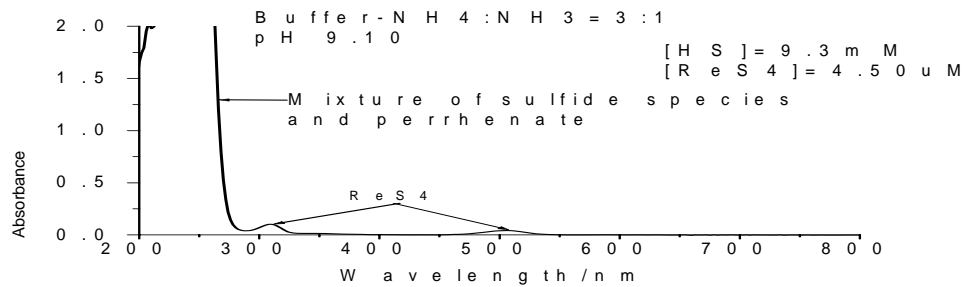
a)



b)



c)



d)

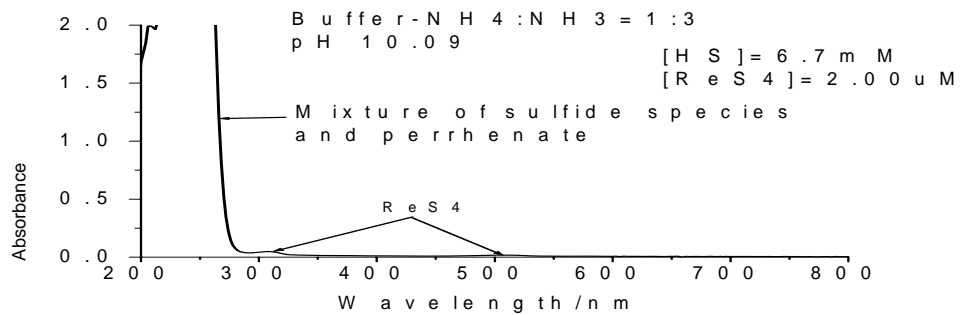
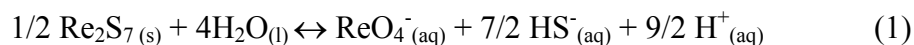


Fig. 19. UV-Vis Spectra of sulfide, 10 μM perrhenate and 95mM buffer mixtures equilibrated at 75 $^\circ\text{C}$ for 33 days. Path length 1 cm.

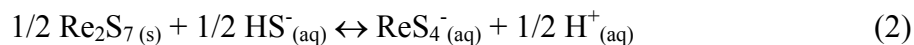
3.3.5 Solubility of Dirhenium Heptasulfide (Re₂S₇)

The buffers and ampoule sealing methods described in Section 2.3.2 were used in this experiment. The rhenium-containing species in these experiments was Re₂S₇ (Sigma-Aldrich). Each ampoule contained 0.5 mM Re₂S₇, 95mM buffer and 1 mM NaHS. These ampoules were equilibrated on a shaker for 5 ½ weeks. They were then opened in an N₂ filled glovebox and the contents filtered with 0.02 µm syringe filters (Whatman). The pH was measured and the total sulfide was also measured using the method described in Section 2.2.2. An aliquot of each sample was acidified with HNO₃ and total rhenium concentration was measured by ICP-MS.

Dirhenium heptasulfide is described as insoluble (Weast and Astle, 1979) and appeared to be insoluble when these ampoules were prepared. The black solid settled to the bottom of the ampoules when they were not shaken. I expected the Re₂S₇ solution to resemble the ampoules from Results section 3.3.2. that had become a dark brown color after equilibration for two weeks. I would then be able to determine whether equilibrium had been reached in these ampoules. Since the solid did not dissolve completely I decided to use these ampoules to determine an equilibrium constant for dissolution of Re₂S₇. Two of the equilibrium reactions proposed are:



$$K = [\text{ReO}_4^-][\text{HS}^-]^{7/2}[\text{H}^+]^{9/2}$$



$$K = [\text{ReS}_4^-][\text{H}^+]^{1/2}/[\text{HS}^-]^{1/2}$$

For both reactions, the concentration of the aqueous Re species should vary considerably with pH. However the following table illustrates that this is not the case.

Table 6. Solubility of Re_2S_7 experiments: pH, final [HS] and $[\text{Re}_{(\text{aq})}]$.

Type of Buffer/95mM	Initial concentration Re_2S_7 (g/L)	Final [Re]/ μM	Final pH	Final [HS]/ mM
Phosphate 3:1	1.2	12	6.3	0.042
Phosphate 1:3	1.2	18	7.28	0.076
Ammonia 3:1	1.2	38	9.13	0.91
Ammonia 1:3	1.2	46	10.12	0.64

These results suggest that there is no solubility equilibrium in these experiments. The two equilibrium reactions presented indicate that Re solubility should vary considerably with pH. It is likely that actual Re_2S_7 solubility is lower than presented above. The Re concentration values I obtained could be a measure of colloidal Re particles that are smaller than the smallest filter I used, $0.02 \mu\text{m}$. ICP-MS was used to obtain these concentration measurements and this instrument does not distinguish between aqueous Re and colloidal Re. These experiments establish an upper limit for Re_2S_7 solubility.

3.4 Investigation of thioperrhenate formation and sorption on kaolinite

3.4.1 Experiment with kaolinite over 30 hours

In these experiments I exposed the perrhenate anion to kaolinite after initiating the reaction with sulfide. I expected an increase in rhenium loss from solution since the rhenium would be in a form more susceptible to sorption. By exposing perrhenate to H₂S gas I expected to form a mixture of thioperrhenates. Following the model of thiomolybdate, I expected increased sorption of the thiolated species.

Fifty milliliters of 0.002M NaReO₄ and 0.05M NH₃-H₂O was prepared and placed in a three-neck round-bottom flask. The flask was placed on a cork stand on a magnetic stirrer. The solution was deoxygenated by bubbling with N₂ gas for 15mins. H₂S gas was bubbled into the liquid for 4.5 hours and a sample was taken. 10g of kaolinite was then added to the flask. At approximately 90-minute intervals, aliquots of the slurry were taken. These samples were centrifuged and filtered with 0.45 μm (Pall) and 0.02 μm (Whatman) syringe filters. The pH was measured and 1:10 and 1:100 dilutions were made with deionized water. UV-Vis spectra were taken of the undiluted sample as well as the two dilutions. After 15.5 hours H₂S gas bubbling was stopped and the flask was placed in an N₂ filled glovebox. The slurry was magnetically stirred inside the glovebox and sampled approximately 24 hours later. This sample was handled in the same manner as described above.

All samples were stored in the refrigerator prior to ICP-MS analysis. Two consecutive 100-fold dilutions were made of all samples. Then 6.00 ml of each diluted sample was added to 4.00 ml of 5% HNO₃. On the morning of analysis each

10 ml acidified dilution was filtered using 0.02 μm (Whatman) syringe filters. Figure 20 is the UV-Vis spectrum of the experiment where kaolinite was added after 4.5 hours of bubbling with H_2S gas.

Figures 20 and 14 are remarkably similar. I expected that some of the rhenium in the thioperrhenates and/or perrhenate would be sorbed to the kaolinite and result in smaller UV-Vis peaks. However, this did not occur and may be the result of competition between sorption and thiolation. Figure 21 a) further illustrates the fact that absorbances did not decrease after kaolinite was added. Previously, (Section 3.1) I found that perrhenate sorption on kaolinite occurred at pHs below 8.5. Figure 21 b) illustrates that this pH condition was met. The concentration of kaolinite in both sets of experiments was 200 g/L.

H₂S bubbled w/KGa1b

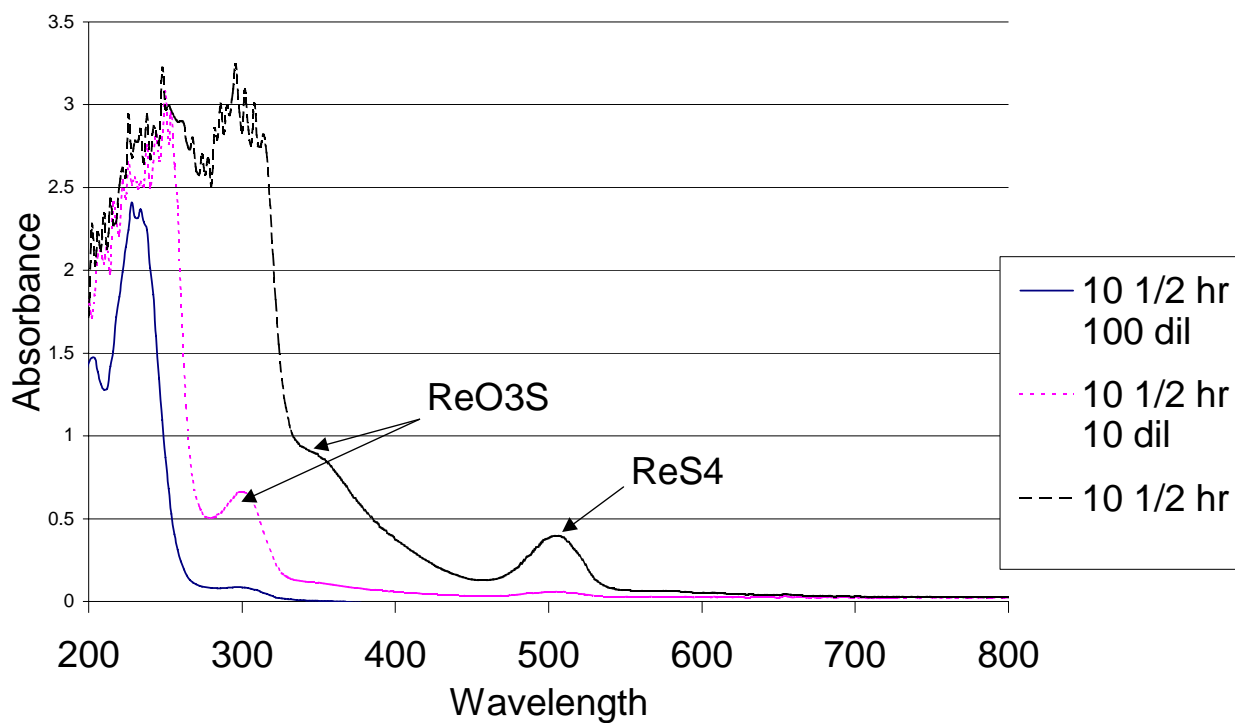
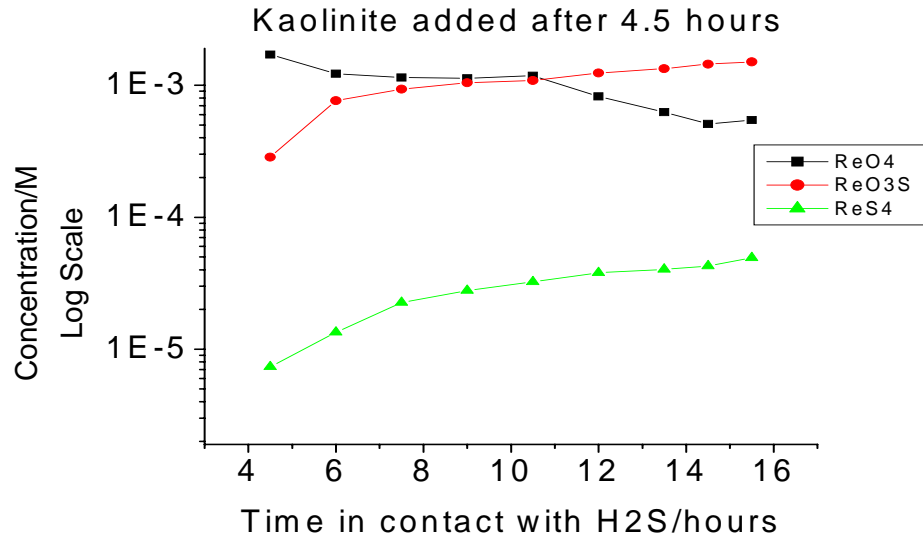


Fig. 20. UV-Vis spectrum of 0.002M NaReO₄ and 0.05M NH₃-H₂O bubbled with H₂S for 10.5 hours; 200 g/L kaolinite was added at 4.5 hours. pH= 6.79. Cell pathlength 1cm.

a)



b)

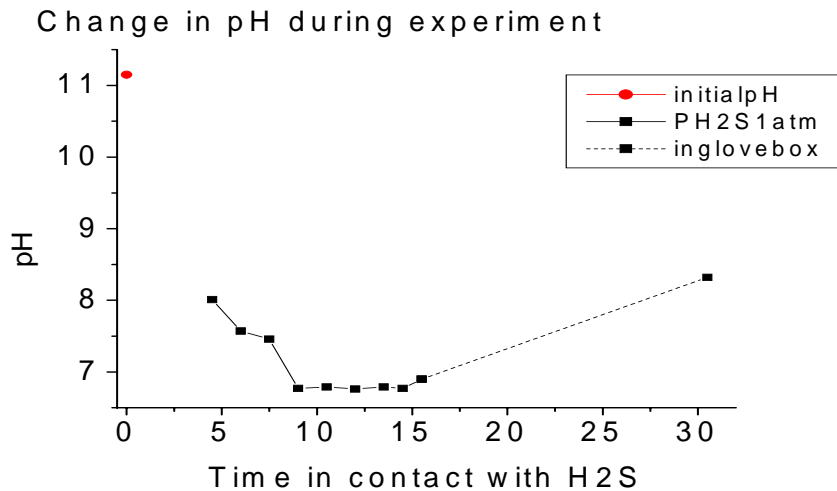


Fig. 21. a) Change in change in concentration of perrhenate and thioperrhenate species vs. time in contact with H₂S at P_{H₂S} = 1atm. Concentration is in a log scale. Initial [ReO₄⁻]=10^{-2.7}M
 b) Change in pH during experiment. Initial pH was measured before H₂S bubbling. The pH remains below 8.5 for all of the experiment.

Note: 200 g/L kaolinite was added after the 4.5 hour sample was taken. Subsequent aliquots were centrifuged for 15 minutes then filtered with 0.45μm (Pall) and 0.02μm (Whatman) syringe filters.

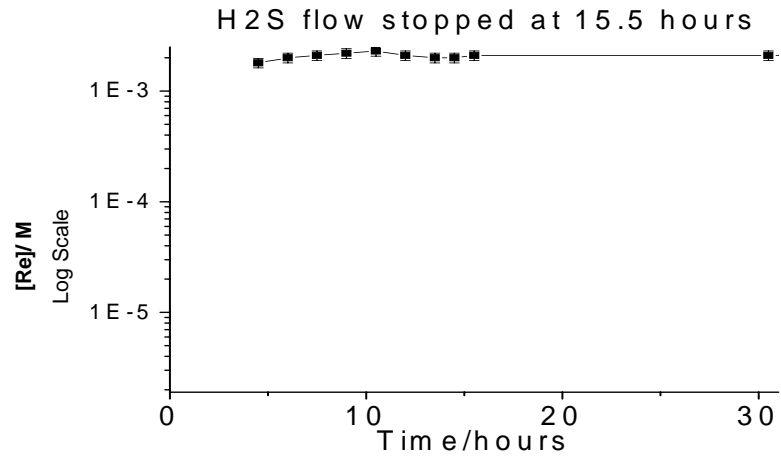
The entire experiment spanned over 30 hours and Fig. 22 illustrates changes in total Re and thioperrhenate/perrhenate concentrations throughout the course of the experiment. The small changes in total rhenium concentration presented in Fig. 22 a) are within 10% of the average value and is most likely analytical drift. In this experiment, perrhenate concentration was 2mM. I have previously found that kaolinite was effective at scavenging perrhenate at a concentration of 0.3mM. Based on these experiments I would expect kaolinite to sorb 25% of the perrhenate in solution at pH 6.7 (Fig. 21. b)). In the above experiments sulfide was present and there may have been competition between thiolation and sorption.

In Fig. 22 b) both ReO_3S^- and ReS_4^- concentrations increase throughout the experiment. This indicates that thioperrhenate formation continued after H_2S was no longer being bubbled through the mixture. Perrhenate (ReO_4^-) concentrations were determined by difference, using total Re concentration determined by ICP-MS:

$$[\text{ReO}_4^-] = [\text{Total Re}] - [\text{ReS}_4^-] - [\text{ReO}_3\text{S}^-]$$

A possible source of error in these calculated perrhenate concentrations is the presence of colloidal particles in the reaction mixture. Figure 23 contains the UV-Vis spectra of the reaction mixture at 30.5 hours. The sample was filtered with 0.45 μm (Pall) and 0.02 μm (Whatman) syringe filters prior to analysis. The baseline of the spectrum is elevated slightly. This is evidence of the presence of a small amount of colloidal particles in the sample. These particles would be measured by the ICP-MS as aqueous Re. Thus, the [Total Re] measurements are the upper limit of dissolved Re and the calculated $[\text{ReO}_4^-]$ presented are the upper limit for perrhenate concentrations.

a)



b)

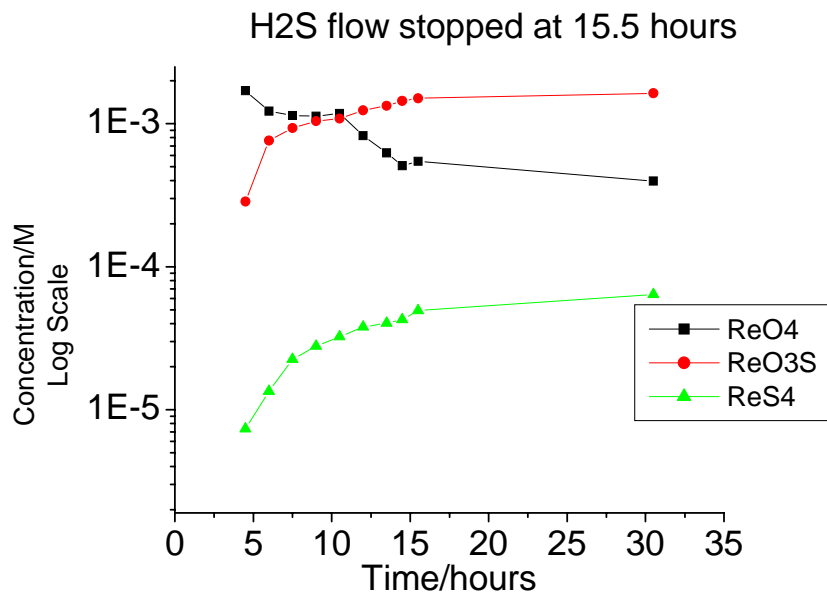


Fig. 22.

a) Change in rhenium concentration over the course of the experiment measured via ICP-MS. Initial perrhenate concentration was approximately $10^{-2.7}$ M, kaolinite concentration was 200g/L

b) Changes in perrhenate and thioperrhenate concentrations during and after H₂S bubbling.

Note: Data up to 15.5 hours are from Fig. 21.

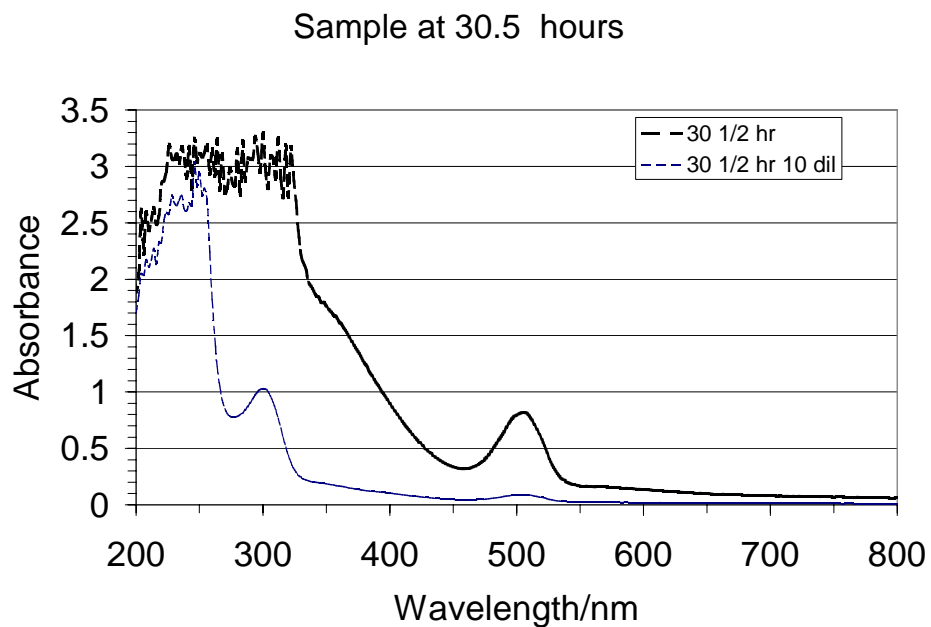


Fig. 23. UV-Vis spectra of 2 mM NaReO_4 and 50mM $\text{NH}_3\text{-H}_2\text{O}$ bubbled with H_2S (g) for 15.5 hours then placed in a N_2 filled glovebox. 200 g/L kaolinite was added after 4.5 hours. Cell pathlength 1cm. pH 8.32. $[\text{ReO}_4^-]_{\text{final}} = 0.34$ mM $[\text{ReO}_3\text{S}^-]_{\text{final}} = 1.6$ mM, $[\text{ReS}_4^-]_{\text{final}} = 0.064$ mM.

3.4.2 Experiment with Kaolinite in the presence of polysulfides and lower Perrhenate concentration

The sorption experiment using kaolinite as a proxy for marine sediments was repeated using a much lower perrhenate concentration: 2.0 μM instead of 2.0mM. Another difference from the experiment outlined in Section 3.4.1 is that polysulfides were added to the reaction vessel. I hypothesized that polysulfides would enhance thiolation of perrhenate and thereby enhance sorption since thioperrhenates are expected to sorb more readily than perrhenate,

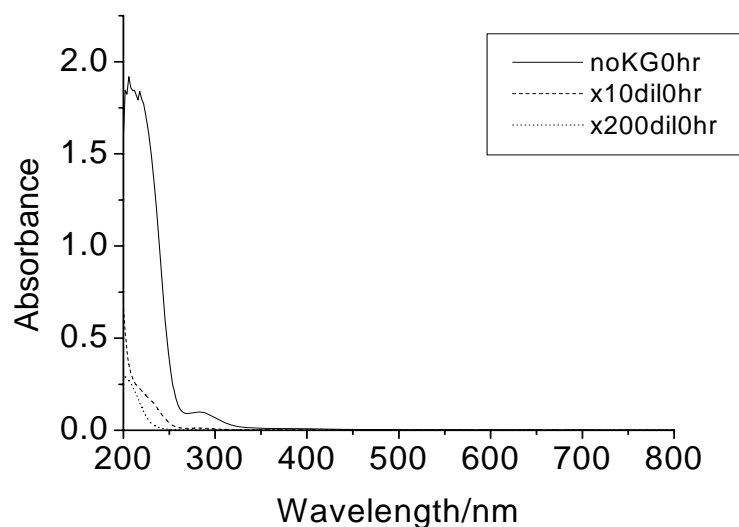
Fifty milliliters of 2.0 μM NaReO_4 , 0.00015 M Na_2S_4 and 0.05M $\text{NH}_3\text{-H}_2\text{O}$ was prepared and placed in a three-neck round-bottom flask. The flask was placed on a cork stand on a magnetic stirrer. The solution was deoxygenated by bubbling with N_2 gas for 15mins. H_2S gas was bubbled into the liquid and samples were taken every 90 minutes. After 4.5 hours 10g of kaolinite was added to the flask. Sampling continued every 90 minutes. Samples were centrifuged for 15 minutes and filtered with 0.45 μm (Pall) and 0.02 μm (Whatman) syringe filters. The pH was measured and 1:10 and 1:200 dilutions were made with deionized water. UV-Vis spectra were taken of the undiluted sample as well as the two dilutions. After 10.5 hours H_2S gas bubbling was stopped and the flask was placed in an N_2 filled glovebox. The slurry was magnetically stirred inside the glovebox and sampled approximately every 24 hours for the next 3 days. These aliquots were handled in the same manner as described above.

All samples were stored in the refrigerator prior to ICP-MS analysis. On the morning of analysis, 0.300 ml of sample was added to 2.70 ml of deionized water and 2.00 ml of 5% HNO₃. Each 5 ml acidified dilution was then filtered using 0.02 μm (Whatman) syringe filter.

Figure 24 a) provides the UV-Vis spectrum of the solution used in this experiment prior to bubbling with H₂S gas. Figure 24 b) provides the UV-Vis spectrum of the centrifuged and filtered mixture after 10.5 hours of H₂S bubbling, kaolinite was added at 4.5 hours. In this experiment I was unable to use peaks in the UV-Vis spectra to track the extent of thiolation. This is because of the much lower perrhenate concentrations.

I estimated the detection limit of ReS₄⁻ using UV-Vis spectra from previous experiments. The smallest peak I observed at wavelength 505 nm (Section 3.3.2) corresponded to an absorbance of 0.0045. Using the extinction coefficient, $\epsilon_{505\text{nm}}=9521 \text{ Lmol}^{-1}\text{cm}^{-1}$ the calculated ReS₄⁻ concentration is 0.5 μM. This is the upper limit on the amount of ReS₄⁻ that could have been produced in this experiment. There was no peak observed at wavelength 505 nm. I was unable to determine whether or not there was a peak at wavelength 350nm, where ReO₃S⁻ absorbs. This is because of the large polysulfide absorption below 400nm.

2 μ M ReO₄, 0.15mM NaS₄ and 0.05M NH₃-H₂O



2 μ M ReO₄, 0.15mM NaS₄ and
0.05M NH₃-H₂O
w/ Kaolinite, 10.5hr H₂S

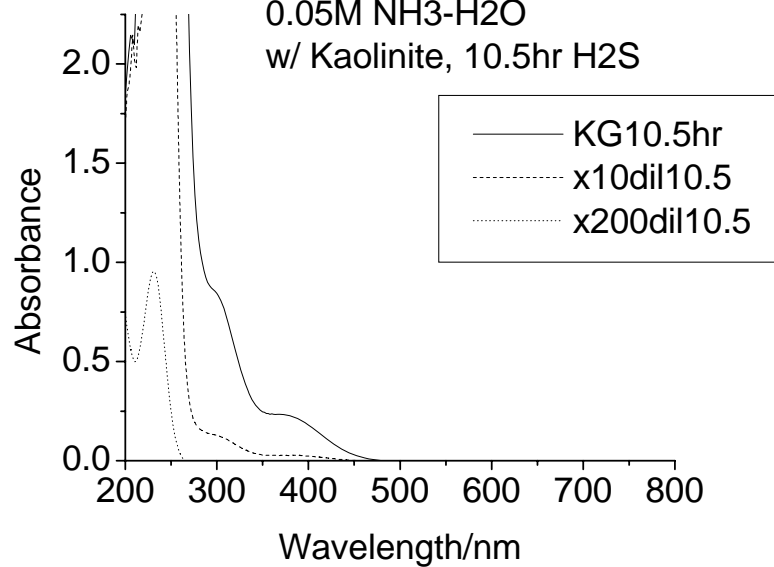


Fig. 24.

a) UV-Vis spectrum of 2 μ M NaReO₄, 0.15mM Na₂S₄ and 50mM NH₃-H₂O.

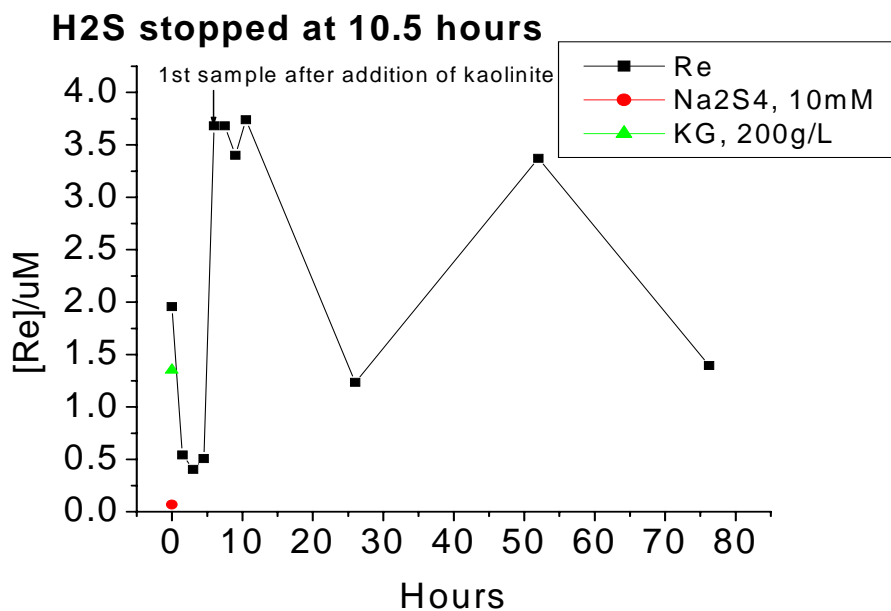
b) UV-Vis spectrum 2 μ M NaReO₄, 0.15mM Na₂S₄ and 50mM NH₃-H₂O bubbled with H₂S for 10.5 hours; kaolinite was added after the 4.5 hour sample was taken.

Cell pathlength: 1cm.

Figure 25 illustrates the change in Re concentration a), and change in pH b), over the course of the experiment. ICP-MS was used to determine the Re concentration in the samples. Figure 25 a) shows that rhenium concentrations decreased initially and then increased after addition of kaolinite at 4.5 hours. The decrease in rhenium concentration when H₂S bubbling was initiated is not understood. Figure 25 a) also illustrates Re contamination introduced by kaolinite and the polysulfide solution (Na₂S_{4(aq)}) The triangle represents Re concentration in a deionized water sample that was mixed with kaolinite, centrifuged, filtered, diluted and acidified in the same manner as the samples. The circle represents Re concentration in a solution of 0.15mM Na₂S₄.

The amount of Re contamination that could have been contributed by kaolinite is the same order of magnitude as the amount of Re used in the experiment, 10⁻⁶ M. It is possible that rhenium was introduced into the solution from the kaolinite since Re concentration increases after kaolinite addition. The increase in rhenium concentration after the addition of kaolinite sheds light on results from previous experiments where perrhenate sorption on kaolinite was investigated in the presence of BH₄⁻ and HS⁻ as reducing agents. If kaolinite releases rhenium into the solution it is not possible to perform sorption experiments at low perrhenate concentrations.

a)



b)

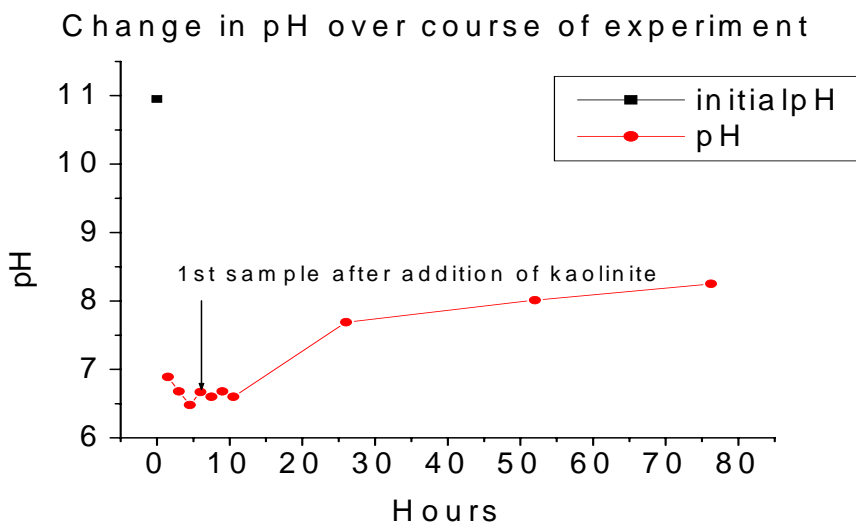


Fig. 25. Initial mixture in reaction vessel was 50 mL 2µM NaReO₄, 0.15mM Na₂S₄ and 50mM NH₃-H₂O. 10g of kaolinite was added at 4.5 hours making the kaolinite concentration 200g/L. H₂S stopped at 10.5 hours
a) Change in [Re] over the course of the experiment.
b) Change in pH over the course of the experiment.

Chapter 4: Discussion

Evidence obtained in this thesis refers to Re sorption under both oxic and anoxic conditions.

Under oxic conditions Re is expected to be in the form of the perrhenate anion, ReO_4^- . I studied ReO_4^- sorption on Aluminum Oxide C ($\delta\text{-Al}_2\text{O}_3$), Aerosil 200 (SiO_2) and KGa1b ($\text{Al}_2\text{Si}_2\text{O}_5[\text{OH}]_4$). Sorption with ionic strength dependence is indicative of outer-sphere surface complex formation (Goldberg et al., 1998). Ionic strength dependence is not evident for any of the solids used, Figs. 3-5. This suggests that the sorption mechanism is inner-sphere.

I have found that sorption of ReO_4^- is weak compared to sorption of MoO_4^{2-} on the same or very similar minerals (Figs. 6 and 7). Perrhenic acid (HReO_4) is a strong acid while H_2MoO_4 is a weak acid ($\text{pK}_a \sim 4.0$). Anions usually bind to oxide surfaces by H atom bridges, so the stronger acid, HReO_4 would be expected bind much less strongly. Goldberg et al., (1996) described molybdate's sorption on both kaolinite and Aluminum Oxid C as outer sphere. I described perrhenate's sorption on these solids as inner sphere.

The fact that neither Mo nor Re are sorbed strongly to oxides or silicates is consistent with the fact that they are conservative in the ocean. If MoO_4^{2-} and ReO_4^- were sorbed strongly to materials of this type, that make up a large part of the sea-floor, they would not be depleted in oxic sediments relative to continental crustal abundance. Their use as paleoredox indicators depends upon their enrichment in anoxic sediments relative to oxic sediments

It appears that kaolinite adsorbs much less Re than silica or alumina. I believe that this is not an artifact due to colloids of the kaolinite getting through the 0.02 μm syringe filter used in these experiments. These colloids would give a false positive in the optical ReO_4^- determination by causing broad scattering in the UV-Vis spectra. This broad scattering was not observed in any of the spectra and an example is illustrated below.

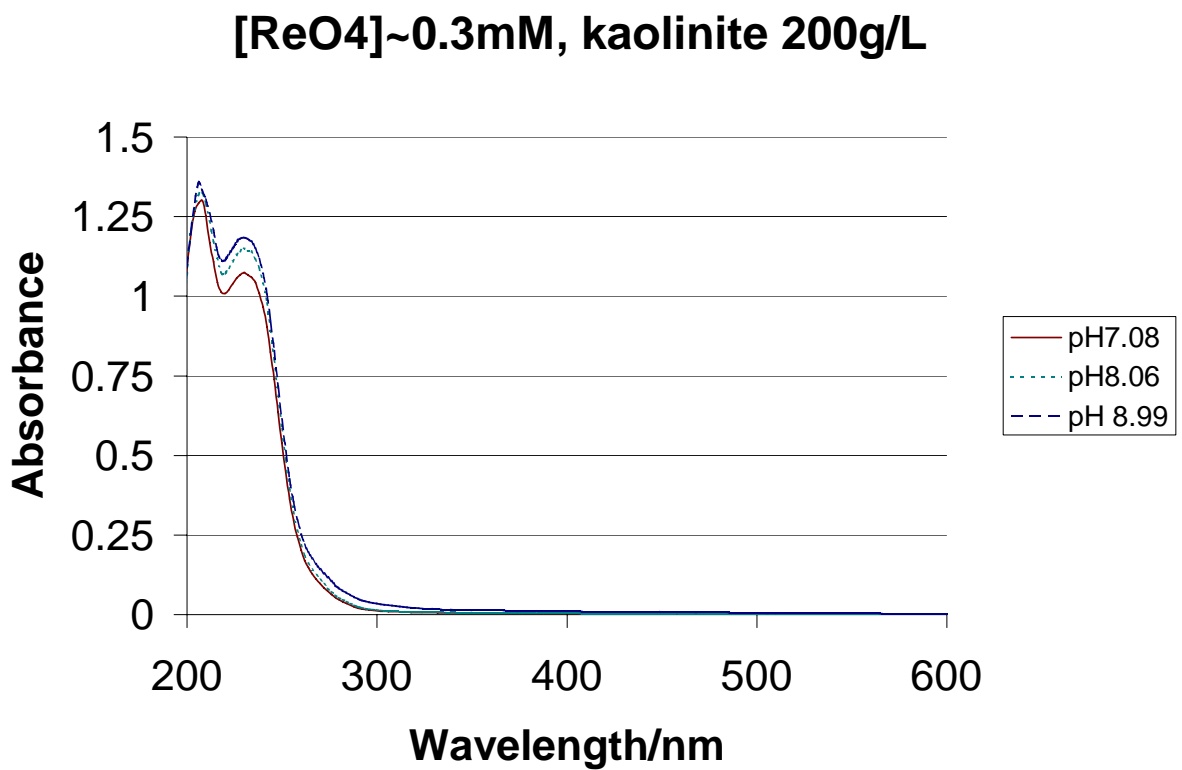


Fig. 26. UV-Vis spectra of 0.3mM ReO_4^- sorption on 200g/L kaolinite, ionic strength 0.01M NaCl. Pathlength: 1cm. Samples were centrifuged for 15 minutes and filtered with 0.45 μm (Pall) and 0.02 μm (Whatman) syringe filters.

The spectra for 3 different pHs are presented. Note that there is no absorption above 300nm.

I calculated a partition coefficient for Re between water and kaolinite using data from the results presented in Fig.5 a) (0.3mM ReO_4^- sorption on 200 g/L KGa1b (BET:12.5 m^2/g) at ionic strength 0.01M NaCl, pH 8.01).

$$P = \frac{[\text{moles Re/kgkaol}]}{\text{moles Re/L}}$$

$$P = \frac{0.00032 \text{ moles Re/kgkaol}}{0.000297 \text{ moles Re/L}}$$

$$P = \mathbf{1.08}$$

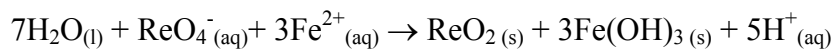
If this partition coefficient described sorption of Re from seawater to sediments, then the concentration of Re on kaolinite in marine sediments would be 0.008 ppb.

Morgan (1999) states that the concentration of rhenium in oxic sediments is much lower than crustal abundances, and ranges from 0.009 – 0.051 ppb. My calculation compares well to the lower-end of this range of concentrations. This finding points to the fact that marine sediments are similar to kaolinite in their capacity to adsorb perrhenate. Olafsson and Riley (1972) found that Re in deep-sea sediments was associated with silicates and not with carbonate or ferromanganese mineral fractions. Thus, in nature, Re is associated with oxic marine sediments that closely resemble kaolinite, a silicate.

Based on previous work by other authors (Colodner et al., 1993 and 1995, Calvert and Pedersen, 1993, Crusius et al. 1996 and Morford and Emerson, 1999), I knew that Re scavenging in nature is more efficient in reducing environments. As mentioned in the Introduction (Section 1.1), the term reducing refers to both suboxic (no O_2 or H_2S) and anoxic (H_2S present but no O_2) conditions (Colodner et al., 1995).

I demonstrated that the presence of a reducing agent improves kaolinite scavenging of rhenium. The reducing agent used was borohydride, chosen because its hydrolysis product, borate, is inert to ReO_4^- . Figure 9 presents the results for Re sorption on kaolinite in the presence of borohydride. These results show that reduction of $\text{Re}^{(\text{VII})}\text{O}_4^-$ promotes the uptake of Re by a simple silicate like kaolinite. Borohydride was used as a reducing agent in these experiments despite the fact that borohydride would never be found in nature. It is likely that there are too many reducing agents in nature to test them each individually, particularly those found in cells. So borohydride was chosen as a proxy.

One of the abundant reducing agents in anoxic environments is Fe^{2+} . Eriksen and Cui (1996a and 1996b) have found that ferrous iron is effective at reducing TcO_4^- . As mentioned in the Introduction (Section 1.4) Tc is Re's chemical analogue, however, in this case the two elements do not exhibit similar behavior. Ferrous iron is not effective at reducing ReO_4^- due to thermodynamic considerations. Consider the following reaction:



$$K = [\text{H}^+]^5 / [\text{ReO}_4^-][\text{Fe}^{2+}]^3$$

I calculated the log K of this reaction using ΔG_f values from Wagman et al., (1982).

$$\Delta G_{\text{rxn}} = [1\text{mol}(-368 \text{ kJ/mol}) + 3\text{mol}(-6593\text{kJ/mol}) + 5\text{mol}(0\text{kJ/mol})] - [7\text{mol}(-237.129\text{kJ/mol}) + 1\text{mol}(-694.5\text{kJ/mol}) + 3\text{mol}(-78.90\text{kJ/mol})] = 245.2 \text{ kJ}$$

$$\log K = -\Delta G_{\text{rxn}} / 2.303RT = -2.452 \times 10^5 \text{ J} / (2.303 * 8.31 \text{ JK}^{-1} * 298.15 \text{ K}) = -42.97$$

I used this log K and the following values: pH = 8 and $[\text{ReO}_4^-] = 40 \text{ pM}$ (Anbar et al., 1992), to determine the value of $[\text{Fe}^{2+}]$ needed for this reaction to go to the right. I calculated that $[\text{Fe}^{2+}]$ would have to be at least 35 μM . Some $[\text{Fe}^{2+}]$ in sulfidic

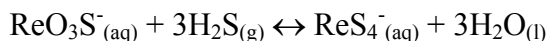
systems are $\leq 0.28\mu\text{M}$ (Haraldsen and Westerlund, 1988), $\leq 4\mu\text{M}$ (Ozturk, 1995), $\leq 1.0\mu\text{M}$ (Seyler and Martin, 1989) and $\leq 10\mu\text{M}$ (Balistreri et al., 1994). Thus, typical values of $[\text{Fe}^{2+}]$ are 1 to 2 orders of magnitude smaller than the concentration required. Even the highest concentration found in nature, $10\mu\text{M}$ is three times smaller than $35\mu\text{M}$. Therefore reduction of perrhenate by ferrous iron is thermodynamically hindered in nature.

Another abundant reducing agent in anaerobic environments is sulfide, which is an important factor in Re chemistry, as shown in this work. In principle sulfide could act as a reducing agent or it could lead to the formation of thioperrhenates. Figure 10 presents the results for Re sorption on kaolinite in the presence of sulfide. These results indicate that sulfide makes kaolinite a slightly better scavenger of Re. I have no evidence that sulfide acts as a reducing agent when it is in contact with perrhenate. When sulfide acts as a reducing agent it is oxidized to polysulfides. These species absorb broadly below 400nm and this type of absorbance was not observed in any UV-Vis spectra of reaction mixtures containing perrhenate and sulfide (e.g. Figs 12, 13, and 14). However, as will be discussed below, it is likely that reduction occurs in solid species formed and not in solution.

I found that when ReO_4^- was exposed to $\text{H}_2\text{S}(\text{g})$ the reaction occurred on a time-scale of hours to form ReO_3S^- and ReS_4^- at near neutral pH. UV-Vis spectra were taken over the course of this experiment and they are presented in Figs. 12-14. Tossell (unpublished work) has predicted that ReO_2S_2^- and ReOS_3^- are unstable compared to ReO_3S^- and ReS_4^- , under environmental conditions. Both ReO_2S_2^- and ReOS_3^- species absorb around 400nm and there are no peaks on or around this

wavelength in any of my UV-Vis spectra. The fact that these species are unstable does not mean that they do not form. The reaction pathway for the formation of ReS_4^- almost certainly involves successive replacement of oxygen atoms in ReO_4^- by sulfur atoms. Thus, ReO_2S_2^- and ReOS_3^- should in fact form during this reaction, but are too unstable to accumulate to concentrations large enough to give rise to absorbances in UV-Vis spectra.

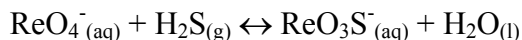
The ratio of ReO_3S^- and ReS_4^- appears to reach a constant value in a period of a few hours in the experiments where perrhenate solutions were in contact with H_2S at $P_{(\text{H}_2\text{S})} = 1 \text{ atm}$ at near neutral pH (Figs. 15 and 21 a)). One way of explaining this observation would be to propose equilibrium reaction and equilibrium constant expression:



$$K = [\text{ReS}_4^-]/([\text{ReO}_3\text{S}^-]P_{\text{H}_2\text{S}})$$

In the absence of kaolinite (Fig. 15.), $K = 4 \pm 1 \times 10^{-2}$, while in the presence of kaolinite (Fig. 21.), $K = 3 \pm 1 \times 10^{-2}$. These K values are the average K's calculated using $[\text{ReS}_4^-]$ and $[\text{ReO}_3\text{S}^-]$ at different reaction times. The uncertainty presented encompasses the range of K values obtained. These two values agree well and indicate that the presence of kaolinite does not affect the reaction between ReO_3S^- and ReS_4^- on the time-scale of this experiment. The tentative equilibrium constant, K, for this reaction is $3.5 \pm 1.5 \times 10^{-2}$.

The ratio of ReO_4^- and ReO_3S^- does not appear to become constant in these experiments (Figs. 15 and 21 b)). If I suppose the existence of an equilibrium:



$$Q_t = [\text{ReO}_3\text{S}^-]/([\text{ReO}_4^-] P_{\text{H}_2\text{S}})$$

Then the reaction quotient, Q , can be used to establish a lower limit for K since $[\text{ReO}_4^-]$ will decrease as the reaction approaches equilibrium. Using data presented in Fig. 21. a), $Q_{15.5 \text{ hours}} = 2.8 \pm 0.1$.

I investigated the effect of sulfide on $\text{Re}^{(\text{VII})}$ by equilibrating perrhenate solutions with sulfide at 4 buffered pH's. The perrhenate concentration was varied, as was the sulfide concentration and equilibration temperature. These experiments and results are outlined in Section 3.4.

I obtained dark poly-thio compounds in reaction mixtures buffered at pHs <10 at both 25°C and 75°C that started with 1mM perrhenate (Results sections 3.3.2 and 3.3.3). In the 25°C experiments this brown polymer created an elevated baseline in the UV-Vis spectra (Fig. 16). These particles were small enough to pass through the 0.02 μm syringe filter used. The concentrations of ReO_3S^- and ReS_4^- were calculated using extinction coefficients (Muller et al., 1967) and compiled in Table 5. The equilibrium constant ($K = 3.5 \pm 1.5 \times 10^{-2}$), calculated above had to be reformatted before being applied to these results.

Reaction	K
$\text{ReO}_3\text{S}^-_{(\text{aq})} + 3\text{H}_2\text{S}_{(\text{g})} \leftrightarrow \text{ReS}_4^-_{(\text{aq})} + 3\text{H}_2\text{O}_{(\text{l})}$	$3.5 \pm 1.5 \times 10^{-2}$
$3\text{H}_2\text{S}_{(\text{aq})} \leftrightarrow 3\text{H}_2\text{S}_{(\text{g})}$	$(10^{+1})^3$
$3\text{H}^+_{(\text{aq})} + 3\text{HS}^-_{(\text{aq})} \leftrightarrow 3\text{H}_2\text{S}_{(\text{aq})}$	$(10^{+7.01})^3$
$\text{ReO}_3\text{S}^-_{(\text{aq})} + 3\text{HS}^-_{(\text{aq})} + 3\text{H}^+ \leftrightarrow \text{ReS}_4^-_{(\text{aq})} + 3\text{H}_2\text{O}_{(\text{l})}$	$3.8 \pm 1.6 \times 10^{22}$

Using the data in Table 3. I calculated K to be 2×10^{27} and 1×10^{29} . Therefore, the long-term experiments at 25°C do not support the equilibrium I discussed above where I calculated K to be $3.8 \pm 1.6 \times 10^{22}$.

In the 75°C experiments the brown polymer did not give a Tyndall beam. I may have not been able to see the beam because of the darkness of the solution, which was the color of Hershey's chocolate syrup. The brown polymer was not extractable into organic solvent, and this indicates that it is not hydrophobic. When the brown mixture was filtered, the black solid was collected on 0.02 μm filter paper. In reaction mixtures exposed to air, the black solid did not dissolve, indicating that it is kinetically stable in the presence of oxygen.

In the experiments containing 10 μM Re, tetra-thioperrhenate, is present at all four pHs (Fig. 19). These results suggest that when tetra-thioperrhenate is formed at pHs < 10 it forms colloidal particles that eventually conglomerate and precipitate as a rhenium-sulfide. My experiments show that longer equilibration time and/or higher reaction temperature lead to the formation of this polymer.

When attempting to synthesize tetra-thioperrhenate, Ranade et al., (1970) observed the formation of a dark brown precipitate that lowered their yield of tetra-thioperrhenate. In my experiments I established that the precipitate I obtained contains rhenium and sulfide (Fig. 18). Semi-quantitative analysis of this rhenium

sulfide suggests that the Re:S ratio is 3:7 . Hibble et al. (1990) and Schwarz et al. (2004) suggest that the structure of this solid cannot be described correctly as dirhenium heptasulfide (Re_2S_7), or rhenium disulfide (ReS_2). Instead they propose that it is a rhenium polysulfide species. Schwarz et al. (2004) proposed that the formula of the compound is structurally related to Re_2S_7 and is best represented as: $\text{Re}^{\text{V}}(\text{S})_{1.5}(\text{S}_2)_1$.

An important characteristic of the UV-Vis spectra (Figs. 17 and 19) is that there is no evidence of polysulfides free in solution (compare to Fig 24 b) in which polysulfide was added). When sulfide (HS^-) acts a reducing agent it is oxidized to polysulfides. Polysulfides absorb strongly between 300 and 400 nm and this type of absorbance is not present in the spectra. This means that any polysulfides formed are not in solution but are in the solids formed.

One proposed hypothesis is that sulfide can enhance Re sorption onto clay minerals like kaolinite. However, the evidence I have collected does not support this hypothesis. In Results section 3.4.1, I described the experiment performed to test this hypothesis. A $10^{-2.7}$ M perrhenate solution in contact with H_2S at $P_{(\text{H}_2\text{S})} = 1\text{atm}$ was exposed to 200g/L of kaolinite. The change in Re concentration over the course of the experiment is shown in Fig. 22 a). The small changes in Re concentration over the course of the experiment are within analytical error. The experiment was repeated using a lower perrhenate concentration and polysulfides and the results are presented in Fig. 25 a). These results show that Re sorption to kaolinite is not enhanced by the presence of polysulfides.

Another proposed hypothesis is that the enrichment of rhenium in reducing sediments is due to the precipitation of an insoluble rhenium sulfide species. I found evidence of this type of species in experiments where rhenium and sulfide were equilibrated on a time-scale of weeks. As I discussed above, the formation of this black solid is preceded by the formation of a brown polymer. The fact that this species formed under all experimental conditions indicates that it is a very stable and insoluble Re species.

Equilibrium constants are needed to evaluate whether this rhenium sulfide species can form under environmental conditions. In the results presented here, sulfide concentrations are 1 to 2 orders of magnitude larger than concentrations found in typical reducing environments. Sulfate concentration in seawater is 10^{-2} M, so this establishes an upper limit on the sulfide that could form. Typical values range from 10^{-5} to 10^{-4} M.

Experimental evidence presented in this thesis, as well as thermodynamic calculations, indicate that sulfide is likely to play an important role in Re enrichment in anaerobic sediments by leading to the formation of a solid Re-S species.

Appendix I. Tables of experimental observations

Table A1. Description of contents of centrifuge tubes used in Kaolinite sorption experiments. S before the tube numbers indicate that the reducing agent used here is sulfide. Control tubes (no reducing agent or mineral surfaces) are in bold.

Tube Number	Perrhenate/ uM	Borate Buffer/ mM	NaHS/mM	KGa1b(g/L)	Re/M (ICP-MS)
S1	1	0.5	0	0	1.51
S2	1	0.4	10	0	1.48
S3	1	0.5	0	80	1.44
S4	1	0.4	10	80	0.98
S5	1	0.5	0	200	1.51
S6	1	0.4	10	200	1.31
S7	0.1	0.95	0	0	0.090
S8	0.1	0.85	10	0	0.033
S9	0.1	0.95	0	80	0.136
S10	0.1	0.85	10	80	0.087
S11	0.1	0.95	0	200	0.075
S12	0.1	0.85	10	200	0.089
S13	0.01	1.0	0	0	0.00578
S14	0.01	0.9	10	0	0.00572
S15	0.01	1.0	0	80	0.01396
S16	0.01	0.9	10	80	0.00547
S17	0.01	1.0	0	200	0.01208
S18	0.01	0.9	10	200	0.00709

Table A2. Description of contents of centrifuge tubes used in Kaolinite sorption experiments. B before the tube numbers indicate that the reducing agent used here is borohydride. Control tubes (no reducing agent or mineral surfaces) are in bold.

Tube Number	Perrhenate/ uM	Borate Buffer/ mM	LiBH₄/mM	KGa1b(g/L)	Re/M (ICP-MS)
B1	1	0.5	0	0	1.49
B2	1	0.4	10	0	1.20
B3	1	0.5	0	80	1.23
B4	1	0.4	10	80	1.12
B5	1	0.5	0	200	1.38
B6	1	0.4	10	200	0.52
B7	0.1	0.95	0	0	0.0924
B8	0.1	0.85	10	0	0.0296
B9	0.1	0.95	0	80	0.0843
B10	0.1	0.85	10	80	0.0607
B11	0.1	0.95	0	200	0.0844
B12	0.1	0.85	10	200	0.0378
B13	0.01	1.0	0	0	0.01063
B14	0.01	0.9	10	0	0.00408
B15	0.01	1.0	0	80	0.01159
B16	0.01	0.9	10	80	0.00477
B17	0.01	1.0	0	200	0.01071
B18	0.01	0.9	10	200	0.00480

Table A3. Visual observations of ampoules containing ~1 mM [ReO₄⁻].
 Temperature: 25°C. Observations in italics correspond to temperature: 75°C.

		Day No.	10	14	24	30	46
Ampoule Name	Buffer pH	[HS]/mM	Description	Description	Description	Description	Description
P312	6.21	10	pale pink-brown	pink-brown	<i>clear brown 75 C oven</i>	<i>dark brown NO Tyndall beam</i>	<i>dark brown w/black solid on bottom</i>
2P312	6.21	10	pale pink-brown	pink-brown	clear brown	brown	dark brown
P312.5 (01	6.21	3	red-brown tint	pale reddish-brown	pale red-brown	pale red-brown	red-brown
P313	6.21	1	red-brown tint	very pale red-brown	very pale red-brown	very pale red-brown	
P132	7.2	10	pale pink	pink	<i>pink 75C oven</i>	<i>pinkish-red NO Tyndall beam</i>	<i>dark brown w/black solid on bottom</i>
2P132	7.2	10	pale pink	pink	pink	brown-pink	brown-pink
P132.5	7.2	3	very pale red-brown	very pale pink-brown	pale pink-brown	pale pink-brown	pink-brown
P133	7.2	1	very pale pink-brown	very pale pink-brown	very pale pink-brown	very pale pink-brown	pale pink-brown
A312	9.24	10	colorless	<i>colorless 75C oven</i>	<i>red-brown tint</i>	<i>reddish-pink</i>	<i>dark brown w/black solid on bottom</i>
2A312	9.24	10	colorless	colorless	colorless	colorless	colorless
A312.5	9.24	3	colorless	colorless	colorless	colorless	colorless
A313	9.24	1	colorless	colorless	colorless	colorless	colorless
A132	10.28	10	colorless	colorless	<i>colorless 75C oven</i>	<i>brown tint Tyndall beam</i>	<i>pink w/black ppt settled at bottom</i>
2A132	10.28	10	colorless	colorless	colorless	colorless	colorless
A132.5	10.28	3	colorless	colorless	colorless	colorless	colorless
A133	10.28	1	colorless	colorless	colorless	colorless	colorless

Table A4. Visual observations of ampoules containing $\sim 10 \mu\text{M}$ $[\text{ReO}_4^-]$.
Temperature: 75°C .

Ampoule Name	Buffer pH	Day No.	1	10	20
		[HS]/mM	Description	Description	Description
P312	6.21	10	colorless	pink-brown tint	pale pink-brown
2P313	6.21	1	colorless	pale pink tint	pink tint
P132	7.2	10	colorless	pale pink tint	pink tint
P133	7.2	1	colorless	colorless	pale pink tint
A312	9.24	10	colorless	colorless	very pale pink tint
A313	9.24	1	colorless	colorless	colorless
A132	10.28	10	colorless	colorless	colorless
A133	10.28	1	colorless	colorless	colorless

Appendix II. Tables of UV-Vis data for ampoules containing ~1mM [ReO₄⁻]. Temperature 25°C. Pathlength: 1cm and 0.1 cm.

1 cm cell						
Equilibration time	8 weeks					
Type of Buffer	Phosphate 3:1	Phosphate 3:1	Phosphate 3:1	Phosphate 1:3	Phosphate 1:3	Phosphate 1:3
Final pH	6.49	6.43	6.36	7.47	7.33	7.31
Final[HS]/mM	4.7	0.92	0.13	6.3	1.8	0.63
Wavelength	1P312	1P3125	1P313	1P132	1P1325	1P133
200	2.4885	1.9970	1.7971	2.0419	1.7808	1.7803
202	2.5973	2.3273	2.1001	2.3506	2.0042	1.9856
204	2.7134	2.2295	2.2610	2.4023	2.0505	2.0255
206	2.5229	2.5219	2.0514	2.4442	2.1643	2.1157
208	2.7818	2.7430	2.3788	2.5664	2.2649	2.1537
210	2.7845	2.5950	2.1315	2.3785	2.2285	2.1415
212	2.4903	2.5734	2.2985	2.7888	2.2919	2.1598
214	2.8155	2.7366	2.3228	2.6686	2.1578	2.2533
216	2.8662	2.7533	2.3652	2.6350	2.5764	2.2334
218	2.9396	2.9396	2.4324	2.9396	2.4415	2.3820
220	3.0053	2.6947	2.4256	2.6747	2.6289	2.4046
222	3.1191	3.1191	2.6397	3.1191	2.6646	2.7322
224	3.1982	2.8765	2.6310	3.0686	2.7515	2.6083
226	3.2543	2.7998	2.8617	3.2543	2.6110	2.6290
228	3.2811	3.2811	2.7568	3.1502	2.9004	2.7093
230	3.2818	3.2029	2.7767	3.0034	2.8115	2.7705
232	3.2670	3.0489	2.6730	3.2670	2.7831	2.5996
234	3.1328	3.1514	2.8449	3.2470	2.6784	3.0298
236	3.1902	3.0401	2.6638	3.2306	2.6861	2.6467
238	3.0921	3.2217	2.8528	3.1601	3.0311	2.8275
240	3.2230	3.2230	2.6956	3.2213	2.6209	2.6156
242	3.2357	3.1215	2.6777	3.1554	2.8651	2.6493
244	3.2621	3.0200	2.5957	2.9713	2.8468	2.6808
246	3.2981	3.1512	2.4742	3.2981	2.8070	2.7887
248	3.3422	2.8719	2.4085	3.3422	2.7923	2.7374
250	3.3657	3.3872	2.2977	3.2100	2.8748	2.5024
252	3.4271	3.4271	2.1151	3.1372	2.8953	2.2181
254	3.4539	3.0825	1.9551	3.2118	2.7379	1.8732
256	3.3149	2.9779	1.8130	3.3489	2.3363	1.6012
258	3.4506	2.9884	1.7105	3.2471	2.1572	1.3871
260	3.4216	2.9986	1.6403	3.4216	1.9171	1.2097
262	3.3788	2.9891	1.5932	3.1882	1.7713	1.0995
264	3.0735	2.8240	1.5947	3.1529	1.7063	1.0279
266	3.2808	2.9294	1.6163	2.9479	1.6792	0.9909
268	3.2368	2.7981	1.6476	3.0596	1.6902	0.9766
270	3.2004	2.8779	1.6997	3.2004	1.7226	0.9721
272	3.1760	2.8431	1.7432	2.9320	1.7669	0.9849
274	3.1646	3.1447	1.8056	3.1646	1.8690	1.0087
276	3.0875	2.9493	1.8850	3.1664	1.9123	1.0432
278	3.1799	2.9497	1.9535	3.0504	1.9882	1.0774
280	3.2059	2.9639	2.0748	2.9747	2.1342	1.1255
282	3.2393	3.0487	2.1693	3.2393	2.1584	1.1863
284	3.2787	3.1164	2.2054	3.2787	2.3223	1.2512
286	3.3215	3.3215	2.3943	3.2795	2.4762	1.3288
288	3.1220	3.1338	2.4824	3.3650	2.5487	1.4093
290	3.4054	3.4054	2.5342	3.4054	2.6092	1.5000
292	3.4391	3.2934	2.7300	3.1272	2.8535	1.5899
294	3.4617	3.4617	2.8351	3.4617	2.8434	1.6673
296	3.4727	3.3270	2.8612	3.2681	2.9041	1.7309
298	3.4709	3.2538	2.8495	3.4709	2.9590	1.7581
300	3.3438	3.4581	2.7748	3.1150	3.0181	1.7513
302	3.1948	3.1712	2.8069	3.4379	2.8200	1.7283

Wavelength	1P312	1P3125	1P313	1P132	1P1325	1P133
304	3.4101	3.4118	2.7337	3.0228	2.8373	1.6329
306	3.3832	3.1651	2.6788	3.3832	2.7251	1.5275
308	3.2434	2.8786	2.3929	3.2267	2.6323	1.3843
310	3.2466	3.3070	2.2122	2.9658	2.3584	1.2225
312	3.3022	2.9591	1.9330	3.3022	2.1750	1.0512
314	3.2796	2.9184	1.6727	3.1327	1.8613	0.8843
316	3.1454	2.9371	1.3941	3.2381	1.5516	0.7280
318	3.2441	2.6820	1.1484	3.2441	1.2648	0.5895
320	3.2337	2.3795	0.9464	2.6901	1.0131	0.4707
322	3.2256	2.0041	0.7827	2.4059	0.8149	0.3787
324	3.2216	1.7482	0.6585	2.0499	0.6641	0.3081
326	3.2217	1.5719	0.5715	1.8159	0.5575	0.2594
328	3.2242	1.4255	0.5112	1.6525	0.4884	0.2263
330	3.2308	1.3636	0.4746	1.5531	0.4456	0.2070
332	3.1785	1.3120	0.4530	1.5029	0.4214	0.1956
334	3.2504	1.2812	0.4422	1.4697	0.4111	0.1901
336	3.0603	1.2704	0.4392	1.4543	0.4088	0.1905
338	3.2771	1.2630	0.4394	1.4443	0.4096	0.1906
340	3.2918	1.2647	0.4417	1.4288	0.4140	0.1934
342	3.2643	1.2555	0.4439	1.4252	0.4175	0.1958
344	3.3179	1.2534	0.4447	1.4135	0.4207	0.1969
346	3.3280	1.2452	0.4462	1.4012	0.4220	0.1983
348	3.0932	1.2374	0.4435	1.3871	0.4202	0.1976
350	3.3413	1.2201	0.4404	1.3597	0.4171	0.1963
352	3.3436	1.1993	0.4338	1.3306	0.4111	0.1938
354	3.0996	1.1802	0.4256	1.3053	0.4024	0.1901
356	3.2953	1.1536	0.4151	1.2745	0.3926	0.1852
358	3.2863	1.1282	0.4037	1.2440	0.3789	0.1786
360	3.2953	1.1006	0.3896	1.2060	0.3647	0.1716
362	3.3025	1.0649	0.3747	1.1689	0.3486	0.1639
364	3.2704	1.0363	0.3597	1.1373	0.3326	0.1559
366	2.7309	1.0035	0.3447	1.0975	0.3158	0.1477
368	3.1801	0.9693	0.3269	1.0615	0.2982	0.1372
370	3.1706	0.9386	0.3125	1.0300	0.2809	0.1299
372	2.8918	0.9065	0.2962	0.9999	0.2657	0.1214
374	3.1482	0.8790	0.2828	0.9651	0.2489	0.1144
376	3.1530	0.8492	0.2690	0.9352	0.2348	0.1079
378	3.1063	0.8248	0.2558	0.9119	0.2202	0.1001
380	2.9563	0.8028	0.2446	0.8912	0.2080	0.0960
382	3.1672	0.7786	0.2340	0.8677	0.1965	0.0883
384	3.1702	0.7606	0.2252	0.8503	0.1870	0.0855
386	3.1805	0.7429	0.2152	0.8354	0.1771	0.0791
388	3.0214	0.7261	0.2075	0.8228	0.1700	0.0762
390	3.0902	0.7106	0.2006	0.8112	0.1624	0.0723
392	2.9470	0.6987	0.1931	0.7992	0.1553	0.0686
394	3.1369	0.6871	0.1875	0.7926	0.1496	0.0658
396	3.1221	0.6760	0.1830	0.7823	0.1450	0.0635
398	3.2387	0.6655	0.1777	0.7800	0.1405	0.0605
400	2.8365	0.6568	0.1742	0.7719	0.1373	0.0586
402	2.8433	0.6499	0.1687	0.7685	0.1341	0.0565
404	2.9151	0.6408	0.1646	0.7659	0.1304	0.0544
406	2.7539	0.6336	0.1612	0.7620	0.1276	0.0528
408	3.2406	0.6270	0.1595	0.7584	0.1240	0.0515
410	2.9379	0.6199	0.1541	0.7548	0.1217	0.0492
412	2.7670	0.6146	0.1526	0.7515	0.1194	0.0484
414	2.9936	0.6058	0.1494	0.7500	0.1166	0.0465
416	3.0981	0.5997	0.1462	0.7446	0.1141	0.0457

Wavelength	1P312	1P3125	1P313	1P132	1P1325	1P133
418	2.8076	0.5937	0.1441	0.7413	0.1115	0.0446
420	3.1016	0.5853	0.1411	0.7390	0.1090	0.0432
422	2.7831	0.5785	0.1386	0.7340	0.1063	0.0424
424	2.7938	0.5717	0.1360	0.7300	0.1037	0.0412
426	2.8709	0.5647	0.1339	0.7269	0.1011	0.0405
428	2.8573	0.5572	0.1313	0.7212	0.0982	0.0392
430	2.9740	0.5497	0.1288	0.7180	0.0958	0.0383
432	2.7166	0.5417	0.1269	0.7137	0.0934	0.0375
434	2.7186	0.5355	0.1244	0.7088	0.0904	0.0367
436	2.7043	0.5273	0.1222	0.7070	0.0886	0.0356
438	2.9421	0.5215	0.1202	0.7022	0.0857	0.0351
440	2.7336	0.5149	0.1185	0.7011	0.0844	0.0345
442	2.7222	0.5106	0.1167	0.6982	0.0822	0.0337
444	2.6482	0.5038	0.1148	0.6956	0.0811	0.0334
446	2.6965	0.4990	0.1135	0.6946	0.0798	0.0327
448	2.5942	0.4954	0.1113	0.6952	0.0784	0.0320
450	2.6460	0.4918	0.1098	0.6960	0.0780	0.0316
452	2.6362	0.4880	0.1083	0.6984	0.0770	0.0314
454	2.6019	0.4862	0.1068	0.7005	0.0770	0.0312
456	2.5893	0.4835	0.1052	0.7048	0.0763	0.0302
458	2.5874	0.4817	0.1037	0.7096	0.0761	0.0299
460	2.6058	0.4819	0.1026	0.7171	0.0764	0.0297
462	2.5716	0.4838	0.1009	0.7290	0.0769	0.0290
464	2.5763	0.4850	0.0994	0.7400	0.0774	0.0286
466	2.5923	0.4880	0.0991	0.7557	0.0787	0.0287
468	2.5372	0.4935	0.0974	0.7747	0.0800	0.0282
470	2.5354	0.5020	0.0964	0.7990	0.0834	0.0278
472	2.5334	0.5105	0.0953	0.8277	0.0854	0.0280
474	2.5414	0.5206	0.0945	0.8572	0.0882	0.0277
476	2.5945	0.5322	0.0930	0.8913	0.0911	0.0275
478	2.6054	0.5460	0.0919	0.9283	0.0951	0.0274
480	2.4939	0.5627	0.0914	0.9735	0.0996	0.0274
482	2.5218	0.5806	0.0904	1.0252	0.1048	0.0269
484	2.5995	0.6002	0.0893	1.0717	0.1102	0.0268
486	2.6379	0.6159	0.0888	1.1206	0.1136	0.0258
488	2.5621	0.6355	0.0876	1.1677	0.1201	0.0267
490	2.5627	0.6572	0.0873	1.2214	0.1250	0.0268
492	2.5957	0.6780	0.0863	1.2796	0.1313	0.0267
494	2.5242	0.6964	0.0854	1.3180	0.1357	0.0264
496	2.5245	0.7143	0.0851	1.3690	0.1403	0.0271
498	2.6623	0.7256	0.0819	1.3909	0.1430	0.0265
500	2.5462	0.7311	0.0830	1.4188	0.1466	0.0259
502	2.6056	0.7386	0.0815	1.4353	0.1476	0.0257
504	2.5027	0.7385	0.0811	1.4459	0.1491	0.0261
506	2.6033	0.7387	0.0782	1.4403	0.1496	0.0254
508	2.5868	0.7302	0.0770	1.4236	0.1477	0.0247
510	2.4558	0.7104	0.0780	1.3826	0.1448	0.0250
512	2.4376	0.6853	0.0751	1.3434	0.1376	0.0230
514	2.4166	0.6577	0.0749	1.2774	0.1327	0.0240
516	2.3712	0.6309	0.0747	1.2167	0.1258	0.0240
518	2.3381	0.5980	0.0726	1.1522	0.1179	0.0228
520	2.2800	0.5700	0.0705	1.0766	0.1109	0.0224
522	2.1590	0.5319	0.0705	0.9936	0.1012	0.0224
524	2.0631	0.4944	0.0684	0.9098	0.0931	0.0213
526	2.0242	0.4539	0.0670	0.8257	0.0830	0.0209
528	1.9613	0.4196	0.0656	0.7462	0.0748	0.0199
530	1.8805	0.3885	0.0644	0.6798	0.0674	0.0194

Wavelength	1P312	1P3125	1P313	1P132	1P1325	1P133
532	1.7959	0.3645	0.0633	0.6258	0.0622	0.0191
534	1.7742	0.3475	0.0616	0.5860	0.0580	0.0183
536	1.7475	0.3299	0.0619	0.5509	0.0538	0.0191
538	1.6925	0.3189	0.0604	0.5215	0.0515	0.0178
540	1.6632	0.3065	0.0598	0.4963	0.0490	0.0178
542	1.6632	0.2980	0.0583	0.4752	0.0466	0.0167
544	1.6121	0.2878	0.0562	0.4587	0.0443	0.0172
546	1.5724	0.2851	0.0580	0.4444	0.0449	0.0177
548	1.5595	0.2773	0.0567	0.4318	0.0437	0.0167
550	1.5440	0.2720	0.0549	0.4193	0.0407	0.0169
552	1.5131	0.2688	0.0555	0.4120	0.0418	0.0158
554	1.4902	0.2652	0.0544	0.4031	0.0408	0.0156
556	1.4725	0.2605	0.0524	0.3932	0.0389	0.0157
558	1.4431	0.2592	0.0535	0.3886	0.0401	0.0149
560	1.4350	0.2542	0.0515	0.3791	0.0385	0.0145
562	1.4008	0.2512	0.0512	0.3708	0.0375	0.0156
564	1.3907	0.2471	0.0505	0.3643	0.0383	0.0147
566	1.3715	0.2434	0.0500	0.3577	0.0362	0.0146
568	1.3508	0.2433	0.0500	0.3535	0.0376	0.0143
570	1.3492	0.2397	0.0495	0.3482	0.0357	0.0138
572	1.3273	0.2381	0.0485	0.3442	0.0357	0.0134
574	1.3187	0.2351	0.0481	0.3394	0.0351	0.0134
576	1.2991	0.2325	0.0473	0.3338	0.0348	0.0129
578	1.2841	0.2293	0.0468	0.3288	0.0342	0.0126
580	1.2715	0.2274	0.0463	0.3243	0.0339	0.0125
582	1.2577	0.2231	0.0462	0.3192	0.0327	0.0121
584	1.2422	0.2222	0.0454	0.3151	0.0331	0.0126
586	1.2296	0.2192	0.0447	0.3107	0.0320	0.0119
588	1.2180	0.2170	0.0443	0.3070	0.0317	0.0121
590	1.2018	0.2142	0.0438	0.3021	0.0315	0.0121
592	1.1938	0.2129	0.0427	0.2986	0.0310	0.0123
594	1.1797	0.2100	0.0426	0.2943	0.0307	0.0117
596	1.1671	0.2072	0.0421	0.2899	0.0299	0.0117
598	1.1547	0.2041	0.0416	0.2856	0.0293	0.0116
600	1.1423	0.2024	0.0408	0.2816	0.0292	0.0115

1 cm cell						
Equilibration time	12 weeks	12 weeks	12 weeks	8 weeks	8 weeks	8 weeks
Type of Buffer	Ammonia 3:1	Ammonia 3:1	Ammonia 3:1	Ammonia 1:3	Ammonia 1:3	Ammonia 1:3
Final pH	9.11	9.10	9.10	10.19	10.2	10.19
Final[HS]/mM	9.05	2.86	0.58	9.6	2.7	0.96
Wavelength	1A312	1A3125	1A313	1A132	1A1325	1A133
200	1.7977	1.6977	1.5870	1.7458	1.7093	1.6729
202	1.8421	1.7775	1.8089	1.8485	1.8451	1.7320
204	1.9304	1.8638	1.9011	1.8813	1.9485	1.9826
206	2.0494	2.0113	1.9042	1.9909	2.0014	1.9302
208	2.0305	1.9288	1.9625	2.0466	2.0197	2.0500
210	2.0772	2.1000	2.0135	2.0314	2.0057	1.9807
212	2.1142	2.0021	1.9691	2.0207	2.1694	2.0355
214	2.0426	2.0756	2.0667	2.1205	2.1208	2.0910
216	2.3547	2.1042	2.0692	2.0799	2.1985	2.0870
218	2.1650	2.2333	2.3680	2.1983	2.1983	2.2864
220	2.3540	2.2407	2.2256	2.3369	2.3231	2.3647
222	2.4317	2.3733	2.3904	2.3981	2.4107	2.3506
224	2.4747	2.4617	2.4453	2.3708	2.4733	2.4615
226	2.5060	2.4371	2.5887	2.4758	2.5386	2.5732
228	2.6009	2.5085	2.5091	2.5316	2.5393	2.5087
230	2.5875	2.5215	2.5514	2.3779	2.4727	2.4938
232	2.6277	2.4718	2.4720	2.5527	2.5399	2.5837
234	2.4945	2.5295	2.4667	2.4765	2.4172	2.5366
236	2.6069	2.5500	2.4701	2.5692	2.5450	2.5316
238	2.5969	2.4934	2.4979	2.4597	2.6321	2.5086
240	2.6204	2.4855	2.4521	2.4524	2.3958	2.4677
242	2.6388	2.4809	2.5733	2.4495	2.5853	2.6056
244	2.6533	2.5886	2.5029	2.5374	2.5914	2.4818
246	2.7775	2.5585	2.7054	2.5359	2.6817	2.5245
248	2.6380	2.5894	2.4860	2.6600	2.5715	2.5947
250	2.7822	2.6298	2.5023	2.5265	2.7585	2.6391
252	2.8405	2.6663	2.2186	2.8660	2.6290	2.5073
254	2.7594	2.7996	1.8511	2.6664	2.7835	2.1118
256	2.7773	2.6368	1.4716	2.6702	2.5497	1.6918
258	2.7331	2.2591	1.1476	2.6770	2.2261	1.2944
260	2.7946	1.7591	0.8822	2.6959	1.6861	0.9793
262	2.4829	1.3235	0.6863	2.4389	1.2512	0.7441
264	2.1001	0.9858	0.5420	1.9706	0.9210	0.5733
266	1.5110	0.7288	0.4293	1.4305	0.6724	0.4412
268	1.1012	0.5395	0.3396	1.0076	0.4896	0.3412
270	0.8060	0.4065	0.2689	0.7040	0.3605	0.2649
272	0.6000	0.3087	0.2122	0.4918	0.2659	0.2045
274	0.4599	0.2384	0.1671	0.3462	0.1971	0.1581
276	0.3665	0.1874	0.1317	0.2474	0.1462	0.1219
278	0.3058	0.1504	0.1038	0.1809	0.1100	0.0931
280	0.2684	0.1245	0.0822	0.1373	0.0834	0.0731
282	0.2451	0.1064	0.0651	0.1080	0.0647	0.0562
284	0.2325	0.0950	0.0538	0.0904	0.0517	0.0450
286	0.2283	0.0863	0.0441	0.0772	0.0411	0.0348
288	0.2298	0.0810	0.0367	0.0688	0.0340	0.0282
290	0.2364	0.0784	0.0320	0.0642	0.0288	0.0231
292	0.2436	0.0770	0.0282	0.0617	0.0252	0.0193
294	0.2526	0.0770	0.0255	0.0602	0.0226	0.0163
296	0.2603	0.0764	0.0232	0.0596	0.0206	0.0137
298	0.2670	0.0757	0.0216	0.0595	0.0193	0.0123
300	0.2705	0.0746	0.0203	0.0594	0.0180	0.0107
302	0.2702	0.0725	0.0188	0.0588	0.0170	0.0095

Wavelength	1A312	1A3125	1A313	1A132	1A1325	1A133
304	0.2649	0.0693	0.0175	0.0571	0.0153	0.0081
306	0.2551	0.0646	0.0159	0.0551	0.0141	0.0074
308	0.2408	0.0591	0.0144	0.0516	0.0129	0.0063
310	0.2190	0.0524	0.0121	0.0476	0.0113	0.0056
312	0.1980	0.0456	0.0104	0.0433	0.0092	0.0046
314	0.1706	0.0390	0.0084	0.0374	0.0077	0.0038
316	0.1454	0.0319	0.0065	0.0315	0.0054	0.0027
318	0.1190	0.0261	0.0054	0.0252	0.0038	0.0017
320	0.0970	0.0199	0.0030	0.0201	0.0022	0.0010
322	0.0788	0.0167	0.0031	0.0161	0.0010	0.0004
324	0.0630	0.0126	0.0012	0.0128	0.0004	0.0005
326	0.0528	0.0104	-0.0001	0.0105	-0.0007	-0.0002
328	0.0467	0.0090	0.0006	0.0085	-0.0012	-0.0004
330	0.0419	0.0076	-0.0003	0.0077	-0.0017	-0.0009
332	0.0399	0.0066	-0.0005	0.0069	-0.0021	-0.0011
334	0.0383	0.0065	-0.0006	0.0069	-0.0015	-0.0006
336	0.0385	0.0068	0.0001	0.0066	-0.0014	-0.0010
338	0.0376	0.0060	-0.0006	0.0063	-0.0019	-0.0012
340	0.0374	0.0058	-0.0009	0.0067	-0.0016	-0.0004
342	0.0380	0.0063	-0.0005	0.0061	-0.0017	-0.0014
344	0.0382	0.0066	-0.0002	0.0061	-0.0019	-0.0013
346	0.0374	0.0060	-0.0005	0.0058	-0.0018	-0.0012
348	0.0372	0.0064	0.0001	0.0059	-0.0018	-0.0013
350	0.0369	0.0068	0.0004	0.0056	-0.0017	-0.0011
352	0.0366	0.0065	0.0003	0.0056	-0.0020	-0.0014
354	0.0357	0.0067	0.0006	0.0049	-0.0020	-0.0013
356	0.0344	0.0066	0.0001	0.0050	-0.0019	-0.0016
358	0.0338	0.0063	0.0006	0.0043	-0.0023	-0.0019
360	0.0328	0.0063	0.0005	0.0044	-0.0023	-0.0017
362	0.0309	0.0063	0.0008	0.0039	-0.0021	-0.0024
364	0.0302	0.0063	0.0006	0.0040	-0.0026	-0.0020
366	0.0276	0.0046	-0.0009	0.0035	-0.0022	-0.0026
368	0.0278	0.0057	0.0010	0.0030	-0.0027	-0.0021
370	0.0258	0.0048	0.0002	0.0023	-0.0031	-0.0028
372	0.0245	0.0046	0.0002	0.0020	-0.0027	-0.0028
374	0.0234	0.0042	0.0004	0.0017	-0.0031	-0.0027
376	0.0221	0.0041	0.0002	0.0025	-0.0028	-0.0021
378	0.0212	0.0041	0.0005	0.0012	-0.0032	-0.0027
380	0.0196	0.0028	-0.0007	0.0013	-0.0035	-0.0029
382	0.0192	0.0032	0.0003	0.0014	-0.0032	-0.0025
384	0.0184	0.0033	0.0000	0.0012	-0.0033	-0.0025
386	0.0170	0.0022	-0.0006	0.0009	-0.0032	-0.0027
388	0.0165	0.0022	-0.0004	0.0006	-0.0033	-0.0025
390	0.0166	0.0025	0.0001	0.0011	-0.0033	-0.0024
392	0.0161	0.0022	-0.0003	0.0006	-0.0025	-0.0022
394	0.0160	0.0022	-0.0007	0.0007	-0.0035	-0.0025
396	0.0153	0.0017	-0.0007	-0.0003	-0.0038	-0.0030
398	0.0150	0.0015	-0.0009	0.0013	-0.0033	-0.0020
400	0.0146	0.0012	-0.0005	0.0003	-0.0031	-0.0025
402	0.0147	0.0016	-0.0004	0.0007	-0.0032	-0.0024
404	0.0141	0.0013	-0.0008	0.0006	-0.0028	-0.0025
406	0.0148	0.0016	-0.0002	0.0005	-0.0034	-0.0028
408	0.0138	0.0008	-0.0008	0.0002	-0.0033	-0.0025
410	0.0146	0.0015	-0.0003	0.0008	-0.0029	-0.0023
412	0.0143	0.0013	-0.0005	0.0005	-0.0035	-0.0024
414	0.0137	0.0009	-0.0002	0.0003	-0.0035	-0.0027
416	0.0136	0.0011	-0.0006	0.0004	-0.0033	-0.0028

Wavelength	1A312	1A3125	1A313	1A132	1A1325	1A133
418	0.0131	0.0007	-0.0007	-0.0001	-0.0034	-0.0025
420	0.0131	0.0009	-0.0003	0.0004	-0.0033	-0.0022
422	0.0130	0.0008	-0.0007	0.0000	-0.0032	-0.0024
424	0.0124	0.0007	-0.0006	-0.0003	-0.0034	-0.0028
426	0.0122	0.0007	-0.0007	0.0000	-0.0032	-0.0026
428	0.0117	0.0005	0.0000	-0.0003	-0.0037	-0.0027
430	0.0110	0.0005	-0.0006	-0.0003	-0.0029	-0.0020
432	0.0107	0.0007	-0.0003	-0.0004	-0.0036	-0.0027
434	0.0097	0.0001	-0.0006	-0.0005	-0.0031	-0.0022
436	0.0099	0.0003	-0.0004	-0.0010	-0.0034	-0.0028
438	0.0093	0.0002	-0.0005	-0.0012	-0.0036	-0.0028
440	0.0091	0.0002	-0.0005	-0.0005	-0.0033	-0.0020
442	0.0087	0.0001	-0.0007	-0.0009	-0.0032	-0.0023
444	0.0082	-0.0001	-0.0008	-0.0011	-0.0033	-0.0024
446	0.0082	0.0001	-0.0005	-0.0010	-0.0033	-0.0026
448	0.0084	0.0002	-0.0002	-0.0010	-0.0033	-0.0026
450	0.0083	0.0001	-0.0006	-0.0012	-0.0037	-0.0027
452	0.0083	0.0002	-0.0002	-0.0008	-0.0033	-0.0026
454	0.0083	-0.0003	-0.0007	-0.0014	-0.0036	-0.0029
456	0.0082	0.0001	-0.0002	-0.0008	-0.0033	-0.0023
458	0.0082	0.0001	-0.0006	-0.0011	-0.0035	-0.0025
460	0.0085	0.0005	-0.0003	-0.0013	-0.0035	-0.0028
462	0.0090	0.0001	-0.0003	-0.0010	-0.0032	-0.0022
464	0.0094	0.0004	-0.0002	-0.0011	-0.0034	-0.0027
466	0.0093	0.0002	-0.0003	-0.0011	-0.0036	-0.0026
468	0.0103	0.0005	0.0001	-0.0008	-0.0032	-0.0027
470	0.0110	0.0005	0.0000	-0.0001	-0.0028	-0.0029
472	0.0121	0.0007	0.0000	-0.0005	-0.0031	-0.0024
474	0.0125	0.0002	-0.0005	0.0004	-0.0030	-0.0024
476	0.0139	0.0011	0.0003	0.0002	-0.0029	-0.0024
478	0.0147	0.0011	0.0002	0.0004	-0.0027	-0.0025
480	0.0156	0.0007	0.0003	0.0011	-0.0029	-0.0021
482	0.0171	0.0009	-0.0001	0.0014	-0.0021	-0.0024
484	0.0193	0.0011	0.0001	0.0015	-0.0029	-0.0022
486	0.0207	0.0020	0.0012	0.0010	-0.0034	-0.0036
488	0.0216	0.0015	0.0004	0.0019	-0.0031	-0.0034
490	0.0229	0.0010	-0.0002	0.0031	-0.0023	-0.0017
492	0.0248	0.0017	-0.0001	0.0034	-0.0020	-0.0017
494	0.0269	0.0023	0.0009	0.0037	-0.0024	-0.0028
496	0.0275	0.0025	0.0007	0.0043	-0.0014	-0.0015
498	0.0282	0.0014	-0.0002	0.0047	-0.0019	-0.0018
500	0.0288	0.0015	0.0005	0.0046	-0.0020	-0.0022
502	0.0301	0.0023	0.0006	0.0045	-0.0023	-0.0024
504	0.0303	0.0019	0.0003	0.0045	-0.0020	-0.0025
506	0.0298	0.0019	-0.0003	0.0054	-0.0014	-0.0020
508	0.0287	0.0020	0.0008	0.0050	-0.0016	-0.0020
510	0.0301	0.0028	0.0008	0.0050	-0.0014	-0.0019
512	0.0281	0.0012	0.0000	0.0042	-0.0017	-0.0018
514	0.0270	0.0022	0.0010	0.0045	-0.0019	-0.0023
516	0.0248	0.0020	0.0005	0.0029	-0.0023	-0.0026
518	0.0228	0.0017	0.0000	0.0038	-0.0013	-0.0010
520	0.0213	0.0014	0.0000	0.0025	-0.0020	-0.0023
522	0.0193	0.0012	-0.0001	0.0019	-0.0027	-0.0023
524	0.0166	0.0013	0.0008	0.0019	-0.0022	-0.0021
526	0.0151	0.0018	0.0001	0.0005	-0.0028	-0.0027
528	0.0127	0.0004	0.0004	0.0004	-0.0030	-0.0027
530	0.0121	0.0013	0.0007	-0.0006	-0.0031	-0.0027

Wavelength	1A312	1A3125	1A313	1A132	1A1325	1A133
532	0.0092	0.0011	-0.0003	-0.0002	-0.0027	-0.0028
534	0.0088	0.0007	0.0009	-0.0006	-0.0033	-0.0028
536	0.0073	0.0002	-0.0004	-0.0009	-0.0035	-0.0027
538	0.0068	-0.0002	-0.0004	-0.0013	-0.0036	-0.0032
540	0.0065	0.0003	-0.0001	-0.0013	-0.0033	-0.0032
542	0.0056	-0.0002	-0.0006	-0.0023	-0.0038	-0.0032
544	0.0054	-0.0002	-0.0002	-0.0019	-0.0040	-0.0039
546	0.0052	-0.0003	-0.0010	-0.0022	-0.0037	-0.0032
548	0.0046	-0.0001	0.0000	-0.0019	-0.0034	-0.0030
550	0.0047	-0.0003	-0.0011	-0.0027	-0.0045	-0.0036
552	0.0044	0.0001	-0.0005	-0.0020	-0.0036	-0.0031
554	0.0045	0.0002	-0.0005	-0.0028	-0.0040	-0.0038
556	0.0041	-0.0007	-0.0010	-0.0025	-0.0043	-0.0040
558	0.0039	0.0001	-0.0004	-0.0027	-0.0039	-0.0033
560	0.0045	0.0002	-0.0005	-0.0026	-0.0039	-0.0032
562	0.0042	-0.0001	-0.0005	-0.0027	-0.0044	-0.0038
564	0.0040	-0.0004	-0.0004	-0.0025	-0.0043	-0.0038
566	0.0034	-0.0007	-0.0007	-0.0033	-0.0052	-0.0038
568	0.0037	-0.0004	-0.0006	-0.0033	-0.0045	-0.0037
570	0.0035	-0.0004	-0.0006	-0.0032	-0.0045	-0.0043
572	0.0034	-0.0003	-0.0003	-0.0030	-0.0047	-0.0043
574	0.0036	-0.0001	-0.0002	-0.0037	-0.0051	-0.0046
576	0.0036	0.0000	-0.0001	-0.0033	-0.0049	-0.0044
578	0.0034	0.0002	0.0002	-0.0037	-0.0052	-0.0047
580	0.0035	0.0004	0.0002	-0.0036	-0.0052	-0.0047
582	0.0036	0.0006	0.0005	-0.0043	-0.0057	-0.0058
584	0.0037	0.0003	0.0004	-0.0034	-0.0050	-0.0046
586	0.0031	0.0000	-0.0002	-0.0039	-0.0054	-0.0049
588	0.0027	-0.0002	-0.0002	-0.0034	-0.0049	-0.0045
590	0.0030	-0.0003	-0.0006	-0.0031	-0.0047	-0.0044
592	0.0027	-0.0004	-0.0005	-0.0033	-0.0046	-0.0039
594	0.0024	-0.0005	-0.0007	-0.0031	-0.0048	-0.0041
596	0.0025	-0.0006	-0.0006	-0.0032	-0.0048	-0.0043
598	0.0022	-0.0004	-0.0006	-0.0031	-0.0045	-0.0040
600	0.0023	-0.0005	-0.0006	-0.0033	-0.0047	-0.0042

0.1 cm cell						
Equilibration time	8 weeks					
Type of Buffer	Phosphate 3:1	Phosphate 3:1	Phosphate 3:1	Phosphate 1:3	Phosphate 1:3	Phosphate 1:3
Final pH	6.49	6.43	6.36	7.47	7.33	7.31
Final[HS]/mM	4.7	0.92	0.13	6.3	1.8	0.63
Wavelength	0.1P312	0.1P3125	0.1P313	0.1P132	0.1P1325	0.1P133
200	1.9056	1.3154	0.8128	1.7078	1.3154	1.0741
202	1.9487	1.1967	0.7822	1.8626	1.1967	0.9942
204	1.8425	1.0897	0.7431	1.8010	1.0897	0.9100
206	1.8877	0.9779	0.6927	1.8128	0.9779	0.8294
208	1.7495	0.8812	0.6483	1.6817	0.8812	0.7637
210	1.7695	0.8199	0.5966	1.6295	0.8199	0.6922
212	1.6971	0.7899	0.5574	1.6074	0.7899	0.6457
214	1.7490	0.7777	0.5240	1.7327	0.7777	0.6071
216	1.7104	0.7992	0.5015	1.8017	0.7992	0.5903
218	1.7885	0.8411	0.4929	1.9756	0.8411	0.5887
220	1.8308	0.8975	0.4895	2.1356	0.8975	0.6068
222	1.8616	0.9553	0.4915	2.3257	0.9553	0.6324
224	1.9266	1.0116	0.4927	2.4512	1.0116	0.6560
226	1.9545	1.0627	0.4901	2.6175	1.0627	0.6757
228	1.9988	1.0854	0.4810	2.5998	1.0854	0.6867
230	1.9748	1.0969	0.4654	2.5987	1.0969	0.6874
232	1.9352	1.0811	0.4453	2.5828	1.0811	0.6772
234	1.9043	1.0424	0.4209	2.6941	1.0424	0.6510
236	1.8053	0.9823	0.3973	2.4476	0.9823	0.6217
238	1.7372	0.9104	0.3732	2.4053	0.9104	0.5823
240	1.6373	0.8276	0.3492	2.2992	0.8276	0.5348
242	1.5434	0.7404	0.3301	2.1196	0.7404	0.4880
244	1.4456	0.6484	0.3068	1.8499	0.6484	0.4317
246	1.3606	0.5626	0.2852	1.5928	0.5626	0.3796
248	1.2773	0.4809	0.2625	1.3431	0.4809	0.3264
250	1.2083	0.4071	0.2403	1.1248	0.4071	0.2755
252	1.1463	0.3448	0.2204	0.9373	0.3448	0.2348
254	1.0917	0.2925	0.2002	0.7840	0.2925	0.1948
256	1.0466	0.2501	0.1842	0.6643	0.2501	0.1642
258	1.0064	0.2193	0.1734	0.5706	0.2193	0.1412
260	0.9736	0.1965	0.1649	0.5022	0.1965	0.1226
262	0.9458	0.1823	0.1611	0.4534	0.1823	0.1110
264	0.9241	0.1752	0.1603	0.4225	0.1752	0.1040
266	0.9038	0.1730	0.1632	0.4033	0.1730	0.1006
268	0.8902	0.1748	0.1669	0.3945	0.1748	0.0988
270	0.8743	0.1777	0.1713	0.3921	0.1777	0.0990
272	0.8622	0.1842	0.1773	0.3945	0.1842	0.1001
274	0.8569	0.1923	0.1854	0.4000	0.1923	0.1010
276	0.8495	0.2027	0.1936	0.4085	0.2027	0.1068
278	0.8417	0.2116	0.2022	0.4184	0.2116	0.1083
280	0.8397	0.2233	0.2120	0.4291	0.2233	0.1154
282	0.8349	0.2347	0.2226	0.4450	0.2347	0.1201
284	0.8381	0.2499	0.2353	0.4621	0.2499	0.1270
286	0.8379	0.2652	0.2497	0.4831	0.2652	0.1350
288	0.8424	0.2845	0.2664	0.5077	0.2845	0.1436
290	0.8500	0.3011	0.2822	0.5354	0.3011	0.1524
292	0.8577	0.3207	0.2981	0.5651	0.3207	0.1618
294	0.8668	0.3377	0.3118	0.5949	0.3377	0.1700
296	0.8763	0.3506	0.3230	0.6226	0.3506	0.1762
298	0.8835	0.3587	0.3282	0.6472	0.3587	0.1795
300	0.8872	0.3597	0.3277	0.6645	0.3597	0.1794

Wavelength	0.1P312	0.1P3125	0.1P313	0.1P132	0.1P1325	0.1P133
302	0.8865	0.3543	0.3204	0.6744	0.3543	0.1751
304	0.8820	0.3409	0.3060	0.6738	0.3409	0.1674
306	0.8693	0.3187	0.2850	0.6610	0.3187	0.1557
308	0.8506	0.2939	0.2597	0.6357	0.2939	0.1417
310	0.8229	0.2605	0.2301	0.5951	0.2605	0.1249
312	0.7869	0.2290	0.1986	0.5444	0.2290	0.1076
314	0.7471	0.1919	0.1693	0.4839	0.1919	0.0910
316	0.7017	0.1613	0.1398	0.4199	0.1613	0.0745
318	0.6565	0.1309	0.1149	0.3556	0.1309	0.0604
320	0.6154	0.1051	0.0936	0.2973	0.1051	0.0480
322	0.5781	0.0847	0.0764	0.2476	0.0847	0.0389
324	0.5508	0.0690	0.0637	0.2107	0.0690	0.0319
326	0.5281	0.0582	0.0542	0.1841	0.0582	0.0260
328	0.5116	0.0505	0.0484	0.1673	0.0505	0.0238
330	0.5013	0.0464	0.0444	0.1569	0.0464	0.0211
332	0.4899	0.0436	0.0422	0.1515	0.0436	0.0199
334	0.4828	0.0426	0.0409	0.1474	0.0426	0.0195
336	0.4750	0.0419	0.0407	0.1457	0.0419	0.0195
338	0.4690	0.0424	0.0401	0.1447	0.0424	0.0195
340	0.4626	0.0423	0.0407	0.1429	0.0423	0.0197
342	0.4562	0.0427	0.0402	0.1423	0.0427	0.0202
344	0.4501	0.0428	0.0407	0.1408	0.0428	0.0200
346	0.4440	0.0428	0.0406	0.1387	0.0428	0.0201
348	0.4375	0.0426	0.0406	0.1374	0.0426	0.0206
350	0.4315	0.0425	0.0402	0.1348	0.0425	0.0199
352	0.4263	0.0418	0.0392	0.1322	0.0418	0.0197
354	0.4191	0.0410	0.0389	0.1293	0.0410	0.0197
356	0.4139	0.0395	0.0370	0.1259	0.0395	0.0185
358	0.4070	0.0387	0.0360	0.1228	0.0387	0.0184
360	0.4021	0.0373	0.0350	0.1197	0.0373	0.0177
362	0.3954	0.0351	0.0336	0.1153	0.0351	0.0167
364	0.3909	0.0339	0.0321	0.1123	0.0339	0.0164
366	0.3854	0.0322	0.0306	0.1088	0.0322	0.0155
368	0.3794	0.0297	0.0279	0.1027	0.0297	0.0144
370	0.3752	0.0288	0.0274	0.1003	0.0288	0.0132
372	0.3698	0.0264	0.0257	0.0984	0.0264	0.0129
374	0.3644	0.0256	0.0238	0.0941	0.0256	0.0117
376	0.3622	0.0237	0.0219	0.0917	0.0237	0.0105
378	0.3576	0.0224	0.0211	0.0889	0.0224	0.0105
380	0.3532	0.0208	0.0202	0.0880	0.0208	0.0100
382	0.3505	0.0204	0.0197	0.0840	0.0204	0.0100
384	0.3459	0.0196	0.0175	0.0842	0.0196	0.0087
386	0.3440	0.0179	0.0173	0.0811	0.0179	0.0083
388	0.3412	0.0172	0.0159	0.0804	0.0172	0.0077
390	0.3381	0.0163	0.0152	0.0792	0.0163	0.0070
392	0.3360	0.0159	0.0152	0.0782	0.0159	0.0072
394	0.3330	0.0149	0.0141	0.0767	0.0149	0.0071
396	0.3310	0.0146	0.0132	0.0755	0.0146	0.0067
398	0.3293	0.0142	0.0131	0.0757	0.0142	0.0063
400	0.3271	0.0132	0.0123	0.0749	0.0132	0.0061
402	0.3255	0.0142	0.0119	0.0748	0.0142	0.0056
404	0.3237	0.0127	0.0116	0.0738	0.0127	0.0056
406	0.3213	0.0125	0.0112	0.0734	0.0125	0.0058
408	0.3196	0.0132	0.0112	0.0738	0.0132	0.0059
410	0.3173	0.0119	0.0107	0.0726	0.0119	0.0051
412	0.3159	0.0121	0.0104	0.0728	0.0121	0.0055
414	0.3132	0.0114	0.0099	0.0722	0.0114	0.0047

Wavelength	0.1P312	0.1P3125	0.1P313	0.1P132	0.1P1325	0.1P133
416	0.3120	0.0115	0.0098	0.0717	0.0115	0.0053
418	0.3098	0.0118	0.0096	0.0715	0.0118	0.0050
420	0.3081	0.0110	0.0092	0.0713	0.0110	0.0045
422	0.3060	0.0110	0.0092	0.0708	0.0110	0.0047
424	0.3050	0.0103	0.0087	0.0699	0.0103	0.0044
426	0.3014	0.0102	0.0083	0.0695	0.0102	0.0040
428	0.2985	0.0096	0.0078	0.0689	0.0096	0.0044
430	0.2965	0.0095	0.0080	0.0689	0.0095	0.0041
432	0.2962	0.0095	0.0076	0.0682	0.0095	0.0041
434	0.2921	0.0092	0.0071	0.0680	0.0092	0.0039
436	0.2896	0.0088	0.0074	0.0676	0.0088	0.0041
438	0.2875	0.0086	0.0072	0.0668	0.0086	0.0042
440	0.2869	0.0083	0.0067	0.0668	0.0083	0.0038
442	0.2843	0.0086	0.0069	0.0668	0.0086	0.0039
444	0.2822	0.0082	0.0064	0.0669	0.0082	0.0037
446	0.2803	0.0082	0.0063	0.0666	0.0082	0.0036
448	0.2778	0.0079	0.0060	0.0665	0.0079	0.0037
450	0.2757	0.0080	0.0061	0.0663	0.0080	0.0035
452	0.2738	0.0078	0.0060	0.0665	0.0078	0.0035
454	0.2717	0.0076	0.0056	0.0670	0.0076	0.0037
456	0.2704	0.0079	0.0057	0.0672	0.0079	0.0039
458	0.2685	0.0078	0.0053	0.0677	0.0078	0.0032
460	0.2672	0.0077	0.0055	0.0683	0.0077	0.0036
462	0.2648	0.0077	0.0048	0.0698	0.0077	0.0033
464	0.2653	0.0078	0.0049	0.0705	0.0078	0.0035
466	0.2641	0.0079	0.0049	0.0719	0.0079	0.0032
468	0.2628	0.0076	0.0046	0.0735	0.0076	0.0033
470	0.2626	0.0088	0.0049	0.0768	0.0088	0.0036
472	0.2617	0.0084	0.0047	0.0795	0.0084	0.0036
474	0.2623	0.0090	0.0054	0.0819	0.0090	0.0036
476	0.2623	0.0089	0.0044	0.0851	0.0089	0.0036
478	0.2636	0.0098	0.0041	0.0888	0.0098	0.0034
480	0.2653	0.0099	0.0039	0.0936	0.0099	0.0030
482	0.2664	0.0106	0.0040	0.0989	0.0106	0.0032
484	0.2670	0.0105	0.0040	0.1029	0.0105	0.0032
486	0.2685	0.0105	0.0033	0.1063	0.0105	0.0033
488	0.2720	0.0117	0.0042	0.1131	0.0117	0.0032
490	0.2713	0.0119	0.0040	0.1167	0.0119	0.0033
492	0.2727	0.0128	0.0035	0.1237	0.0128	0.0028
494	0.2734	0.0130	0.0037	0.1278	0.0130	0.0027
496	0.2744	0.0136	0.0036	0.1317	0.0136	0.0034
498	0.2746	0.0131	0.0034	0.1346	0.0131	0.0032
500	0.2744	0.0141	0.0033	0.1365	0.0141	0.0035
502	0.2726	0.0143	0.0034	0.1390	0.0143	0.0031
504	0.2715	0.0143	0.0030	0.1395	0.0143	0.0034
506	0.2696	0.0138	0.0026	0.1395	0.0138	0.0027
508	0.2658	0.0138	0.0030	0.1381	0.0138	0.0033
510	0.2624	0.0134	0.0032	0.1362	0.0134	0.0031
512	0.2571	0.0133	0.0027	0.1308	0.0133	0.0027
514	0.2507	0.0126	0.0031	0.1240	0.0126	0.0036
516	0.2437	0.0115	0.0029	0.1179	0.0115	0.0029
518	0.2377	0.0112	0.0016	0.1117	0.0112	0.0016
520	0.2302	0.0105	0.0027	0.1045	0.0105	0.0034
522	0.2234	0.0100	0.0025	0.0967	0.0100	0.0025
524	0.2157	0.0090	0.0021	0.0884	0.0090	0.0034
526	0.2077	0.0081	0.0023	0.0792	0.0081	0.0022
528	0.1993	0.0077	0.0015	0.0715	0.0077	0.0026

Wavelength	0.1P312	0.1P3125	0.1P313	0.1P132	0.1P1325	0.1P133
530	0.1939	0.0067	0.0017	0.0642	0.0067	0.0028
532	0.1873	0.0058	0.0012	0.0601	0.0058	0.0024
534	0.1834	0.0060	0.0014	0.0551	0.0060	0.0018
536	0.1781	0.0045	0.0002	0.0516	0.0045	0.0020
538	0.1748	0.0054	0.0015	0.0489	0.0054	0.0028
540	0.1705	0.0050	0.0011	0.0469	0.0050	0.0019
542	0.1671	0.0045	0.0004	0.0441	0.0045	0.0019
544	0.1629	0.0039	0.0001	0.0411	0.0039	0.0018
546	0.1616	0.0040	0.0013	0.0420	0.0040	0.0028
548	0.1590	0.0043	0.0002	0.0401	0.0043	0.0019
550	0.1552	0.0046	-0.0001	0.0375	0.0046	0.0011
552	0.1551	0.0040	0.0009	0.0385	0.0040	0.0028
554	0.1520	0.0035	0.0001	0.0366	0.0035	0.0012
556	0.1485	0.0043	0.0005	0.0349	0.0043	0.0026
558	0.1481	0.0037	0.0001	0.0352	0.0037	0.0020
560	0.1458	0.0041	0.0002	0.0344	0.0041	0.0021
562	0.1422	0.0037	-0.0003	0.0324	0.0037	0.0009
564	0.1401	0.0037	-0.0002	0.0323	0.0037	0.0015
566	0.1375	0.0035	-0.0003	0.0311	0.0035	0.0021
568	0.1370	0.0034	-0.0005	0.0323	0.0034	0.0017
570	0.1355	0.0030	-0.0011	0.0310	0.0030	0.0012
572	0.1346	0.0035	-0.0005	0.0305	0.0035	0.0017
574	0.1325	0.0031	-0.0005	0.0299	0.0031	0.0016
576	0.1309	0.0032	-0.0009	0.0295	0.0032	0.0016
578	0.1293	0.0032	-0.0009	0.0289	0.0032	0.0016
580	0.1280	0.0029	-0.0011	0.0285	0.0029	0.0013
582	0.1267	0.0031	-0.0010	0.0277	0.0031	0.0015
584	0.1256	0.0030	-0.0013	0.0278	0.0030	0.0014
586	0.1238	0.0028	-0.0011	0.0271	0.0028	0.0013
588	0.1222	0.0028	-0.0013	0.0263	0.0028	0.0013
590	0.1217	0.0028	-0.0011	0.0263	0.0028	0.0012
592	0.1198	0.0028	-0.0009	0.0253	0.0028	0.0016
594	0.1182	0.0027	-0.0015	0.0258	0.0027	0.0009
596	0.1180	0.0027	-0.0004	0.0247	0.0027	0.0017
598	0.1160	0.0023	-0.0015	0.0249	0.0023	0.0010
600	0.1143	0.0025	-0.0015	0.0244	0.0025	0.0010

0.1 cm cell						
Equilibration time	12 weeks	12 weeks	12 weeks	8 weeks	8 weeks	8 weeks
Type of Buffer	Ammonia 3:1	Ammonia 3:1	Ammonia 3:1	Ammonia 1:3	Ammonia 1:3	Ammonia 1:3
Final pH	9.11	9.10	9.10	10.19	10.2	10.19
Final[HS]/mM	9.05	2.86	0.58	9.6	2.7	0.96
Wavelength	0.1A312	0.1A3125	0.1A313	0.1A132	0.1A1325	0.1A133
200	1.7137	1.5048	1.2343	1.7510	1.5964	1.4516
202	1.8519	1.6159	1.0965	1.8360	1.6725	1.3135
204	1.9048	1.5853	1.0226	1.9386	1.6378	1.1745
206	1.9844	1.4792	0.9539	1.9819	1.5313	1.0534
208	2.0001	1.4273	0.9080	2.0311	1.4343	0.9646
210	2.1013	1.3745	0.8491	1.9966	1.3955	0.8967
212	2.0290	1.3897	0.8181	2.0139	1.3861	0.8481
214	2.1179	1.4132	0.7786	2.0930	1.4076	0.8176
216	2.1274	1.4928	0.7681	2.1448	1.5014	0.8231
218	2.3094	1.6084	0.7724	2.2774	1.5930	0.8528
220	2.2764	1.7809	0.7980	2.2563	1.7560	0.9054
222	2.3367	1.9300	0.8289	2.4057	1.9195	0.9630
224	2.5146	2.0547	0.8650	2.4876	2.0783	1.0249
226	2.4801	2.2166	0.8930	2.5633	2.1909	1.0911
228	2.5417	2.2351	0.9125	2.4901	2.2466	1.1362
230	2.5087	2.3030	0.9181	2.5347	2.2852	1.1622
232	2.5360	2.3467	0.9105	2.5800	2.2921	1.1617
234	2.4650	2.2660	0.8857	2.4973	2.2928	1.1424
236	2.5165	2.2219	0.8464	2.5329	2.1723	1.0954
238	2.5178	2.1144	0.7905	2.4860	2.1206	1.0222
240	2.5299	1.9672	0.7247	2.5218	1.9393	0.9327
242	2.5052	1.8049	0.6523	2.5054	1.7528	0.8318
244	2.5303	1.5590	0.5667	2.5336	1.5234	0.7205
246	2.6094	1.3086	0.4864	2.5532	1.2794	0.6100
248	2.3820	1.0666	0.4036	2.4223	1.0413	0.5023
250	2.0768	0.8509	0.3283	2.1922	0.8286	0.4042
252	1.6730	0.6621	0.2644	1.7602	0.6445	0.3204
254	1.2810	0.5036	0.2060	1.3427	0.4866	0.2472
256	0.9545	0.3775	0.1598	1.0031	0.3638	0.1888
258	0.6957	0.2799	0.1238	0.7281	0.2686	0.1435
260	0.4978	0.2039	0.0945	0.5176	0.1944	0.1075
262	0.3519	0.1488	0.0734	0.3621	0.1401	0.0811
264	0.2474	0.1093	0.0583	0.2500	0.1020	0.0627
266	0.1744	0.0809	0.0467	0.1713	0.0746	0.0488
268	0.1252	0.0604	0.0377	0.1189	0.0546	0.0385
270	0.0902	0.0468	0.0305	0.0815	0.0405	0.0301
272	0.0681	0.0359	0.0247	0.0572	0.0304	0.0239
274	0.0529	0.0284	0.0199	0.0407	0.0233	0.0192
276	0.0431	0.0238	0.0163	0.0295	0.0179	0.0155
278	0.0371	0.0202	0.0141	0.0217	0.0138	0.0123
280	0.0331	0.0174	0.0116	0.0174	0.0114	0.0110
282	0.0305	0.0154	0.0098	0.0137	0.0093	0.0083
284	0.0296	0.0145	0.0091	0.0117	0.0077	0.0073
286	0.0290	0.0135	0.0075	0.0106	0.0069	0.0068
288	0.0287	0.0126	0.0065	0.0096	0.0062	0.0059
290	0.0300	0.0125	0.0066	0.0089	0.0055	0.0057
292	0.0307	0.0128	0.0059	0.0087	0.0052	0.0051
294	0.0316	0.0125	0.0056	0.0085	0.0050	0.0047
296	0.0325	0.0123	0.0056	0.0083	0.0044	0.0045
298	0.0332	0.0126	0.0052	0.0086	0.0047	0.0045
300	0.0334	0.0124	0.0051	0.0079	0.0043	0.0041

Wavelength	0.1A312	0.1A3125	0.1A313	0.1A132	0.1A1325	0.1A133
302	0.0336	0.0123	0.0051	0.0083	0.0043	0.0045
304	0.0327	0.0116	0.0046	0.0079	0.0041	0.0041
306	0.0321	0.0115	0.0047	0.0077	0.0042	0.0042
308	0.0305	0.0108	0.0046	0.0072	0.0035	0.0039
310	0.0285	0.0104	0.0043	0.0068	0.0034	0.0039
312	0.0263	0.0093	0.0040	0.0064	0.0037	0.0044
314	0.0235	0.0090	0.0039	0.0056	0.0027	0.0037
316	0.0212	0.0086	0.0039	0.0047	0.0027	0.0036
318	0.0186	0.0075	0.0038	0.0043	0.0022	0.0039
320	0.0164	0.0077	0.0036	0.0036	0.0022	0.0034
322	0.0145	0.0069	0.0032	0.0037	0.0023	0.0038
324	0.0127	0.0066	0.0035	0.0024	0.0017	0.0032
326	0.0121	0.0068	0.0036	0.0024	0.0018	0.0032
328	0.0117	0.0063	0.0033	0.0023	0.0012	0.0036
330	0.0109	0.0060	0.0031	0.0018	0.0012	0.0033
332	0.0104	0.0060	0.0029	0.0016	0.0009	0.0030
334	0.0107	0.0060	0.0033	0.0019	0.0015	0.0036
336	0.0107	0.0061	0.0032	0.0020	0.0014	0.0036
338	0.0111	0.0068	0.0038	0.0017	0.0012	0.0038
340	0.0105	0.0060	0.0030	0.0015	0.0016	0.0034
342	0.0107	0.0067	0.0031	0.0017	0.0012	0.0036
344	0.0111	0.0067	0.0037	0.0019	0.0011	0.0038
346	0.0108	0.0063	0.0029	0.0015	0.0009	0.0039
348	0.0109	0.0066	0.0032	0.0016	0.0009	0.0037
350	0.0106	0.0063	0.0032	0.0014	0.0010	0.0037
352	0.0109	0.0065	0.0033	0.0014	0.0013	0.0040
354	0.0107	0.0068	0.0037	0.0015	0.0009	0.0038
356	0.0104	0.0064	0.0033	0.0015	0.0009	0.0041
358	0.0102	0.0063	0.0034	0.0010	0.0005	0.0038
360	0.0107	0.0065	0.0038	0.0009	0.0001	0.0035
362	0.0102	0.0061	0.0034	0.0010	0.0005	0.0037
364	0.0101	0.0061	0.0034	0.0010	0.0003	0.0035
366	0.0096	0.0059	0.0032	0.0010	0.0003	0.0039
368	0.0099	0.0060	0.0032	0.0006	0.0002	0.0038
370	0.0097	0.0066	0.0033	0.0006	0.0000	0.0039
372	0.0095	0.0061	0.0031	0.0011	0.0002	0.0043
374	0.0094	0.0058	0.0032	0.0004	0.0001	0.0037
376	0.0089	0.0061	0.0031	0.0003	0.0002	0.0042
378	0.0090	0.0056	0.0031	0.0005	-0.0001	0.0039
380	0.0085	0.0059	0.0030	0.0006	-0.0004	0.0040
382	0.0087	0.0062	0.0029	0.0000	-0.0001	0.0046
384	0.0083	0.0058	0.0033	0.0009	0.0002	0.0043
386	0.0083	0.0060	0.0031	0.0000	0.0000	0.0046
388	0.0090	0.0063	0.0035	0.0000	-0.0004	0.0040
390	0.0091	0.0063	0.0037	0.0007	-0.0001	0.0047
392	0.0082	0.0054	0.0029	0.0004	0.0001	0.0043
394	0.0089	0.0068	0.0037	0.0002	0.0001	0.0046
396	0.0084	0.0061	0.0034	0.0005	0.0000	0.0042
398	0.0090	0.0066	0.0037	-0.0002	-0.0001	0.0049
400	0.0086	0.0060	0.0036	0.0003	-0.0002	0.0046
402	0.0086	0.0061	0.0035	-0.0001	-0.0006	0.0043
404	0.0088	0.0062	0.0031	0.0000	-0.0002	0.0047
406	0.0083	0.0059	0.0030	0.0002	0.0002	0.0047
408	0.0085	0.0066	0.0036	0.0005	-0.0001	0.0046
410	0.0087	0.0063	0.0034	0.0001	-0.0004	0.0046
412	0.0086	0.0063	0.0034	0.0001	-0.0002	0.0047
414	0.0085	0.0061	0.0034	-0.0002	-0.0004	0.0043

Wavelength	0.1A312	0.1A3125	0.1A313	0.1A132	0.1A1325	0.1A133
416	0.0087	0.0064	0.0032	0.0004	0.0002	0.0054
418	0.0086	0.0062	0.0036	0.0001	-0.0004	0.0043
420	0.0086	0.0062	0.0033	-0.0001	-0.0002	0.0049
422	0.0089	0.0064	0.0036	-0.0002	-0.0003	0.0048
424	0.0085	0.0062	0.0035	0.0000	-0.0002	0.0047
426	0.0084	0.0061	0.0033	-0.0002	-0.0003	0.0049
428	0.0085	0.0064	0.0034	-0.0001	-0.0003	0.0046
430	0.0079	0.0062	0.0032	-0.0004	-0.0003	0.0050
432	0.0085	0.0061	0.0037	0.0003	0.0001	0.0048
434	0.0085	0.0067	0.0036	-0.0002	-0.0002	0.0048
436	0.0086	0.0064	0.0038	0.0000	-0.0003	0.0049
438	0.0081	0.0064	0.0035	-0.0004	-0.0004	0.0050
440	0.0083	0.0062	0.0037	-0.0005	-0.0004	0.0049
442	0.0081	0.0062	0.0036	-0.0002	-0.0006	0.0048
444	0.0083	0.0063	0.0038	0.0002	0.0001	0.0053
446	0.0082	0.0060	0.0037	-0.0002	-0.0002	0.0051
448	0.0084	0.0067	0.0038	0.0000	-0.0002	0.0050
450	0.0083	0.0065	0.0039	-0.0002	-0.0002	0.0050
452	0.0088	0.0067	0.0040	0.0001	-0.0001	0.0052
454	0.0082	0.0063	0.0037	0.0000	-0.0002	0.0052
456	0.0085	0.0062	0.0038	-0.0001	-0.0002	0.0054
458	0.0081	0.0065	0.0037	0.0000	-0.0001	0.0053
460	0.0085	0.0063	0.0036	-0.0002	-0.0006	0.0048
462	0.0084	0.0066	0.0039	0.0000	0.0000	0.0057
464	0.0083	0.0066	0.0035	0.0001	-0.0005	0.0051
466	0.0088	0.0066	0.0042	0.0000	-0.0002	0.0053
468	0.0088	0.0067	0.0041	0.0002	0.0000	0.0055
470	0.0091	0.0070	0.0042	0.0004	-0.0003	0.0056
472	0.0093	0.0066	0.0038	0.0008	0.0007	0.0060
474	0.0088	0.0063	0.0037	-0.0001	0.0002	0.0055
476	0.0095	0.0074	0.0043	0.0000	-0.0002	0.0055
478	0.0093	0.0069	0.0040	0.0005	0.0001	0.0057
480	0.0092	0.0067	0.0041	0.0002	-0.0002	0.0058
482	0.0094	0.0069	0.0039	0.0007	0.0004	0.0058
484	0.0096	0.0067	0.0039	0.0001	-0.0002	0.0054
486	0.0099	0.0073	0.0043	0.0000	-0.0002	0.0061
488	0.0098	0.0063	0.0036	0.0001	-0.0005	0.0050
490	0.0103	0.0072	0.0041	0.0010	0.0004	0.0058
492	0.0101	0.0066	0.0038	-0.0002	-0.0002	0.0055
494	0.0103	0.0072	0.0038	0.0013	0.0000	0.0055
496	0.0108	0.0069	0.0037	0.0004	0.0000	0.0052
498	0.0111	0.0074	0.0043	0.0008	0.0002	0.0060
500	0.0106	0.0071	0.0039	0.0006	0.0002	0.0057
502	0.0110	0.0069	0.0036	0.0005	0.0004	0.0052
504	0.0108	0.0066	0.0038	0.0005	-0.0004	0.0056
506	0.0113	0.0071	0.0043	0.0004	-0.0002	0.0057
508	0.0108	0.0074	0.0038	0.0009	-0.0001	0.0056
510	0.0107	0.0066	0.0034	0.0009	0.0003	0.0058
512	0.0106	0.0063	0.0039	0.0006	-0.0004	0.0053
514	0.0108	0.0066	0.0032	0.0009	0.0000	0.0053
516	0.0117	0.0074	0.0044	0.0005	-0.0008	0.0050
518	0.0103	0.0068	0.0042	0.0001	-0.0004	0.0058
520	0.0102	0.0064	0.0033	0.0010	-0.0002	0.0056
522	0.0098	0.0064	0.0037	0.0008	0.0001	0.0052
524	0.0098	0.0064	0.0037	-0.0001	-0.0008	0.0047
526	0.0080	0.0058	0.0034	-0.0005	-0.0006	0.0054
528	0.0084	0.0066	0.0032	-0.0001	-0.0008	0.0050

Wavelength	0.1A312	0.1A3125	0.1A313	0.1A132	0.1A1325	0.1A133
530	0.0090	0.0064	0.0037	0.0000	-0.0005	0.0055
532	0.0078	0.0055	0.0027	-0.0008	-0.0014	0.0045
534	0.0088	0.0069	0.0039	-0.0011	-0.0003	0.0051
536	0.0084	0.0063	0.0033	-0.0002	-0.0009	0.0050
538	0.0079	0.0067	0.0036	-0.0002	0.0000	0.0060
540	0.0085	0.0064	0.0042	-0.0006	-0.0017	0.0043
542	0.0077	0.0060	0.0033	-0.0002	-0.0002	0.0056
544	0.0079	0.0060	0.0034	-0.0010	-0.0012	0.0054
546	0.0086	0.0070	0.0044	-0.0006	-0.0007	0.0046
548	0.0075	0.0061	0.0033	-0.0007	-0.0007	0.0058
550	0.0073	0.0060	0.0034	-0.0008	-0.0014	0.0048
552	0.0081	0.0061	0.0031	-0.0009	-0.0007	0.0054
554	0.0078	0.0064	0.0034	-0.0014	-0.0011	0.0045
556	0.0063	0.0051	0.0033	-0.0007	-0.0004	0.0053
558	0.0080	0.0070	0.0040	-0.0009	-0.0012	0.0049
560	0.0082	0.0066	0.0031	-0.0002	-0.0006	0.0054
562	0.0059	0.0049	0.0036	-0.0014	-0.0018	0.0040
564	0.0085	0.0074	0.0036	-0.0009	-0.0007	0.0056
566	0.0066	0.0055	0.0034	-0.0009	-0.0009	0.0052
568	0.0079	0.0061	0.0032	-0.0009	-0.0009	0.0056
570	0.0081	0.0071	0.0038	-0.0011	-0.0012	0.0050
572	0.0077	0.0064	0.0036	-0.0011	-0.0012	0.0052
574	0.0079	0.0068	0.0035	-0.0010	-0.0009	0.0056
576	0.0080	0.0065	0.0038	-0.0009	-0.0009	0.0058
578	0.0081	0.0069	0.0042	-0.0013	-0.0015	0.0054
580	0.0078	0.0069	0.0038	-0.0010	-0.0009	0.0062
582	0.0082	0.0070	0.0043	-0.0018	-0.0018	0.0051
584	0.0081	0.0069	0.0040	-0.0007	-0.0006	0.0063
586	0.0080	0.0068	0.0039	-0.0014	-0.0015	0.0051
588	0.0078	0.0066	0.0037	-0.0011	-0.0008	0.0054
590	0.0078	0.0066	0.0039	-0.0010	-0.0013	0.0049
592	0.0074	0.0063	0.0035	-0.0008	-0.0011	0.0051
594	0.0075	0.0068	0.0036	-0.0012	-0.0009	0.0053
596	0.0072	0.0057	0.0033	-0.0011	-0.0014	0.0046
598	0.0074	0.0067	0.0036	-0.0010	-0.0008	0.0051
600	0.0075	0.0066	0.0036	-0.0009	-0.0009	0.0052

References

- Adelson J. M., Helz G. R., and Miller C. V. (2001) Reconstructing the Rise of Recent Coastal Anoxia; Molybdenum in Chesapeake Bay Sediments. *Geochimica et Cosmochimica Acta* **65**, 237-252.
- Anbar A. D., Creaser R.A., Papanastassiou D.A. and Wasserburg G.J. (1992) Rhenium in Seawater - Confirmation of Generally Conservative Behavior. *Geochimica et Cosmochimica Acta* **56**, 4099-4103.
- Balistreri L. S., Murray J. W. and Paul B. (1994) The geochemical cycling of trace elements in a biogenic meromictic lake. *Geochimica et Cosmochimica Acta* **58**, 3993-4008.
- Bea F. (1999) Inductively Couple Plasma Mass Spectrometry *In* Marshall C.P. and Fairbridge R.W. (Eds) Encyclopedia of Geochemistry, Kluwer Academic Publishers, Boston, Massachusetts pp. 340-341
- Bereznitski Y., Jaroniec M. and Maurice P. (1998) Adsorption characteristics of two clay minerals society standard kaolinites. *Journal of Colloid Interface Science* **205**, 528-530.
- Birks J. L. (1975) Medical radionuclides in marine environments. *Nature* **255**, 621-622.
- Bostick B. C., Fendorf S., and Helz G. R. (2003) Differential Adsorption of Molybdate and Tetrathiomolybdate on Pyrite (FeS₂). *Environmental Science & Technology* **37**, 285-291.
- Broadbent H. S. and Johnson J. H. (1962) Rhenkum Catalysts. IV. Rhenium(III) Oxide from Perrhenate via Borohydride Reduction. *Journal of Organic Chemistry*. **27**, 4400-4402.
- Calvert S. E. and Pedersen T. F. (1993) Geochemistry of Recent Oxidic and Anoxic Marine-Sediments - Implications for the Geological Record. *Marine Geology* **113**, 67-88.
- Colodner D. (1991) The Marine Geochemistry of Rhenium, Iridium and Platinum. Ph.D. dissertation, Massachusetts Institute of Technology, Cambridge, Massachusetts, 269 pp.
- Colodner D., Sachs J., Ravizza G., Turekian K., Edmond J. and Boyle E. (1993) The Geochemical Cycle of Rhenium - a Reconnaissance. *Earth and Planetary Science Letters* **117**, 205-221.

- Colodner D., Boyle E., Edmond J. and Thomson J. (1992) Postdepositional Mobility of Platinum, Iridium and Rhenium in Marine-Sediments. *Nature* **358**, 402-404.
- Colodner D., Edmond J., and Boyle E. (1995) Rhenium in the Black Sea: comparison with molybdenum and uranium. *Earth and Planetary Science Letters* **131**, 1-15.
- Colton R. (1965) The Chemistry of Rhenium and Technetium. Interscience Publishers, New York, New York, 185 pp.
- Cronin T., Willard D., Karlsen A., Ishman S., Verardo S., McGeehin J., Kerhin R., Holmes C., Colman S. and Zimmerman A. (2000) Climatic Variability in the Eastern United States Over the Past Millennium From Chesapeake Bay Sediments. *Geology* **28**, 3-6.
- Crusius J. and Thomson J. (2000) Comparative Behavior of Authigenic Re, U, and Mo During Reoxidation and Subsequent Long-Term Burial in Marine Sediments. *Geochimica et Cosmochimica Acta* **64**, 2233-2242.
- Crusius J., Calvert S., Pedersen T. and Sage D. (1996) Rhenium and molybdenum enrichments in sediments as indicators of oxic, suboxic and sulfidic conditions of deposition. *Earth and Planetary Science Letters* **145**, 65-78.
- Cui D. and Eriksen T. E. (1996a) Reduction of Per technetate by Ferrous Iron in Solution: Influence of Sorbed and Precipitated Fe(II). *Environmental Science and Technology* **30**, 2259-2262.
- Cui D. and Eriksen T. E. (1996b) Reduction of Per technetate in Solution by Heterogenous Electron Transfer from Fe(II)-Containing Geological Material. *Environmental Science and Technology* **30**, 2263-2269.
- Erickson B. E. and Helz G. R. (2000) Molybdenum(VI) Speciation in Sulfidic Waters: Stability and Lability of Thiomolybdates. *Geochimica et Cosmochimica Acta* **64**, 1149-1158.
- Galloway J. N., Schlesinger W. H., Levy H., Michaels A. and Schnoor J.L. (1995) Nitrogen-Fixation - Anthropogenic Enhancement-Environmental Response. *Global Biogeochemical Cycles* **9**, 235-252.
- Goldberg S., Su C., Forster H.S. (1998) Sorption of Molybdenum on Oxides, Clay Minerals, and Soils –Mechanisms and Models. In Jenne E. A. (Ed), Adsorption of Metals by Geomedia: variables, mechanisms and model application. Academic Press, San Diego, California, pp.401-426.
- Haraldsen C. and Westerlund S. (1988) Trace metals in the water columns of the Black Sea and Framvaren Fjord. *Marine Chemistry* **23**, 417-424.

- Hibble S. J., Walton R. I., Feaviour M. R. and Smith A. D. (1999) Sulfur-Sulfur bonding in amorphous sulfides WS₃, WS₅, and Re₂S₇ from sulfur K-edge EXAFS studies. *Journal of the Chemical Society Dalton transactions* **16**, 2877-2883.
- Jarvis K. E., Gray A. L., Houk R. S. (1992) Handbook of ICP-MS. Blackie, Glasgow, United Kingdom, pp10-57.
- Ketterer M. E. (1990) Determination of Rhenium in Groundwater by Inductively Coupled Plasma Mass-Spectrometry With Online Cation-Exchange Membrane Sample Cleanup. *Analytical Chemistry* **62**, 2522-2526.
- Koide M., Hodge V., Yang J.S. and Goldberg E.D. (1987) Determination of Rhenium in Marine Waters and Sediments by Graphite-Furnace Atomic-Absorption Spectrometry. *Analytical Chemistry* **59**, 1802-1805.
- Laws E.A. (2000) Aquatic Pollution, An Introductory Text. John Wiley & Sons Inc., New York, New York. 639 pp.
- Lloyd J. R., Lovley D. R., and Macaskie L. E. (1999) Application of microbial technetium reduction to the treatment of nuclear wastes. Wissenschaftlich-Technische Berichte - Forschungszentrum Rossendorf.
- Lloyd J. R., Sole V.A., Van Praagh V.G., and Lovley D.R. (2000) Direct and Fe(II)-mediated reduction of technetium by Fe(III)-reducing bacteria. *Applied and Environmental Microbiology* **66**, 3743-3749.
- Maes A. et al. (2004) Evidence for the Interaction of Technetium Colloids With Humic Substances by X-Ray Absorption Spectroscopy. *Environmental Science & Technology* **38**, 2044-2051.
- Morford J. L. and Emerson S. (1999) The Geochemistry of Redox Sensitive Trace Metals in Sediments. *Geochimica et Cosmochimica Acta* **63**, 1735-1750.
- Morgan J.W. (1999) Rhenium-Osmium Dating Method. In Marshall C.P. and Fairbridge R.W. (Eds) Encyclopedia of Geochemistry, Kluwer Academic Publishers, Boston, Massachusetts pp. 547-550
- Müller A., Krebs B. and Diemann E. (1967) Reaction of pertechnetate and perrhenate with hydrogen sulfide. Preparation of tetrathio-perrhenate ions in solution. *Zeitschrift für anorganische und allgemeine Chemie* **353**, 259-264.
- Müller A., Diemann E. and Rao V. V. (1970) Darstellung Eigenschaften und röntgenographische Untersuchung von Tetathio-perrhenaten. *Chemische Berichte* **103**, 2961-2971.

- Müller A., Diemann E., Jostes R. and Bögge H. (1981) Transition Metal Thiometalates: Properties and Significance in Complex and Bioinorganic Chemistry. *Angewandte Chemie (International edition in English)* **20**, 934-955.
- Murray J.W., Izdar E. (1991) Black Sea Oceanography. Kluwer Academic Publishers, Dordrecht, Netherlands, 487 pp.
- Nameroff T. J., Balistrieri L. S., and Murray J. W. (2002) Suboxic Trace Metal Geochemistry in the Eastern Tropical North Pacific. *Geochimica et Cosmochimica Acta* **66**, 1139-1158.
- Olafsson J. and Riley J. P. (1972) Some data on the marine geochemistry of rhenium. *Chemical Geology* **9**, 227-230.
- Ozturk M. (1995) Trends of trace metal (Mn, Fe, Co, Ni, Cu, Zn, Cd and Pb) distributions at the oxic-anoxic interface and in sulfidic water of the Drammensfjord. *Marine Chemistry* **48**, 329-342.
- Pacer R. A. (1973) Borohydride reduction of the perrhenate ion. *Journal of Inorganic and Nuclear Chemistry* **35**, 1375-1377.
- Peacock R. D. (1966) The Chemistry of Technetium and Rhenium. Elsevier Publishing Company, New York, New York, 137 pp.
- Ranade A. C., Müller A. and Diemann E. (1970) Evidence for the Existence of new Thioanions of Vanadium and Rhenium by their Electronic Spectra. *Zeitschrift für anorganische und allgemeine Chemie* **373**, 258-264.
- Ravizza G. and Turekian K. K. (1989) Application of the rhenium-187-osmium-187 system to black shale geochronometry. *Geochimica et Cosmochimica Acta* **53**, 3257-3262.
- Schwarz D. E., Frenkel A. I., Nuzzo R. G., Rauchfuss T. B. and Vairavamurthy A. (2004) Electrosynthesis of ReS₄. XAS Analysis of ReS₂, Re₂S₇, and ReS₄. *Chemistry of Materials* **16**, 151-158.
- Seyler P. and Martin J. M. (1989) Biogeochemical processes affecting arsenic species distribution in a permanently stratified lake. *Environmental Science & Technology* **23**, 1258-1263.
- Sposito G. (1984) The Surface Chemistry of Soils. Oxford University Press, New York, 234 pp.
- Tuttle J. H., Jonas R. B., Malone C. M., (1987) Origin, Development and Significance of Chesapeake. In Majumdar S.K., Hall L.W. Jr. and Austin H.M., (Eds.), Contaminant Problems and Management of Living Chesapeake Bay Resources. The Pennsylvania Academy of Science, Phillipsburg, New Jersey, pp.442-472

- Vorlicek T. P. and Helz G. R. (2002) Catalysis by Mineral Surfaces: Implications for Mo Geochemistry in Anoxic Environments. *Geochimica et Cosmochimica Acta* **66**, 3679-3692.
- Vorlicek T.P., Kahn M.D., Kasuya Y., and Helz G.R. (2004) Capture of Molybdenum in Pyrite-Forming Sediments: Role of Ligand-Induced Reduction by Polysulfides. *Geochimica et Cosmochimica Acta* **68**, 547-556.
- Wagman D.D., Evans W.H., Parker V.B., Schumm R.H., Halow I., Bailey S.M., Churney K.L., and Nuttall R.L. (1982) The NBS table of chemical and thermodynamic properties. *Journal of Physical and Chemical Reference Data* **11**, Suppl. 2.
- Wakoff B. and Nagy K.L. (2004) Perrhenate Uptake by Iron and Aluminum Oxyhydroxides: an Analogue for Pertechnetate Incorporation in Hanford Waste Tank Sludges. *Environmental Science & Technology* **38**, 1765-1771.
- Weast R.C. and Astle M.J. (Eds.), (1979) CRC Handbook of Chemistry and Physics. CRC Press Inc. Boca Raton, Florida, p. B-117.
- Wilkinson G., Gillard R.D. and McCleverty J.A. (Eds.), (1987) Comprehensive Coordination Chemistry. Pergamon Press, New York, vol. 2, p.521
- Xiong Y. L. and Wood S. A. (1999) Experimental Determination of the Solubility of ReO_2 and the Dominant Oxidation State of Rhenium in Hydrothermal Solutions. *Chemical Geology* **158**, 245-256.
- Xiong Y. L. and Wood S. A. (2001) Hydrothermal Transport and Deposition of Rhenium Under Subcritical Conditions (up to 200 Degrees C) in Light of Experimental Studies. *Economic Geology and the Bulletin of the Society of Economic Geologists* **96**, 1429-1444.
- Young, J. R. (1981) A Study of the adsorption of Nickel(II) onto an amorphous silica surface by chemical and NMR Methods. Ph.D. Thesis. California Institute of Technology.